



Analysis of the Phreatic Line on Various Types of Primary Flood Defences

IS THE PHREATIC LINE SCHEMATISATION TOO CONSERVATIVE?

BACHELOR THESIS CIVIL ENGINEERING



UNIVERSITY OF TWENTE.

A.J. Denkers

UNIVERSITY OF TWENTE

WATERSCHAP DRENTS OVERIJSSELSE DELTA

19 October 2020 – 1 February 2021

COLOPHON

This document is a Bachelor Thesis for the completion of the Bachelor Civil Engineering at the University of Twente, Enschede, The Netherlands

Title:	Analysis of the Phreatic Line on Various Types of Primary Flood Defences
Version:	Final Version
Date:	25 January 2021
Author:	Bram Denkers Student No. s1828053
Educational Institute:	University of Twente Postbus 217 7500 AE Enschede Faculty of Engineering Technology Bachelor Civil Engineering
Host Company:	Waterschap Drents Overijsselse Delta Dokter van Deenweg 186 8025BM Zwolle, the Netherlands
Supervisors:	ir. P.T. Hopman (Waterschap Drents Overijsselse Delta) V.M. van Bergeijk MSc (University of Twente)
Duration	19 October 2020 – 1 February 2021

PREFACE

Before you lies my bachelor thesis *Analysis of the Phreatic Line on Various Types of Primary Flood Defences* as part of my bachelor study Civil Engineering at the University of Twente. The past 12 weeks I carried out my research at the waterboard Drents Overijsselse Delta, in the Water Safety group within the Research and Advice Department. Unfortunately, working at the office turned out impossible for almost the whole period due to COVID-19. Nonetheless, I was warmly welcomed at the Waterboard Drents Overijsselse Delta and had the opportunity to meet online all the colleagues within the department.

First of all, I would like to thank Peter Hopman from the Waterboard Drents Overijsselse Delta. He was always willing to answer all my questions and provided a lot of feedback during my research. In all our online meetings, you were very enthusiastic and proactive in providing new insights for this research. Furthermore, I would like to thank Jan Gruppen for this guidance at the start of my research. Also, I want to thank Vera van Bergeijk from the University of Twente for all your constructive feedback and ensuring the scientific justification of my research. Moreover, I want to thank everyone within the Research and Advice Department for making it even online a pleasant period. Lastly, I would like to thank my family and friends for listening to all the struggles I encountered during my thesis.

Finally, I would like to conclude with expressing the hope that you will enjoy reading my thesis. If you have any questions or comments, please do not hesitate to contact me.

Bram Denkers

Hengelo (GLD), 25 January 2021

SUMMARY

The Dutch primary flood defences protect the land from the sea and the large rivers in the Netherlands. The waterboard and the Ministry of Infrastructure and Environment are in charge to guarantee the protection of the hinterland from future flooding. The Dutch waterboards are obliged to assess whether the primary flood defences meet the given legal safety standards once every twelve years. Part of this assessment is to check the stability and safety of the flood defences against the given safety standards. The important factor for the inner slope macro stability of the dike is the phreatic line defined as the groundwater table in the dike. This phreatic line depends on different factors such as the hydraulic loads, pore pressures and other hydrological processes. When there are no groundwater measurements available to determine the height of the phreatic line, the waterboards have to rely on a conservative schematisation of the phreatic line provided in the *Technische Rapport Waterspanningen bij Dijklichamen* and the *Waternet Creator*. This study is performed in collaboration with the waterboard Drents Overijsselse Delta to answer the main research question: *can the current phreatic line schematisation be improved to provide a more realistic safety factor for the inner macro stability?*

Within the research, 4 research sub-questions were established to answer the main research question in the end. The first sub-question provided insight into the influences of soil and hydrological factors on the phreatic line. The second and third question were used to study the effect of different hydraulic loads on the progression of the phreatic line in the dike compared to the prescribed schematic estimations of the phreatic line. In the last research sub-question, a sensitivity analysis was performed to show which factors have the most impact on the schematic estimation of the phreatic line.

To answer the research questions, a modelling study has been performed on a fictive homogeneous clay and sand dike with simplified but realistic geometries. Since the phreatic line depends on different factors, such as the outside water levels, precipitation and soil properties, to test all these factors a Finite Element Method was constructed. The software Plaxis with Plaxflow module was used to make this Finite Element Method, that can handle different inputs, such as different hydraulic conditions and rainfall events. The model behaviour and soil parameters were calibrated based on literature and the use of analytical formulas.

Different hydraulic conditions, such as storm and discharge dominated high water waves, were applied to the model to see the effect of this on the progression of the phreatic line during such a wave. On top of the high water wave, an 8-days uniform rainfall event had been added. Furthermore, a fictive normative water level as a function of time had been simulated. All these simulations were compared to the prescribed schematic estimation of the phreatic line as described in the *Technisch Rapport Waterspanningen bij Dijklichamen* (TRWD) and the *Waternet Creator* (WC). In the end, a sensitivity analysis was performed to get insight into the most important factors regarding the phreatic line and which should definitely be taken into account in the phreatic line schematisation.

It became clear from the simulation results that when modelling a high water wave, the estimated phreatic line schematisation as described in the TRWD and the WC is exceeded at the inner toe of the homogeneous clay dikes. When an 8-days rainfall event was added, the phreatic line increased even more at the inner side of the homogeneous clay dike. This location is important for the inner macro stability of the dike slope. For homogenous sand dike, the prescribed schematisations of the phreatic line by the TRWD and the WC are not exceeded even when rainfall had been incorporated.

Furthermore, during the simulation of the normative water level as a function of the time. It became clear that that in case of a clay dike with a 4 meter thick sub-soil the phreatic line at the inner toe exceeded the WC and the TRWD prescribed estimation already after 20 days. In case of a 1 meter thick sub-soil, the WC and the TRWD estimation of the phreatic line was already exceeded after 12 days at the inner toe.

From the sensitivity analysis, it became clear that an increase in hydraulic conductivity leads to a higher located phreatic line, however, the variation in height over time will decrease. Next, a relatively low specific volumetric storage leads to a more varying phreatic line under daily circumstances. Lastly, it was concluded that both an intensification and a de-intensification of the 8-days rainfall event on clay and sand dikes lead not a lift or drop in the phreatic line during a discharge and storm dominated high water wave.

This research shows the effect of different hydrological conditions, soil parameters and sub-soils on the progression of the phreatic line during different hydraulic conditions. From all the simulations, it became clear that the phreatic line at the inner side of the clay dike is underestimated by the TRWD and the WC schematisation compared to the simulation results. Based on these results it would be recommended to take the exit point of the phreatic line at the inner toe of the clay dike at a height of $0.25 \cdot$ the peak of the high water wave relative to the surface level. For sand dikes, the TRWD and WC estimated schematisations are not overestimating nor underestimating the phreatic line, therefore no adaptation to improve the schematisation is suggested.

Furthermore, the thickness of the sub-soil has an influence on the height of the phreatic line according to the TRWD. In the simulations, this effect was indeed measurable under the crest of the dike and at the inner toe. The WC schematic estimation of the phreatic line has not incorporated this effect. Based on the results, it would be good to incorporate the thickness of the clay sub-soil in the schematisation of the phreatic line.

Several improvements for the phreatic line schematisations were given in this study to achieve a more realistic safety factor for the inner macro stability. Insights into the effects of different hydraulic conditions, hydrological process and soil parameters on the phreatic line have been provided. Still, due to the scope and other limitations of the research, not all the insights could be explained or supported by literature and simulation outputs. For this, more extensive research into the phreatic line exit point at the inner toe of the dike and the effect of different weather conditions should be performed.

TABLE OF CONTENTS

Colophon	i
Preface	ii
Summary	iii
Table of Contents	v
List of terms and abbreviations	vii
List of Symbols	vii
Table of Figures	viii
Table of Tables	xii
1 Introduction.....	1
1.1 Problem Description	1
1.2 Research Objective and Questions	2
1.3 Brief Overview of Methodology	3
1.4 Scope	5
1.5 Thesis Outline	6
2 Theoretical Framework	7
2.1 Phreatic Line	7
2.1.1 Schematisation of Phreatic Line	8
2.1.2 Factors influencing the phreatic line	11
2.2 Macro Stability.....	15
2.2.1 Uplifting.....	16
2.3 Theory on Groundwater FLOW.....	17
2.3.1 Saturated Zone	18
2.3.2 Unsaturated Zone.....	20
3 Plaxis Model	23
3.1 General Information	23
3.1.1 Limitations.....	23
3.2 Model Set-Up.....	24
3.2.1 Dike Geometry	24
3.2.2 Soil Parameters	25
3.2.3 Precipitation & Evaporation Data	29
3.2.4 Water Levels.....	29
3.2.5 Calibration	29
3.3 Validation & Reliability	30
3.4 Schematic Overview of The Model.....	32

4	Methodology	33
4.1	Phreatic Line under different Hydraulic Conditions	33
4.1.1	Water Level Scenarios	33
4.1.2	Rainfall Scenarios	35
4.1.3	Schematisation of the Phreatic Line.....	35
4.2	Situations leading to prescribed schematisations	36
4.3	Sensitivity Analysis.....	37
5	Model Results	39
5.1	Schematisation of the phreatic line under different hydraulic conditions.....	39
5.1.1	Daily Circumstances 2019	39
5.1.2	Storm and Discharge High Water Wave	40
5.1.3	Rainfall.....	42
5.2	Situations leading to the Prescribed Schematic Estimation of the Phreatic Line	44
5.2.1	Time-dependent Normative Water Level	45
5.2.2	Rainfall.....	47
5.3	Sensitivity Analysis.....	48
5.3.1	Phreatic Line under Daily Circumstances	48
5.3.2	Steady-State & Time-dependent Normative Water Level.....	51
5.3.3	Discharge and Storm Dominated High Water Waves	56
6	Discussion	60
6.1	Modelling Choices	60
6.2	Model Results	61
6.3	Comparison Plaxis Model and Schematisations	61
7	Conclusion	63
8	Recommendations	66
	Bibliography	67
	Appendices.....	73
A	Surface Geometries.....	73
B	Rainfall Time series	74
C	75% Confidence Interval Discharge/Storm High Water Wave.....	75
D	Discharge and Storm High Water Waves Full Time-Series.....	76
E	Time-dependent Normative Water Level Sand 1 Meter.....	78
F	Sensitivity Analysis Other Parameters	79

LIST OF TERMS AND ABBREVIATIONS

Term / Abbreviation	Meaning
Phreatic Line	Groundwater table level
KNMI	Dutch meteorological institute. (Koninklijk Nederlands Meteorologisch Instituut)
WBN	Water level in normative (Waterstand Bij Norm)
Hydraulic Conductivity	Property of vascular plants, soils and rocks, that describes the ease with which a fluid can move through pore spaces or fractures.
Surface Level	Ground level (Maaiveld)
FEM	Finite Element Method
TAW	Technical advisory committee for flood defences (<i>Technische Adviescommissie voor de Waterkingen</i>)
Waterboard	Regional government responsible for the management of flood defences, water levels and water quality (<i>Waterschap</i>)
WC	The estimated phreatic line schematisation provided by the Waternet Creator
TRWD	The estimated phreatic line schematisation provided in <i>Technisch Rapport Waterspanningen bij Dijklichamen</i>

LIST OF SYMBOLS

g	Gravitational acceleration	(m/s ²)
g_a	Fitting parameter related to the inverse of the air entry suction	(L ⁻¹)
g_c	Fitting parameter Van Genuchten	(-)
g_l	Fitting parameter Van Genuchten	(-)
g_n	Measure of the pore-size distribution	(-)
h	Hydraulic head	(m)
K	Hydraulic conductivity	(m/s)
k	Intrinsic permeability	(m ²)
m	Fitting parameter Van Genuchten ($1 - (\frac{1}{n})$)	(-)
m_v	Compressibility of the soil	(m ² /N)
N	Net infiltration due to precipitation	(m/s)
n	(effective phreatic) porosity	(-)
q	Specific discharge	(m/s)
S_{eff}	Effective degree of saturation	(-)
u	Water pressure	(N/m ²)
V_v	Volume of void space	(L)
V_T	Total volume of material	(L)
a	Fitting parameter related to the inverse of the air entry suction	(L ⁻¹)
β	Compressibility of the water	(m ² /N)

C'_{ref}	Effective cohesion	(kN/m ²)
E'	Effective Young's modulus	(kN/m ³)
∇p	Pressure drop over a given distance	(Pa)
ρ	Density of water	(kg/m ³)
γ_{unsat}	The unsaturated unit weight	(kg/m ³)
γ_{sat}	The saturated unit weight	(kg/m ³)
$ \psi $	Suction pressure	(L)
ψ	Pore pressure head	(m)
μ	Dynamic viscosity of the fluid	(Pa s)
ν'	Effective Poisson's ratio	(-)
θ	Volumetric water content	(-)
θ_s	Saturated water content	(-)
θ_r	Residential water content	(-)
φ	Hydraulic head	(m)

TABLE OF FIGURES

Figure 1-1: Methodology Flowchart.....	3
Figure 1-2: Schematic representation of dike with a clay core.	5
Figure 1-3: Schematic representation of dike with a sand core.	5
Figure 2-1: Cross-section of a Dutch dike profile (Van der Meer et al., 2004).	7
Figure 2-2: Overview interaction between soil layers (Van der Meer et al., 2004).	8
Figure 2-3: Phreatic Line situation 1 (Van der Meer et al., 2004).	9
Figure 2-4: Phreatic line situation 2 (Van der Meer et al., 2004).	10
Figure 2-5: Schematisation of the phreatic line plane for clay dikes (Van der Meij, 2020).	11
Figure 2-6: Schematisation of the phreatic plane for sand dike on clay/peat underground, without drainage construction (Van der Meij, 2020).	11
Figure 2-7: Shape of flood wave for the Rhine river at Lobith with the different previous hydrographs HR2001, WTI20011 (Chbab, 2019).	13
Figure 2-8: Water height normalized to water levels based on average daily measurements – Deventer (Gerritsen, 2019). Dots are measurement points, redline is median, blue shaded 75%-CI and grey shaded 95%-CI.	13
Figure 2-9: Water height normalized to water levels based on average daily measurements – Kampen (Gerritsen, 2019). Dots are measurement points, redline is median, blue shaded 75%-CI and grey shaded 95%-CI.	14
Figure 2-10: Situation of macro instability (Helpdesk Water, n.d.).....	16
Figure 2-11: Equilibrium analysis of macro stability ('t Hart et al., 2016).	16
Figure 2-12: The effect of sliding due to uplift on a dike (Warmink, 2018).	17

Figure 2-13: Visualisation of the effects of different climatological processes on the pore water pressure (D. G. Fredlund, 2000, p. 984).	17
Figure 2-14: Typical Water Retention Curves for the soil of different texture (Tuller & Or, 2005, p. 278).	21
Figure 3-1: Sand Dike (yellow) with 1 meter clay (green) and 13 meter sand layer (orange) (square = 1 by 1 meter).	24
Figure 3-2: Generated Mesh Clay Dike with 4 meter clay sub-soil.	25
Figure 3-3: Phreatic line after 90 years of precipitation with and without altered Van Genuchten Parameter...	26
Figure 3-4: Starting situation of the phreatic line (dark blue line) clay dike with 4 meter clay colours indicates the effective saturation.....	30
Figure 3-5: Starting situation of the phreatic line (dark blue line) 1 meter clay dike with 1 meter clay colours indicates the effective saturation.	30
Figure 3-6: Starting situation of the phreatic line (dark blue line) sand dike with 4 meter clay colours indicates the effective saturation.....	30
Figure 3-7: Starting situation of the phreatic line (dark blue line) sand dike with 1 meter clay colours indicates the effective saturation.....	30
Figure 3-8: Effect of hydraulic conductivity (K) under daily circumstances.	31
Figure 3-9: Effect of the width of clay sub-soil (D) below the dike under daily circumstances.	32
Figure 3-10 Overview of the model setup in relation to the research sub-questions (RQ).	32
Figure 4-1: The discharge and storm high water waves normalised on the WBN water level.	34
Figure 4-2: The upper bound of the 75% Confidence Interval (solid lines) of the discharge and storm dominated high water waves.	35
Figure 4-3 The phreatic line schematisations of the four different dike bodies based on the TRWD and WC.....	36
Figure 5-1: The phreatic line over the year 2019 together with the net precipitation of 2019 and the 3 days moving average net precipitation.	39
Figure 5-2: The phreatic line at different time steps in days together with the dike body and the schematizations of the WC and TRWD for a clay dike with a 4 meter clay sub-soil for: (a) the discharge dominated high water wave, (b) the storm dominated high water wave.	40
Figure 5-3: The phreatic line at different time steps in days together with the dike body and the schematizations of the WC and TRWD for a clay dike with a 1 meter clay sub-soil for: (a) the discharge dominated high water wave, (b) the storm dominated high water wave.	41
Figure 5-4: The phreatic line at different time steps in days together with the dike body and the schematizations of the WC and TRWD for a sand dike with a 4 meter clay sub-soil for: (a) the discharge dominated high water wave, (b) the storm dominated high water wave.	42
Figure 5-5: The phreatic line at different time steps in days together with the dike body and the schematizations of the WC and TRWD for a sand dike with a 1 meter clay sub-soil for: (a) the discharge dominated high water wave, (b) the storm dominated high water wave.	42
Figure 5-6: The phreatic line at different time steps in days together with the dike body and the schematizations of the WC and TRWD for a clay dike with a 4 meter clay sub-soil for: (a) the discharge dominated high water wave with a 1/500 year rainfall event, (b) the storm dominated high water wave with a 1/500 year rainfall event.....	43

Figure 5-7: The phreatic line at different time steps in days together with the dike body and the schematizations of the WC and TRWD for a clay dike with a 1 meter clay sub-soil for: (a) the discharge dominated high water wave with a 1/500 year rainfall event, (b) the storm dominated high water wave with a 1/500 year rainfall event.	43
Figure 5-8: The phreatic line at different time steps in days together with the dike body and the schematizations of the WC and TRWD for a clay dike with a 4 meter clay sub-soil for: (a) the discharge dominated high water wave with and without 1/500 year rainfall event, (b) the storm dominated high water wave with and without a 1/500 year rainfall event.	44
Figure 5-9: The phreatic line at different time steps in days together with the dike body and the schematizations of the WC and TRWD for a clay dike with a 1 meter clay sub-soil for: (a) the discharge dominated high water wave with and without 1/500 year rainfall event, (b) the storm dominated high water wave with and without a 1/500 year rainfall event.	44
Figure 5-10: The phreatic line for a normative water level at different time steps in days together with the dike body and the schematizations of the WC and the TRWD for a clay dike with a 4 meter sub-soil.	45
Figure 5-11: The phreatic line for a normative water level at different time steps in days together with the dike body and the schematizations of the WC and the TRWD for a clay dike with a 1 meter sub-soil.	46
Figure 5-12: The phreatic line for a normative water level at different time steps in days together with the dike body and the schematizations of the WC and the TRWD for a sand dike with a 4 meter sub-soil.	47
Figure 5-13: The phreatic line for a normative water level with winter rainfall at different time steps in days together with the dike body and the schematizations of the WC and the TRWD for a clay dike with a 4 meter sub-soil.	47
Figure 5-14: The phreatic line for a normative water level with winter rainfall at different time steps in days together with the dike body and the schematizations of the WC and the TRWD for a clay dike with a 1 meter sub-soil.	48
Figure 5-15: The effect of different hydraulic conductivity (K) on the phreatic line over the year 2019 together with the net precipitation of 2019 and the 3 days moving average net precipitation.	49
Figure 5-16: The effect of different Volumetric Storage Capacity (B) on the phreatic line over the year 2019 together with the net precipitation of 2019 and the 3 days moving average net precipitation.	49
Figure 5-17: The effect of different clay sub-soil thickness (D) on the phreatic line over the year 2019 together with the net precipitation of 2019 and the 3 days moving average net precipitation.	50
Figure 5-18: The effect of different clay dike widths (W) on the phreatic line over the year 2019 together with the net precipitation of 2019 and the 3 days moving average net precipitation.	50
Figure 5-19: The phreatic line during a steady-state simulation with the dike body and the schematizations of the WC and TRWD for a clay dike with a 4 meter clay sub-soil for: (a) different hydraulic conductivities, (b) different volumetric specific storage capacities, (c) different sub-soil thicknesses.	52
Figure 5-20: The phreatic line during a steady state simulation with the dike body and the schematizations of the WC and TRWD for a sand dike with a 4 meter clay sub-soil for: (a) different hydraulic conductivities, (b) different volumetric specific storage capacities, (c) different sub-soil thicknesses.	53
Figure 5-21: The phreatic line for a normative water level with different hydraulic conductivities at different time steps in days together with the dike body and the schematizations of the WC and the TRWD for a clay dike with a 4 meter sub-soil.	54

Figure 5-22: The phreatic line for a normative water level with different volumetric specific storage capacity at different time steps in days together with the dike body and the schematizations of the WC and the TRWD for a clay dike with a 4 meter sub-soil.....	54
Figure 5-23: The phreatic line for a normative water level with different sub-soil thickness at different time steps in days together with the dike body and the schematizations of the WC and the TRWD for a clay dike with a 4 meter sub-soil.....	54
Figure 5-24: The phreatic line for a normative water level with different hydraulic conductivities (unit m/day) at different time steps in days together with the dike body and the schematizations of the WC and the TRWD for a sand dike with a 4 meter sub-soil.	55
Figure 5-25: The phreatic line for a normative water level with different volumetric storage capacity (unit 1/m) at different time steps in days together with the dike body and the schematizations of the WC and the TRWD for a sand dike with a 4 meter sub-soil.	55
Figure 5-26: The phreatic line for a normative water level with different sub-soil thickness (unit meter) at different time steps in days together with the dike body and the schematizations of the WC and the TRWD for a sand dike with a 4 meter sub-soil.	55
Figure 5-27: The phreatic line for a discharge highwater wave with different hydraulic conductivities (unit m/day) at different time steps in days together with the dike body and the schematizations of the WC and the TRWD for a clay dike with a 4 meter sub-soil.	56
Figure 5-28: The phreatic line for a storm highwater wave with different hydraulic conductivities (unit m/day) at different time steps in days together with the dike body and the schematizations of the WC and the TRWD for a clay dike with a 4 meter sub-soil.	56
Figure 5-29: The phreatic line for a discharge highwater wave with different specific volumetric storage capacities (unit 1/m) at different time steps in days together with the dike body and the schematizations of the WC and the TRWD for a clay dike with a 4 meter sub-soil.....	57
Figure 5-30: The phreatic line for a storm highwater wave with different specific volumetric storage capacities (unit 1/m) at different time steps in days together with the dike body and the schematizations of the WC and the TRWD for a clay dike with a 4 meter sub-soil.	57
Figure 5-31: The phreatic line for a discharge highwater wave with different rainfall intensities (R = return period 1/... year) at different time steps in days together with the dike body and the schematizations of the WC and the TRWD for a clay dike with a 4 meter sub-soil.	58
Figure 5-32: The phreatic line for a storm highwater wave with different rainfall intensities (R = return period 1/... year) at different time steps in days together with the dike body and the schematizations of the WC and the TRWD for a clay dike with a 4 meter sub-soil.	58
Figure 5-33: The phreatic line for a discharge highwater wave with different hydraulic conductivities (unit m/day) at different time steps in days together with the dike body and the schematizations of the WC and the TRWD for a sand dike with a 4 meter sub-soil.	59
Figure 5-34: The phreatic line for a storm highwater wave with different hydraulic conductivities (unit m/day) at different time steps in days together with the dike body and the schematizations of the WC and the TRWD for a sand dike with a 4 meter sub-soil.	59
Figure 5-35: The phreatic line for a discharge highwater wave with different rainfall intensities (R = return period 1/... year) at different time steps in days together with the dike body and the schematizations of the WC and the TRWD for a sand dike with a 4 meter sub-soil.....	59

Figure 5-36: The phreatic line for a storm highwater wave with different rainfall intensities (R = return period 1/... year) at different time steps in days together with the dike body and the schematizations of the WC and the TRWD for a sand dike with a 4 meter sub-soil..... 59

TABLE OF TABLES

Table 1: Schematisation points for different situations according to the Waternet Creator (Van der Meij, 2020).	10
Table 2: Range of horizontal hydraulic conductivities per soil type (Billen, 2020).	19
Table 3 Soils per layer for different dike types.	25
Table 4: Van Genuchten Fitting Parameters (* = Original value) (Vogel et al., 2000).	26
Table 5: Hydraulic Conductivity Clay.	27
Table 6: Hydraulic Conductivity Sand.	27
Table 7: Hydraulic Conductivity Sand Aquifer.	28
Table 8: Volumetric Specific Storage overview.	28
Table 9: Other Soil Properties for the different soil layers.	28
Table 10: 8-days precipitation volumes (mm) for the different return periods (Beersma et al., 2019, pp. 15–22).	29
Table 11: Overview of different scenarios with different hydraulic conditions.	33
Table 12: The scenarios of the sensitivity analysis based on the previous research sub-questions.	37
Table 13: Sensitivity analysis for Clay Dike.	37
Table 14: Sensitivity analysis for Sand Dike.	38

1 INTRODUCTION

The Netherlands has a long history in water management to protect the hinterland from flooding. Around 26 percent of the area of the Netherlands is below sea level. Therefore, flood protection is a national priority, since more than half of the country is vulnerable to flooding (Planbureau voor de Leefomgeving, 2014). The primary flood defences were built to protect against flooding during the high water from the North Sea, the Wadden Sea, and the major rivers in the Netherlands.

In the Netherlands, the waterboards and the Ministry of Infrastructure and Environment are in charge to guarantee the protection of the hinterland from future flooding. Due to global warming, the ongoing land subsidence and sea level rising, a larger responsibility lies in the hands of these authorities. The need for a good flood risk management is becoming more important. To guarantee protection for the people of the hinterland, the Water Act framework has been created for the upcoming decades to deal with these kinds of issues. According to this act, the Dutch waterboards are obliged to assess whether the primary flood defences meet the given legal safety standards once every twelve years. In 2017, the rules and assessment tools that have to be used were formalised in the Wettelijke Beoordelingsinstrumentarium (WBI)

Within the WBI, there are different assessment level for the safety assessment of the primary flood defences. One of the applications of the WBI is the *Ringtoets*, in which the assessment of the flood defences can be analysed. Calculating the flood probabilities of the primary flood defences not only requires insight into the strength of the dike body but also the hydraulic loads and pore water pressure have an impact on the failure probabilities. This concerns the duration of high water levels and wave patterns. Insight in these pore water pressures is therefore essential in the assessment of these flood defences (Helpdesk Water, 2017).

When a dike becomes saturated with water, the effective stress in the soil decreases. Therefore, these effective stresses, pore pressures and the location of the phreatic line are important for the inner slope macro stability of a dike (Kanning et al., 2015). In cases where little or no pore water pressure measurements are available, the waterboards have to rely on conservative estimates to determine the location of the phreatic line and the pore water pressure developments in the body of the dike.

Technisch Rapport Waterspanningen bij Dijklichamen (Van der Meer et al., 2004) provides a method to make an initial estimate of the pore pressures without water pressure measurements or groundwater flow calculations. Another method within the WBI for the initial estimate can be provided by the *Waternet Creator*. The research is conducted in cooperation with the Waterboard Drents Overijsselse Delta (WDODelta). This waterboard wants to know if these estimations are very conservative for the inner slope stability of a dike body. What kind of situation describes the suggested estimations of the phreatic line?

1.1 PROBLEM DESCRIPTION

Since the waterboard has limited (ground)water pressure measurements points in the dike bodies. Even in cases where there is a measurement point in the dike body, high water situations have not occurred yet and therefore no measurements are available. Therefore, the waterboard is depending on the methods described in the *Technisch Rapport Waterspanning bij dijklichamen* and the *Waternet Creator* to give a first estimation of the location of the phreatic line and the pore pressure in dike bodies.

The scientific basis for how conservative the schematisations are is not entirely clear. An expert report from 2009 (Expertisenetwerk waterveiligheid, 2009) shows that there is no information about whether the schematisations are based on measurements or expert judgements.

For macro stability, the calculations are based on this estimated schematic representation of the phreatic line. However, there is not clearly defined on which assumptions and situations this schematic representation of the phreatic line is based.

Furthermore, the location of the phreatic line depends on many different factors. Factors that influence the phreatic line according to the *Technisch rapport waterkerende grondconstructies* (Kremer et al., 2001) are:

- Soil types of the dike body
- The geometry of the dike
- Duration and peak of high water wave
- Whether or not the groundwater flow is stationary
- The cover layer of the outer slope
- (Extreme) Rainfall

Since the phreatic line depends on the river high water wave and many other different factors, it is important to look at these effects on the phreatic line, and the inner macro stability. Currently, it is unknown which situations lead to the estimated schematic representation of the phreatic line, and how realistic those situations are.

Therefore, there is need for an investigation into the method for the phreatic line approximation and to determine how well this method describes the phreatic line in dikes. All of this is to provide insights for the waterboard into how realistic it could be to move away from this conservative estimation of the phreatic line and carry out more research to the exact location of this phreatic line. Since the waterboard has to assess many kilometres of dikes, a more reliable schematisation of the phreatic line gives a better dike assessment.

1.2 RESEARCH OBJECTIVE AND QUESTIONS

The main research objective is to provide insight into what degree the estimated schematisation of the phreatic line approximation, as currently stipulated in the *Technisch Rapport Waterspanning bij dijklichamen* and provided by the *Waternet Creator*, are conservative approximations (Van der Meer et al., 2004). These insights can help the waterboard to decide whether they can deviate from this prescribed standard for the dike assessments.

To achieve the aim of the research, the main research question has been formulated as follows:

Main Question: *Can the current phreatic line schematisation be improved to provide a more realistic safety factor for the inner macro stability?*

This main question has been divided into four sub-questions to make it more manageable. First of all, it is important to obtain more insight into the effects of the phreatic line on the inner macro stability of a dike. This indicates the importance of the location of the phreatic line for the assessment of dike rings. It is also a first step in the understanding of influences of the phreatic line in the dike assessments. Because of this, the first research sub-question is formulated as follows:

Sub-question 1: *What are the main factors influencing the phreatic line?*

Next, to provide insight in which different hydraulic conditions, a combination of parameters, gives the estimated schematic representation of the phreatic line the next sub-question has been formulated. Since the location of the phreatic line depends on many factors, different hydraulic conditions will be modelled. This to see the effects of the different hydraulic conditions on the phreatic line.

Sub-question 2: *What are the effects of different hydraulic conditions on the phreatic line?*

To compare the schematisation of the phreatic line given by the *Technisch Rapport Waterspanningen bij Dijklichamen* and the *Waternet Creator* with a realistic situation, the next sub-question has been formulated. A realistic situation is a modelling situation in which average realistic parameter input has been used.

Sub-question 3: *What different realistic situations lead to the prescribed schematic estimation of the phreatic line?*

Furthermore, now the situation describing the estimated schematic representation has been made clear. To show the extent of how conservative this representation is, the impact of the different time-dependent factors should be made clear. Therefore, a sensitivity analysis will be conducted, to show how conservative the estimation is and see which parameters should definitely be taken into account in the phreatic line schematisation. To give insights into this the last sub-question has been formulated.

Sub-question 4: *Which factors have the most impact on the schematic estimation of the phreatic line?*

1.3 BRIEF OVERVIEW OF METHODOLOGY

In this section, all methods that will be used to find the answers for the different research questions are briefly described. In Chapter 3, a more detailed methodology for the modelling related research sub-questions is provided.

A schematic overview of the research methodology is given in Figure 1-1. Clearly, the structure between the different sub-question can be seen. The circular boxes indicate the type of method that is used to answer the particular sub-question. The arrows indicate the information flow that is needed to answer a sub-question via the specific method. Most of the time, the results of previous sub-questions is the input for the next question.

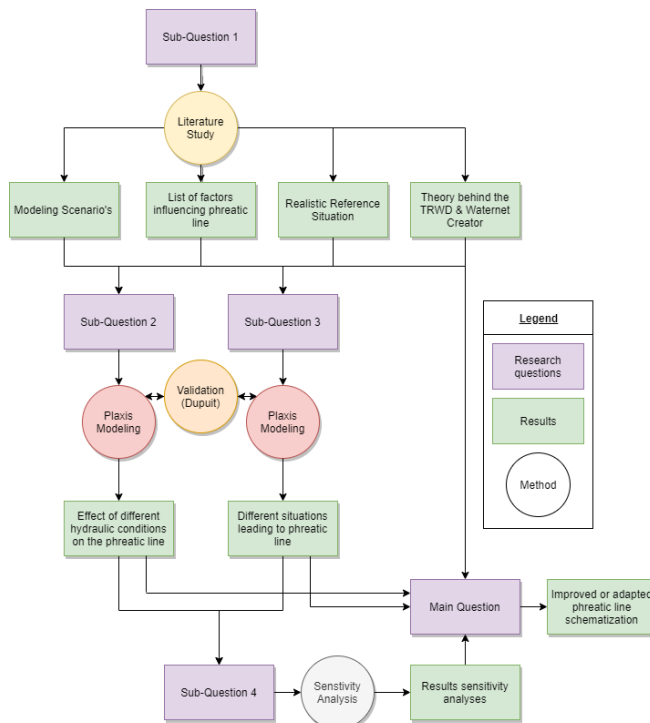


Figure 1-1: Methodology Flowchart.

Next, for each research question a brief methodology is given.

Sub-question 1

- *What are the main factors influencing the phreatic line?*

This sub-question will be answered by performing a literature study and by close communication with the experts at the waterboard. The outcomes of this literature study will be factors which will be used in the modelling study.

The following subjects will be researched for this sub-question:

- The background of the estimated phreatic line schematisations given in the TWRD and the Waternet Creator;
- Factors influencing the position of the phreatic line;
- Theory on time-dependent groundwater flow;

There are already several studies and theses conducted about the phreatic line in general or the application on secondary regional flood defences. For example, de Loor (2018) and Dorst (2019) has researched the effects of precipitation and soil properties on the level of the phreatic line in river dikes. De Raadt, Jaspers Focks, Van Hoven, et al. (2015, p. 511) researched the phreatic line under storm conditions.

These research studies will provide the required information to understand the factors influencing the phreatic line and to answer this sub-question. The results for this sub-question can be found in Chapter 2, Theoretical framework.

The results of the literature study will be used directly as input for the next sub-questions. For example, in sub-question 2, the different factors influencing the phreatic line and the background behind the schematisations will be used to model the different situations leading to the prescribed schematisations. For sub-question 3, realistic values for the different parameters will be used as input for the modelling study.

Sub-question 2 & 3 and 4:

- *What are the effects of different hydraulic conditions on the phreatic line?*
- *What different situations lead to the prescribed schematic estimation of the phreatic line?*
- *Which factors have impact on the schematic estimation of the phreatic line?*

For these sub-questions, a quantitative modelling study will be performed. For some parts, a small statistical comparison will be conducted.

For the modelling parts, a numerical finite element method (FEM) model will be set-up in Plaxis, to determine the time-dependent groundwater flow and the location of the phreatic line. Different situations, a combination of different input parameters, will be evaluated to check which are leading to the prescribed schematic estimation of the phreatic line. Besides that, the model output will be compared against each other, to see the effects of a different set of parameters.

For the last sub-question, a sensitivity analysis will be conducted. For the sensitivity different scenario's will be evaluated. As starting values, the parameter results of the previous sub-questions will be used. The scenarios will be based on the outcomes of the literature study. Examples of various scenarios could be:

- Variation in the permeability of different layers;
- Variation in the rainfall;
- Variation in soil parameters
- Variation in the high water level time.

This to see which parameters have the most influence on the location of the phreatic line. More information on the set-up and the parameter choices of the model for each sub-question can be found in Chapter 3 Plaxis model and Chapter 4 Methodology.

1.4 SCOPE

During the research, the focus will be on the schematisation of the phreatic line. The depth of the phreatic line inside the dike body depends on the soil layers of the dike body, and the structure of the substrate (Van der Meer et al., 2004). There are 4 general dike body situations described corresponding to the standard situations in the report *Technisch rapport waterspanningen bij dijken*.

1. Clay core and an impermeable layer;
2. Clay core and a sand foundation;
3. Sand core (with or without a cover layer) and an impermeable layer;
4. Sand core (with or without a cover layer) and a sand foundation.

Only the first and the third situations are applicable within the waterboard. According to the bachelor thesis of Bootsma (2019), the impact of the phreatic line on the other two situations (2nd and 4th) is very limited due to the high safety factor. Therefore, only the first and third situation will be used in this research. A schematic representation of these 2 dike bodies is given in Figure 1-2 and Figure 1-3.

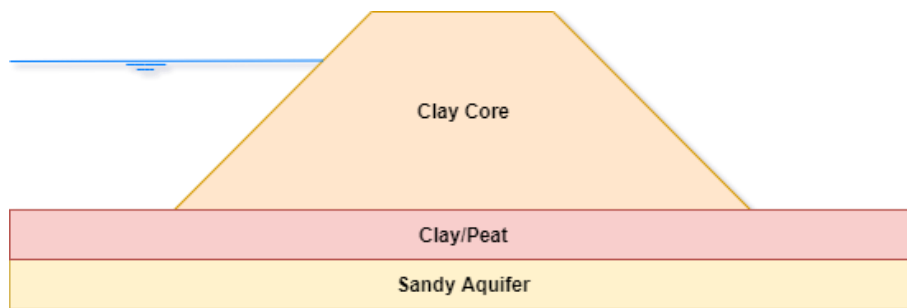


Figure 1-2: Schematic representation of dike with a clay core.

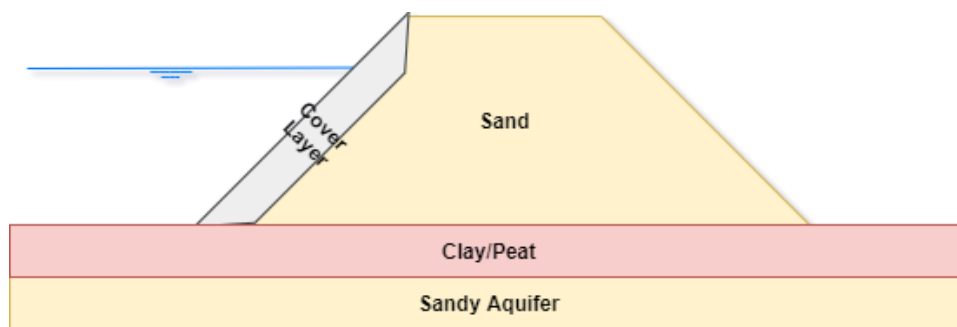


Figure 1-3: Schematic representation of dike with a sand core.

The focus of this research will be mainly on the modelling part. Only a minimum focus will be on the statistical analyses of dike characteristics and the height and duration of the high water waves.

1.5 THESIS OUTLINE

This thesis has the following structure. Chapter 2 contains a review of the relevant literature. Since the first research sub-question forms the foundation for the modelling study, the answer to this sub-question can be found in Chapter 2 as well. Subsequently, The model set-up and the validation of the model can be found in Chapter 3. The methodology for the last three research sub-question is described in Chapter 4. Following, in Chapter 5 the results of the modelling study will be given per research sub-question. Afterwards, the discussion will be provided in Chapter 6. Next, the conclusion and thereby the answer to the different research sub-questions and the main research question will be provided in Chapter 7. In the end, the discussion and recommendations are provided in Chapter 7 and 8.

2 THEORETICAL FRAMEWORK

In this chapter, information is provided regarding the theory on which this research project is based. Furthermore, it gives thereby answers to the first research sub-question. The objective of this research is to provide insights into how conservative the estimated representation of the phreatic line according to the report *Technisch Rapport Waterspanningen bij dijklighamen* and the Waternet Creator is. First, general information on the phreatic line, the schematisation and factors influencing the phreatic line is given. Next, an overview of macro stability in relation to the phreatic line. In the end, the general theoretical background behind groundwater flow is presented.

2.1 PHREATIC LINE

In the Netherlands, a dike is generally built on an incompressible sandy aquifer (Pleistocene) and on top a semi-permeable top-layer (Holocene). These two ground layers together form the Dutch dike profile (See Figure 2-1). The phreatic line is the location of the free groundwater table, being the hypothetical position where the water pressure is equal to the atmospheric pressure. The forces of the outer water level directly influence the hydraulic head in the aquifer and gradually affecting the phreatic line in the dike itself. In general, the top layer has a lower permeability compared to the sandy aquifer.

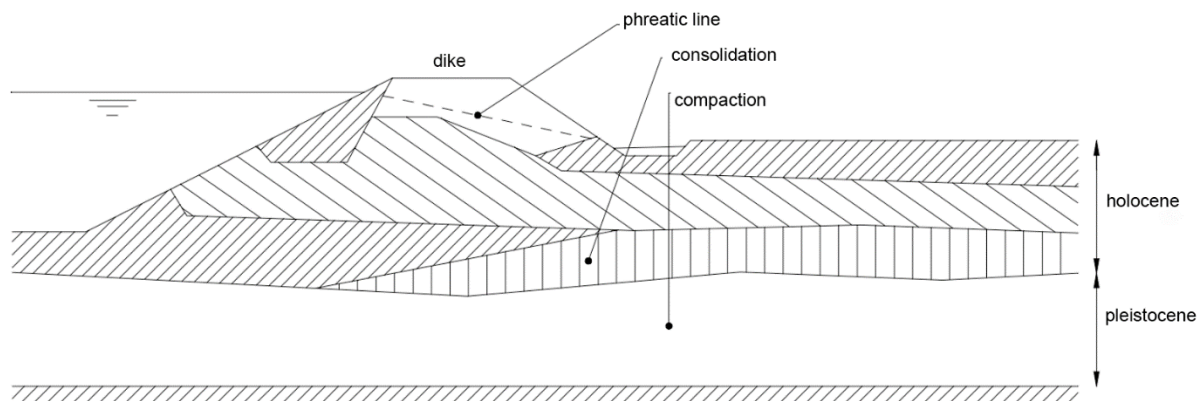


Figure 2-1: Cross-section of a Dutch dike profile (Van der Meer et al., 2004).

Water can be stored in the voids of the soil layers below the phreatic line, phreatic storage. In soft soil layers, extra water can be stored in the extra voids that arise when the soil starts to consolidate. This called the elastic storage capacity. Storage means that the effect of groundwater movement is delayed. This is a time-dependent process since the water levels itself change over time.

In Figure 2-2, the different flow lines and groundwater interaction between the soil layers can be seen for a typical Dutch dike profile. The groundwater flow can be roughly classified as follows;

- A. Two-dimensional slow flow in a vertical plane through the dike body (clay and/or sand with cover)
- B. Slow vertical one-dimensional flow (infiltration and seepage)
- C. The horizontal one-dimensional flow of groundwater in the sandy aquifer (Pleistocene)

The phreatic line is the place where the pore pressure is zero. Above this line the pore pressures are negative, representing capillary tension causing the water to rise against the gravitational force. The soil above the phreatic line is partially in saturated or unsaturated condition.

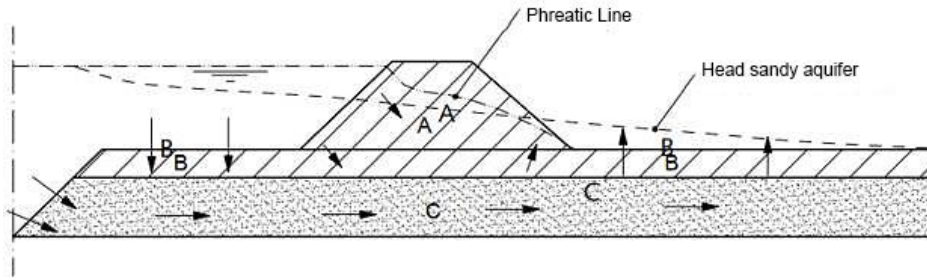


Figure 2-2: Overview interaction between soil layers (Van der Meer et al., 2004).

The initial level of the stationary groundwater table can best be determined based on water pressure measurements under stationary conditions. These measurements are only available for a few dike sections within the waterboard area. When these measurements are not available, an estimation can be made based on the method described in the report *Technisch Rapport Waterspanningen bij dijklichamen (TRWD)* or by the use of the Waternet Creator. For both, the effects of the non-stationary nature of the high water can be analysed.

2.1.1 SCHEMATISATION OF PHREATIC LINE

As described above, the phreatic line is an important variable. Due to uncertainty in a large number of processes and influencing factors, the phreatic line is usually schematised based on a number of points in the geometry of the dike. In this section, the schematisation of the phreatic line according to the TRWD and the Waternet Creator will be discussed.

2.1.1.1 TECHNISCH RAPPORT WATERSPANNINGEN BIJ DIJKLICHAMEN (TRWD)

In the report *Technisch Rapport Waterspanningen bij dijklichamen*, there are four situations for which the estimated schematisations have been made. As described in the scope of this project, only two situations are of importance for this waterboard, due to their relative low safety factors (Bootsma, 2019). Therefore, only the following two situations will be investigated.

1. A clay core and an impermeable layer;
2. Sand core (with or without cover) and an impermeable layer.

2.1.1.1.1 SITUATION 1 (CLAY CORE)

In Figure 2-3, the situation of the schematisation of the phreatic line during the water level in normative (WBN) situation (in Dutch: *Waterstand bij norm*). The schematisation consists of four points (A, B, C and D).

Point C is the height of the phreatic line at the outer toe:

- In case of a ditch, located at the water level of the ditch (Point C2).
- In case of no ditch, located at the outer toe (Point C3).

Point D is the height of the phreatic line at the inner toe:

- In case of a ditch, located at the water level of the ditch (Point D1).
- In case of no ditch, located at the inner toe. (Point D2).

Point A, below the inner slope of the dike body. The height of point A is determined with Equation 1. As can be seen, the height of point A is not depending on the outer water level.

Equation 1

$$A_{height} = \text{Min}(C_{height} + \frac{L}{X}, D_{height} + \frac{L}{X})$$

In which:

A_{height}	=	height of point A (m)
C_{height}	=	height of point C (m)
D_{height}	=	height of point D (m)
L	=	distance between point C and point D (m)
d	=	thickness of clay or peat layer below the dike body (m)
X	=	12 if $d = 0.0$ m
X	=	10 if $0.0 \text{ m} < d < 4.0$ m
X	=	8 if $d > 4.0$ m

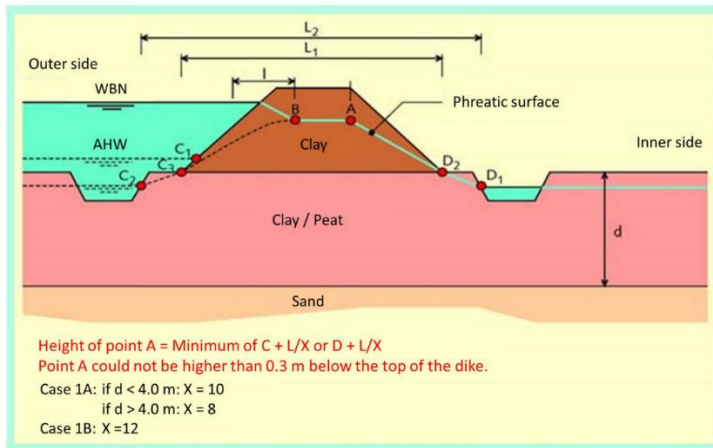


Figure 2-3: Phreatic Line situation 1 (Van der Meer et al., 2004).

The location of point B is determined by the horizontal penetration depth l . This length can be determined by the following formula. (Van der Meer et al., 2004)

Equation 2

$$l = \sqrt{\frac{2 * k_z * H_0 * t}{n_z}}$$

In which:

k_z	=	The permeability of the soil layer (m/s)
H_0	=	Water depth from permeable layers (m)
T	=	Duration of the heigh water wave (s)
n_z	=	Porosity of the dike material (-)

2.1.1.1.2 SITUATION 2 (SAND CORE)

In Figure 2-4, the phreatic line is given for the second situation. In this case, the dike has a sand core layer and a possible cover layer.

A clay cover layer with a thickness of fewer than 1,5 meters serves as an open covering due to its permeability. In this case, it is assumed that the phreatic line goes linear from point C1 tot D1 or D2.

Point D is the height of the phreatic line at the:

- Inner toe at the height of $0.25 * h$ above the ground (Point D1).
- Start of the drainage construction (Point D2) in case of a properly functioning draining construction.

Point E is the height of the phreatic line at the inner toe:

- In case of a ditch, located at the water level of the ditch (Point E1).
- In case of no ditch, located at the inner toe. (Point E2).

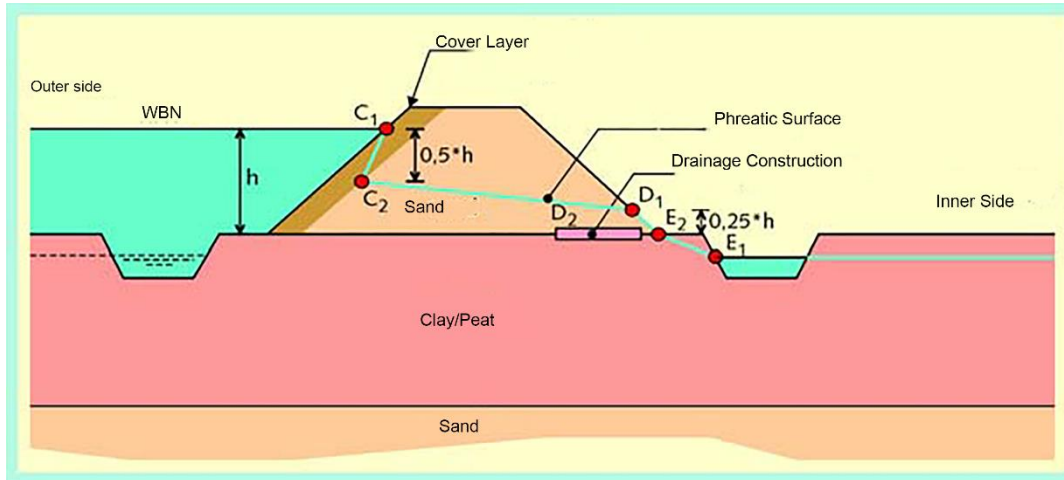


Figure 2-4: Phreatic line situation 2 (Van der Meer et al., 2004).

2.1.1.2 SCHEMATISATION PHREATIC LINE WITH WATERNET CREATOR

As described earlier, the Waternet Creator can also schematise the phreatic line. The same two situations as described in the TRWD are used since those are the most interesting ones due to their relative low safety factor.

In Figure 2-5 & Figure 2-6, the schematisation of the phreatic line for clay dikes and sand dikes can be found (Van der Meij, 2020). In Table 1, the location of points A, B, C, D, E and F can be found.

Table 1: Schematisation points for different situations according to the Waternet Creator (Van der Meij, 2020).

Points	Clay Dikes	Sand dike on clay
A	The intersection of the river water level with the outer slope.	The intersection of the river level with the outer slope.
B	River water level minus offset, with default offset 1 meter.	River water level minus offset, with default offset $0.5 \times (\text{Height point A} - \text{Height point E})$. (Exists only in case there is a clay cover)
C	River water level minus offset, with default offset 1.5 meters.	Linear interpolation between point B and point E.
D	Linear interpolation between C and E.	Linear interpolation between point B and point E.
E	Ground-level at the toe of the dike.	The surface level at dike toe minus offset, with default offset $-0.25 \times (\text{Height point A} - \text{Height point E})$.
F	Intersection point polder and water level polder.	Intersection point polder and water level polder.

As can be seen, the location of the phreatic line in Waternet Creator is not depending on, for example, the duration of the high water or the soil characteristics of the dike.

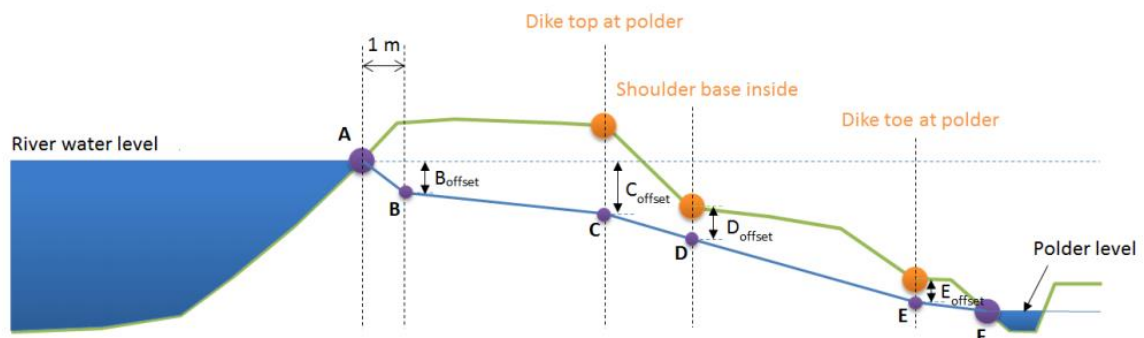


Figure 2-5: Schematisation of the phreatic line plane for clay dikes (Van der Meij, 2020).

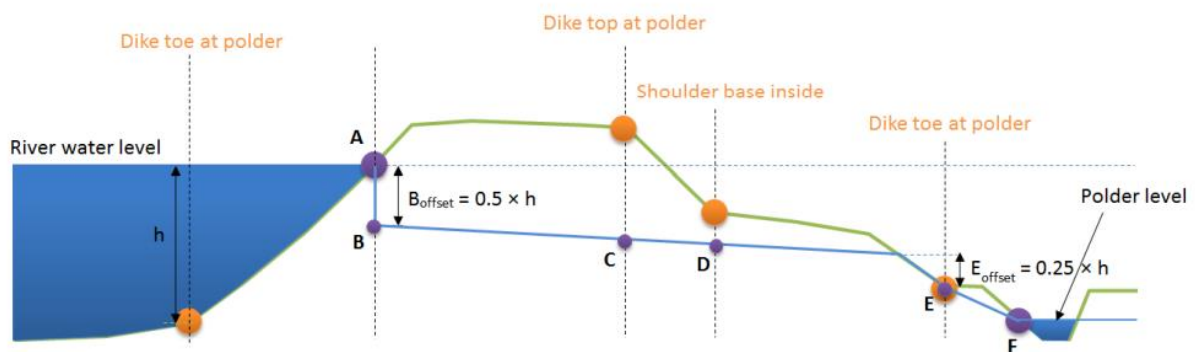


Figure 2-6: Schematisation of the phreatic plane for sand dike on clay/peat underground, without drainage construction (Van der Meij, 2020).

Comparing the TRWD and the Waternet Creator, it can be seen that for clay dikes the TRWD takes into account the thickness of the sub-soil layer. Furthermore, the Waternet Creator depends not on the dike geometry. To conclude, the TRWD estimates the phreatic line always equal or higher than the Waternet Creator.

2.1.2 FACTORS INFLUENCING THE PHREATIC LINE

In this section, the different factors influencing the height of the phreatic line will be discussed and the first research sub-question will be answered. There are already several studies and theses conducted about the phreatic line in general or the effects on (regional) flood defences. For example, de Loor (2018) and Dorst (2019) has researched the effects of precipitation and soil properties on the level of the phreatic line in river dikes. De Raadt, Jaspers Focks, Van Hoven, et al. (2015, p. 511) researched the phreatic line under storm conditions. In addition to this literature, the following reports have been analysed:

- *Technische rapport waterspanningen bij dijken* (Van der Meer et al., 2004)
- *Technisch Rapport Waterkerende Grondconstructies; Geotechnische aspecten van dijken, dammen en boezemkaden* (Kremer et al., 2001)
- *Schematiseringshandleiding macrostabiliteit*. (Ministerie van Infrastructuur en Waterstaat. 2019)

In general, various hydrological processes determine the in- and outflow of water in the dike and therefore determine the height of the phreatic line. For example, these processes are:

- Variations in water level (in- and outside water level, high water waves)
- Precipitation
- Evapotranspiration

2.1.2.1 WATER LEVEL

The largest influence on the position of the phreatic line is the water levels both at the inner and outer side of the dike. The phreatic line describes the progression of the groundwater table between the inner and outer water level (polderlevel). Therefore, these water levels are important as these describe the entry and exit point of the phreatic line in the dike body.

Technisch Rapport Waterspanningen bij dijklichamen (TRWD) state that during a high water wave the pore pressures inside the dike will follow the outer water level with a delay. Even when the water levels are back to daily (lower) level after a period of high water, the pore pressures inside the dike will remain high for a certain time. Especially in clay dikes that have low permeability, the process of returning to the original pore pressures before the high water wave will take some time. This is called the lingering effect of the phreatic line.

The thesis of De Loor (2018) shows that the permeability of the soil layers has a very large impact on the phreatic line during water level changes. It also shows that on a fully homogenous clay dike with rather poor permeability, a high water wave has little or no impact. However, it also shows that clay layers with soil deterioration have a large influence on the phreatic line. This is because of the deterioration of the topsoil layer of the dike, the water can easier infiltrate due to the large hydraulic conductivity of that top layer.

Another principle which influences the 'lingering effect' of the phreatic line is phreatic and elastic water storage in the soil. The phreatic storage occurs when voids in the soil layers become filled with water as the phreatic level is rising. For this principle, the porosity of the soil is thus an important parameter. This is also incorporated in Equation 2. Elastic water storage occurs when pore pressures change but the total soil stresses are constant. As a result, the voids in the soil will be filled by the water change. This storage coefficient is related to the consolidation coefficient. In general, the phreatic storage is several orders larger than the elastic storage (Van der Meer et al., 2004).

Furthermore, the duration of a high water wave differs for the different river deltas. Furthermore, high water is not a maximum static value, this value rises and drops in a certain time frame. A high water wave has a certain duration and shape. In the WAQUA report of Deltares, the different shapes of these high water patterns from the Generator of Rainfall and Discharge Extremes (GRADES) simulations are given. An example of a distribution of shapes at the Rhine in Lobith is given in Figure 2-7. It can be seen that the width of the confidence interval of the GRADE simulation is larger. This shows the uncertainty of the high water pattern. The HR2001 and the WT12011 lines are the hydrographs used in the previous Wettelijke Beoordelingsinstrumentariums for the primary flood defences.

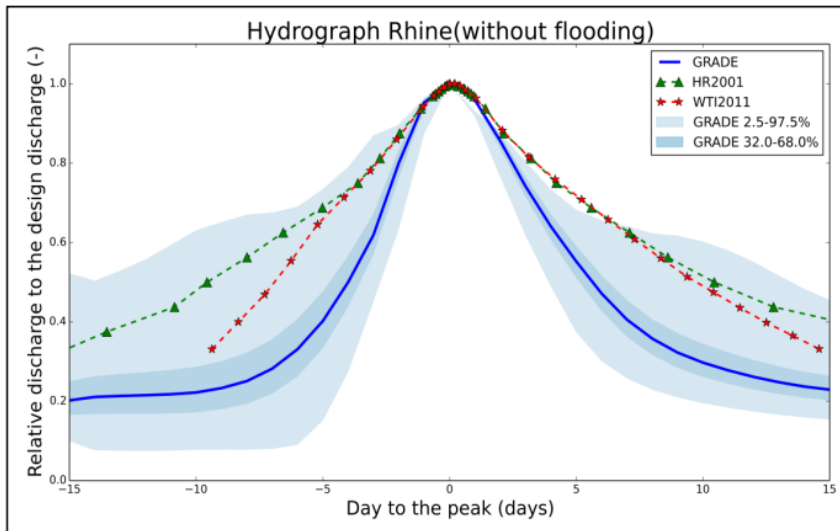


Figure 2-7: Shape of flood wave for the Rhine river at Lobith with the different previous hydrographs HR2001, WTI20011 (Chbab, 2019).

Within the waterboard, research has been conducted by Gerritsen (2019) into the high water patterns of the IJsseldelta. Based on this study a typical discharge and storm dominated high water pattern has been derived. In Figure 2-8 and Figure 2-9, a typical discharge dominated high water wave of Deventer and a storm dominated high water wave of Kampen can be found.

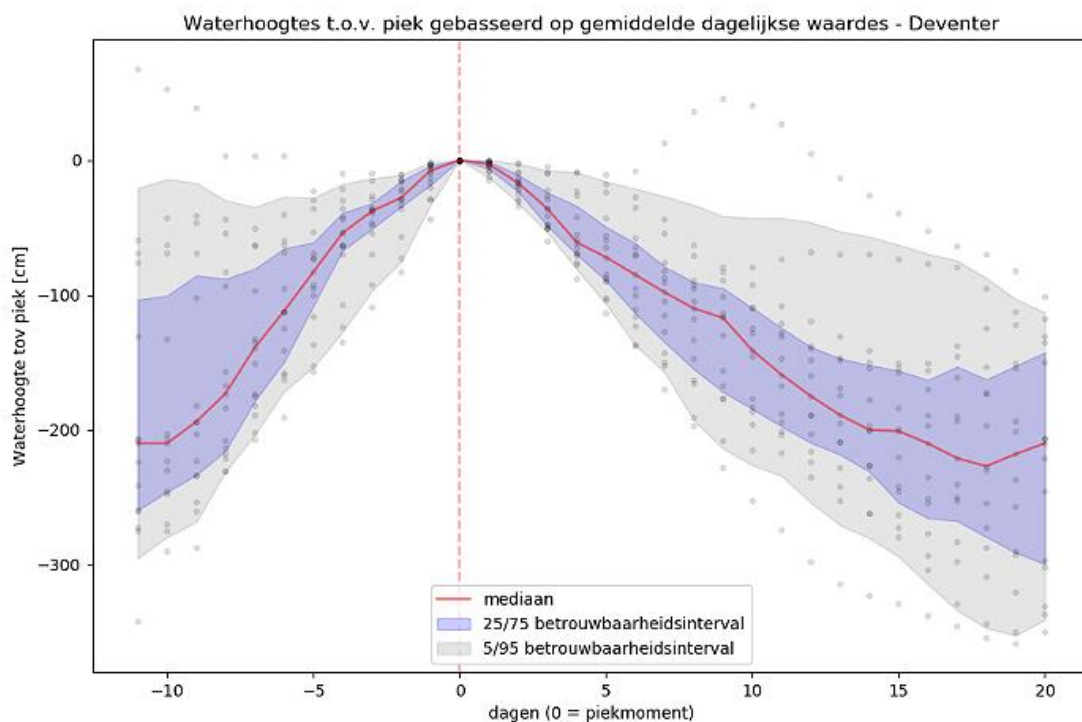


Figure 2-8: Water height normalized to water levels based on average daily measurements – Deventer (Gerritsen, 2019). Dots are measurement points, redline is median, blue shaded 75%-CI and grey shaded 95%-CI.

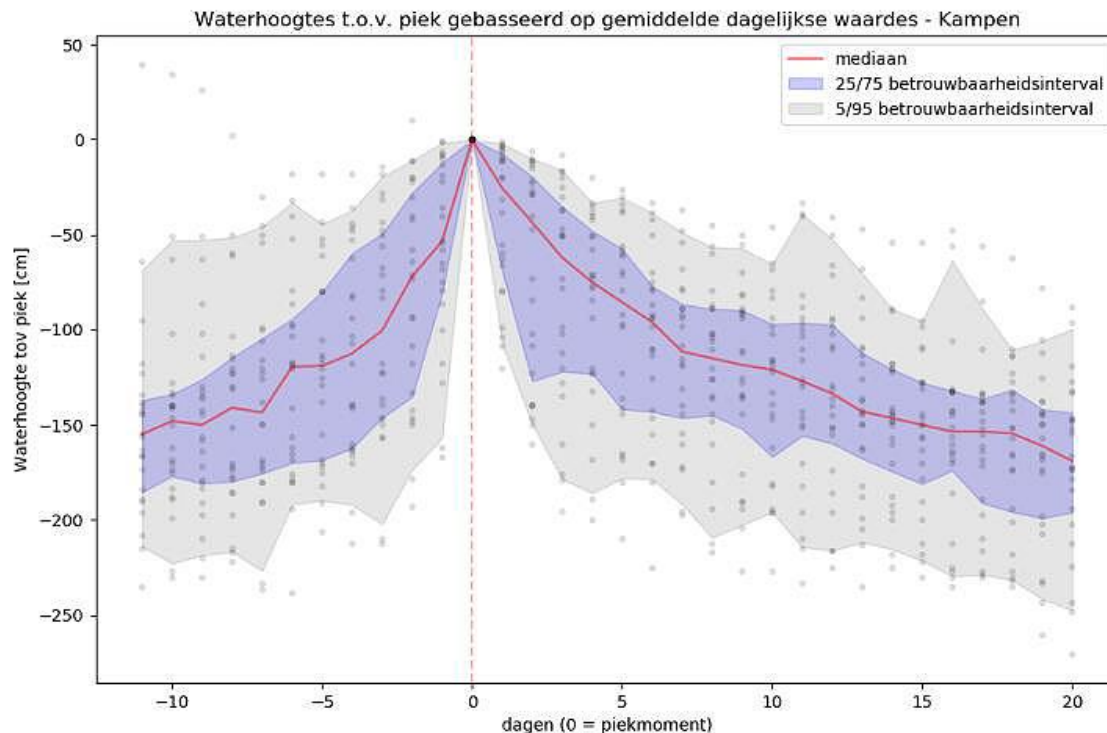


Figure 2-9: Water height normalized to water levels based on average daily measurements – Kampen (Gerritsen, 2019). Dots are measurement points, redline is median, blue shaded 75%-CI and grey shaded 95%-CI.

2.1.2.2 RAINFALL

Another process which influences the location of the phreatic line is precipitation. Not all precipitation is directly infiltrated in the soil. Some of the precipitation will become run-off and will raise the groundwater table. This rising groundwater table first leads to a higher phreatic line at the inner and outer toe of the dike because those locations are close to the outer border of the dike, where the precipitation infiltration takes places.

The composition of the top layers of the dike is an important factor in the influence of precipitation on the phreatic line. For example, a dike with an asphalt layer or another less permeable layer such as a dense clay layer is less influenced by precipitation than a sand or grass cover.

The zone above the phreatic line is called the unsaturated zone. The precipitation will flow through this zone before reaching the phreatic line at which the water table is located. The structure of this unsaturated zone determines mainly the time it takes before the saturated zone is reached. For example, in clay soils, the pores and cracks are finer than a coarse-grained sand layer.

According to the report *Technische Waterspanning bij Dijklichamen*, in case of an extreme rainfall event, the phreatic line will be increased with 0,5 to 1,0 meters between the inner toe and the inner crest line of the dike. Furthermore, an assumption is made that an extreme rainfall event and a high water wave will never simultaneously occur.

As described above the thesis of De Loor (2018) concludes that the soil deterioration of homogenous clay dikes has a significant influence on the response of the phreatic line to a rainfall event. Besides that, a sand dike shows a quicker response to the possible rainfall events. Furthermore, a series of small rainfall events on a dike will contribute more to a rising phreatic line, than a large extreme short rainfall. The thesis of Dorst (2019), confirmed the statements made by De Loor (2018), that precipitation can have a significant impact on the height of the phreatic line depending on the characteristics of the dike and the rainfall event itself.

2.1.2.3 SOIL LAYERS

The soil is divided into two zones by the phreatic line; the saturated and the unsaturated zone. The saturated zone is the part of the soil below the water table, in which relatively all the pores and fractures are saturated with water. Above this zone, there is the unsaturated zone. The water in this unsaturated zone has a pressure head which is less than the atmospheric pressure. This zone is retained by infiltration from precipitation and capillary rise of groundwater.

Normally clay used in dikes is very impermeable, the permeability is in the range from 1 cm to 0.001 cm per day (Billen, 2020). However, in practice, a clay layer is never fully solid mass. Besides that, clay has an an-isotropic soil behaviour due to the orientation of the soil particles. In general, the horizontal conductivity is larger than the vertical conductivity. The ratio of this difference is called the hydraulic conductivity anisotropy ratio and can be calculated as follows:

Equation 3

$$a = \frac{K_v}{K_h}$$

In which:

K_v	=	vertical conductivity (m/day)
K_h	=	horizontal conductivity (m/day)

This deterioration of the clay layer is mainly because of the weathering of the clay layer, the swelling and shrinking of clay particles. Cracks and pores can also be caused by small animals or the roots of vegetation on the dike. (Technisch Adviescommissie voor Waterkeringen, 1996). In the thesis of De Loor (2018), it became clear that the top layer with higher permeability is more affected by the water level changes due to the larger permeability.

Furthermore, Dorts (2019) shows that the soil composition of the cross-section has a large influence on the location of the phreatic line. Especially when permeable layers are present. Variation in the soil composition is very common. A dike is often raised with different soil materials, with materials that are readily available at that moment.

2.2 MACRO STABILITY

Macro instability is one of the direct failure mechanisms. Macro instability occurs when large parts of soil are shearing along a straight or a curve as shown in Figure 2-10. Macro-stability is the resistance against shearing of large sections of the dike slope, along straight or curved slip planes. Instability is a result of a lost equilibrium between the active or driving forces and the passive or resisting forces. (Warmink, 2019, pp. 56–58).

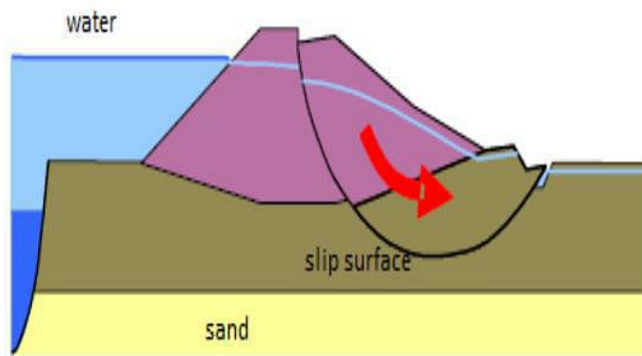


Figure 2-10: Situation of macro instability (Helpdesk Water, n.d.).

If in a sliding plane analysis a circular sliding plane is assumed, then this equilibrium revolves around a moment and an opposing moment. The moment consists of the weight times the arm of the mass body to the left of the centre of the sliding circle. The counteracting moment consists of the weight times the arm of the mass body to the right of the centre and the shear forces along the sliding circle times the radius to the sliding circle ('t Hart et al., 2016), this is shown in Figure 2-11.

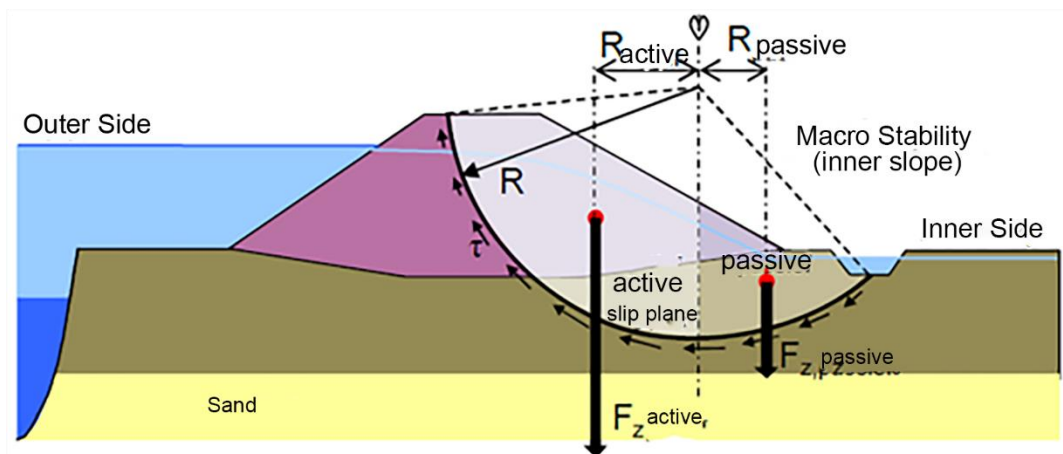


Figure 2-11: Equilibrium analysis of macro stability ('t Hart et al., 2016).

There are several ways the loss of equilibrium between the driving and resisting forces can occur. Since this research is about the macro instability due to high water levels at the outside of the dike, only this mechanism is explained.

Due to the high water levels, the phreatic line in the dike increases. This causes a decrease in the effective stress in the ground, this results in lower shear forces along the slip plane. Besides that, the soil becomes heavier resulting in an increase in the driving forces. Due to both of this, the slope will start to shear along its slip plane (Warmink, 2018).

2.2.1 UPLIFTING

Another phenomenon that could trigger the slope instability of a dike is uplifting. This phenomenon is a result of high water pressures in the sand layer. The high water will lift up the floor of the weak layers behind the dike at the passive zone. This will decrease the passive force ($F_{z,passief}$), this could result in an equilibrium lost

Figure 2-11. As a result, the whole sand layer will move away from the dike along a horizontal slip plane (Warmink, 2018). The active zone will follow, see Figure 2-12.

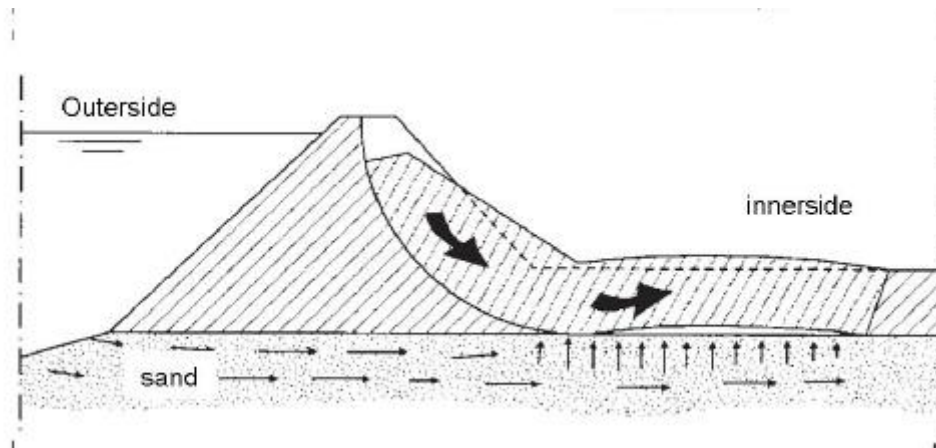


Figure 2-12: The effect of sliding due to uplift on a dike (Warmink, 2018).

2.3 THEORY ON GROUNDWATER FLOW

In this section, the mathematical and theoretical background of the basics behind groundwater flow is discussed. The groundwater flow can be divided into two zones by the phreatic line. In the saturated zone, which is located below the phreatic line, the pore water pressures are negative with respect to the atmospheric pressure. In the unsaturated zone, which is located above the phreatic line, the pore pressure is positive. In this unsaturated zone, water can also be present due to capillary rise and infiltration or precipitation. The location of the phreatic line and the distribution of pore water pressure is controlled by different climatological processes such as evaporation and precipitation. In the case of a zero net surface in and outflow, the pore water pressure profile become in equilibrium at a hydrostatic condition (see Figure 2-13).

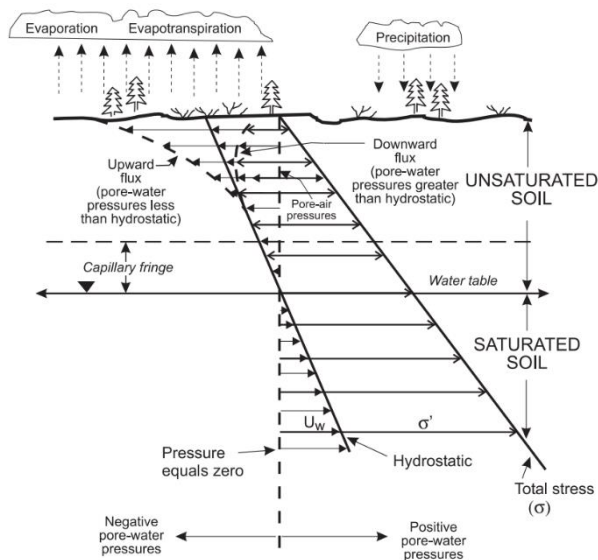


Figure 2-13: Visualisation of the effects of different climatological processes on the pore water pressure (D. G. Fredlund, 2000, p. 984).

2.3.1 SATURATED ZONE

The groundwater flow in the saturated zone is based on two basic principles, Darcy's law and the law of conservation of mass.

2.3.1.1 DARCY'S LAW

Darcy's law can be used for laminar flow through porous aquifers. The flow of water in the saturated zone can thereby be described using Darcy's law (Assaad et al., 2004, pp. 177–184). Darcy (1856) formulated that the rate of water flow through a soil mass is proportional to Darcy's permeability. Darcy's permeability is a property of both the porous soil and the groundwater itself (Equation 4).

Equation 4

$$q = -\frac{k}{\mu} \nabla p$$

In which:

q	=	specific discharge (m/s)
k	=	(intrinsic) permeability (m ²)
μ	=	dynamic viscosity of the fluid (Pa * s)
∇p	=	pressure drop over a given distance (Pa)

For homogenous, incompressible liquid and isotropic permeability, the formula above could be rewritten. The following equations hold under these circumstances:

Equation 5

$$\begin{aligned} q_x &= -K \frac{\partial \phi}{\partial x} \\ q_y &= -K \frac{\partial \phi}{\partial y} \\ q_z &= -K \frac{\partial \phi}{\partial z} \end{aligned}$$

In which:

$q_{x,y,z}$	=	specific discharge in the different axis (m/s)
K	=	hydraulic conductivity (m/s)
ϕ	=	Hydraulic head ($z + u/\rho g$) (m)
x, y, z	=	Height at the location with respect to the reference level (m)
u	=	Water pressure (N/m ²)
ρ	=	density of water (kg/m ³)
g	=	gravitational acceleration (m/s ²)

The intrinsic permeability (k) is part of the proportionality constant in the Darcy formula (Equation 4), this constant relates the discharge and the fluid physical properties (e.g., viscosity), to a pressure gradient applied to the porous media. The hydraulic conductivity (K) is the global physical constant that accounts for how easily the fluid can be moved through the pores in the material. The intrinsic permeability is a part of this. Further research has been done by Muskat (1937) in the physical properties of the fluid and the soil characteristics that determine the intrinsic permeability (Thusyanthan & Madabhushi, 2003). Given the value of the hydraulic conductivity the (intrinsic) permeability can be calculated as follows:

Equation 6

$$k = K \frac{\mu}{\rho g}$$

In which:

k	=	(intrinsic) permeability (m ²)
K	=	hydraulic conductivity (m/s)
μ	=	dynamic viscosity of the fluid (Pa s)
ρ	=	density of the fluid (kg/m ³)
g	=	Acceleration due to gravity (m/s ²)

As can be seen in this formula, there is a relation between the hydraulic conductivity and the intrinsic permeability. For the dike stability assessment, the effect of the viscosity of the fluid can be neglected, since the fluid is constant in this modelling study. Even within one specific soil type, there is a range of (intrinsic) permeabilities possible. This all is depending on grain size, porosity and other characteristics of this soil type. Table 2 illustrates how large the bandwidth of hydraulic conductivity even could be.

Table 2: Range of horizontal hydraulic conductivities per soil type (Billen, 2020).

Soil Type	Minimum Horizontal Hydraulic Conductivity (m/s)	Maximum Horizontal Hydraulic Conductivity (m/s)
Clay	-	$< 10^{-2}$
Sand	10^{-7}	10^{-2}
Gravel	10^{-3}	1

As mentioned above, in Equation 5 isotropic permeability is assumed for all the different directions. In reality, this is often not the case. Usually, the permeability varies significantly between the horizontal and the vertical planes. As a rule of thumb, when no measurements are available, it could be assumed that the vertical permeability to be approximately one-tenth of the horizontal permeability (Fanchi, 2010, p. 67). In this 2D modelling study, the permeability in the depth (z) direction will be neglected.

2.3.1.2 LAW OF CONSERVATION OF MASS

As introduced in Chapter 2.1.2, there is phreatic and elastic storage capacity in different soil types. The principle behind this phenomenon is based on the law of conservation of mass. First of all, in the case of stationary conditions (TRWD), the groundwater flow can be calculated based on the hydraulic conductivity and the geometry of the soil. In this case, the following continuity equation holds (Equation 7):

Equation 7

$$\frac{\partial q_x}{\partial x} + \frac{\partial q_y}{\partial y} + \frac{\partial q_z}{\partial z} = 0$$

For non-stationary groundwater flow, the equation above does not hold. In the case of transient groundwater flow the amount of water changes over time. In order to comply with the law of conservation of mass storage has to occur. The two types of storage are described in Chapter 2.1.2.1.

For elastic storage, the following continuity equation holds:

Equation 8

$$(m_v + n\beta) \frac{\partial u}{\partial t} = \frac{\partial q_x}{\partial x} + \frac{\partial q_y}{\partial y} + \frac{\partial q_z}{\partial z}$$

In which:

m_v	=	compressibility of the soil (m ² /N)
β	=	compressibility of the water (m ² /N)
n	=	effective phreatic porosity (-)

For the phreatic storage, the following continuity equation holds:

Equation 9

$$n \frac{\partial h}{\partial t} + \frac{\partial(hq_x)}{\partial x} + \frac{\partial(hq_y)}{\partial y} = N$$

In which:

h	=	hydraulic head with respect to the base of the topsoil layer (m)
N	=	net infiltration due to precipitation (m/s)
n	=	effective phreatic porosity (-)

When the Darcy's Law and the continuity equation are combined a differential equation describing the groundwater flow flows. This differential equation can be solved by defining the initial- and boundary conditions by a finite element method model.

2.3.2 UNSATURATED ZONE

The groundwater flow in the unsaturated zone has other characteristics than the saturated zone. The theories presented in this subsection are mainly based on the book *Unsaturated Soil Mechanics in Engineering Practice* by Fredlund (2006). In this zone, the water pressure is generally negative, which means that the water pressure is lower than the atmospheric pressure.

Groundwater is recharged by different processes, such as the capillary rise and infiltration of precipitation. In the unsaturated zone, the soil contains air as well as water in its pores. When all voids are filled with water, the soil is fully saturated. The volumetric water content described the ratio of water volume to soil volume. In the equation for the volumetric water content, the porosity of the soil is an important factor.

Equation 10

$$n = \frac{V_V}{V_T}$$

In which:

n	=	porosity (-)
V_V	=	Volume of void space (L)
V_T	=	Total volume of material (L)

When soil is not fully saturated, the permeability of the soil is lower. The unsaturated permeability also depends on the water content of the soil next to the porosity and the distribution of pores (Lind & Lundin, 1990, p. 110). However, this water content is depending on the pore water pressure, which is negative due to the capillary rise. This phenomenon is also called suction or matric potential, the pressure soil exerts on the

surrounding materials to equalise the moisture content in the overall block of soil and is defined as the difference between pore air pressure and pore water pressure.

Due to this, the mechanical properties of the soil changes. The relation between the suction and the soil saturation is described by the so-called Water Retention Curve. The Water Retention Curve gives the capacity of the soil to holds the water in the pores under different stress levels. In literature, several models are describing the shape of the Water Retention Curves. One of the most renowned models is the Van Genuchten Model. In Figure 2-14, an example of typical water retention curves for different types of soil are given.

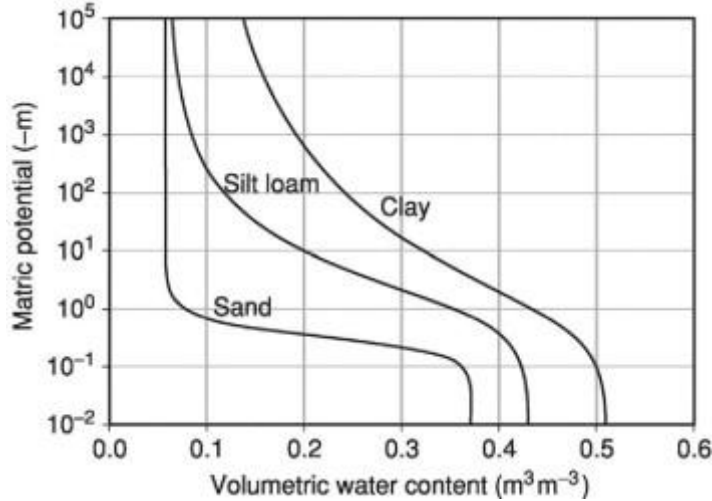


Figure 2-14: Typical Water Retention Curves for the soil of different texture (Tuller & Or, 2005, p. 278).

The Water Retention Curve equation of Van Genuchten (1980) can be found in Equation 11.

Equation 11

$$\theta(\psi) = \theta_r + \frac{\theta_s - \theta_r}{[1 + (g_a |\psi|)^{g_n}]^{1-1/g_n}}$$

In which

- θ_s = Saturated Water content (-)
- θ_r = Residential water content (-)
- g_a = Fitting parameter related to the inverse of the air entry suction (L^{-1})
- $|\psi|$ = Suction pressure (L)
- g_n = Measure of the pore-size distribution (-)

The parameters g_a and g_n can be determined through field tests and are based on soil characteristics. The parameter g_a is related to the air entry suction (AEV) of the soil and the g_n is related to the pore size distribution. The residential water content describes the amount of water that remains in the soil even at high suction. The residential water content is the water content when all the pores are filled with water. In general, all the pores at this saturated condition cannot be completely filled with water because some air bubbles are present.

The permeability of the Van Genuchten model is defined by the following equation:

Equation 12

$$k_r = (S_{eff})^{g_l} \left[1 - \left(1 - (S_{eff})^{\frac{1}{g_c}} \right)^{g_c} \right]^2$$

In which:

S_{eff}	=	Effective degree of saturation (-)
g_c	=	Fitting parameter Van Genuchten (-)
g_l	=	Fitting parameter Van Genuchten (-)

The fitting parameter g_c is related to the measure of the pore-size distribution and can be calculated by $1 - [1/g_n]$. The S_{eff} is the effective degree of saturation, related through Equation 13 (Brooks (1964)).

Equation 13

$$S_{eff} = \frac{\theta - \theta_r}{\theta_s - \theta_r}$$

In which:

S_{eff}	=	Effective degree of saturation (-)
θ	=	Volumetric water content (-)
θ_s	=	Saturated water content (-)
θ_r	=	Residual water content (-)

The material parameters can be determined based on information about the soil type. In the Netherlands, the Staring classification is used. The characteristic values of the Van Genuchten model parameters for the different soil types according to the Staring classification can be found in Chapter 3. Vogel et al. (2000) show that the selection of the curve fitting parameters can significantly affect the results of numerical simulations of transient flow, including the numerical stability and the rate of convergence.

3 PLAXIS MODEL

In this section, the general information on the finite element model Plaxis will be provided. Furthermore, the model set-up for the answering of the last three sub-question will be given. Next, the validation of the model will be evaluated. In the end, a schematic overview of the model set-up will be explained.

3.1 GENERAL INFORMATION

From the theoretical framework, it becomes clear that the height of the phreatic line depends on outside water levels and precipitations. The effects of precipitation on the phreatic line depend on the soil characteristics. Besides the soil characteristics also the geometry of the dike has a larger influence. To test the effects of all these factors is to use a Finite Element Method model for the modelling of the phreatic line. With this type of model, the research questions can be answered.

For this research, the Finite Element Method model Plaxis 2D 2019 with the PlaxFlow module will be used. Within the waterboard, Plaxis is already widely used for different time-dependent applications. For example, the stability of dam walls or for the macro stability assessment of special water structures. According to Van der Meer et al. (2014), the use of Plaxis is recommended for modelling the behaviour of groundwater flow through both saturated as well as the unsaturated soils for individual time steps.

In this numerical model, the different soil layers and subsoils of a dike cross-section will be decomposed into finite elements according to a generated mesh. The number of elements can be determined by the user, which influences the accuracy and calculation times of the model. Since the soil is subjected to changing hydraulic conditions during the simulations, for each finite element hydraulic computations have to be performed. As explained in the Theoretical framework, the basis of the groundwater flow depends on Darcy's Law, the law of conservation of mass and the water retention curve. The in and outflow of the model is based on the boundary conditions such as the difference between water levels, precipitation and seepage.

The PlaxFlow module supports two different types of calculation methods; a steady-state and a transient groundwater flow. The steady-state calculation is not time-dependent and computes an equilibrium situation given the stationary boundary conditions. The transient calculation is time-dependent and can comply with changing boundary conditions over time.

There are several methods to calculate the pore pressures in the unsaturated zone within Plaxis. The different methods are; Van Genuchten, approximate Van Genuchten, Saturated or a user-defined Water Retention Curves. Furthermore, Plaxis has pre-defined soil data for different soil classifications systems. Such as the Staring, Hypres and USDA (Plaxis, 2020).

3.1.1 LIMITATIONS

Outside of the scope of this research is a comparison of the other different possible numerical models that could be used. Only the limitations applicable to the general use of a Finite Element Method model and Plaxis will be discussed in this section.

Finite Element Methods also have their own limitations and disadvantages. Firstly, these methods can be used to solve advanced sophisticated problems and therefore has a lot of different underlying scientific methods and parameter choices. A common mistake that could occur is solving these problems without an understanding of the underlying scientific methods. Secondly, depending on the mesh settings and the time step intervals the Finite Element Method model could have a long computation cost or give numerical instability to the model (Brinkgreve & Swolfs, 2008, p. 5).

Another limitation of the Plaxis is that there is no option to automatically export the phreatic line. A workaround for this limitation is to manually extract some coordinates of the phreatic line and use excel to plot a line through those points. However, this is a lengthy process since it has to be done for all the time steps in a time-dependent simulation.

3.2 MODEL SET-UP

The last 3 research sub-questions all need a starting situation in the calibrated model. Therefore, in this section, the set-up of the starting situation in the Plaxis FEM model will be described. This involves determining or estimating the required input parameters and providing the schematisation of the different soil layers in the dike geometry. Besides that, a mesh has to be chosen and the boundary conditions have to be applied to the model. In the end, the model will be calibrated to fit the daily circumstances as much as possible.

In order to reduce the computation times, the flow only option has been chosen in Plaxis. This method treats the soil as a rigid structure and only calculates the (ground)water flow through it. The effect of soil deformation is neglected in this research. The consequences of this choice is explained in the discussion.

3.2.1 DIKE GEOMETRY

In this research different types of dike bodies will be examined. These correspond to the standard situations described in the TRWD and the Waternet Creator, and common dike geometries in the area of the waterboard. These are a homogenous clay dike and a homogenous sand dike on an incompressible sandy aquifer as explained in the scope. The surface geometry of the dike can be found in Figure 3-1.

Dike Geometry

Slope	1:3
Crest height	4 meter
Crest width	4 meter
Base width	28 meter

Sub-Soil Layers

1. 4 meter clay layer, and 10-meter sand layer (Pleistocene)
2. 1 meter clay layer, and 13 meter sand layer (Pleistocene)

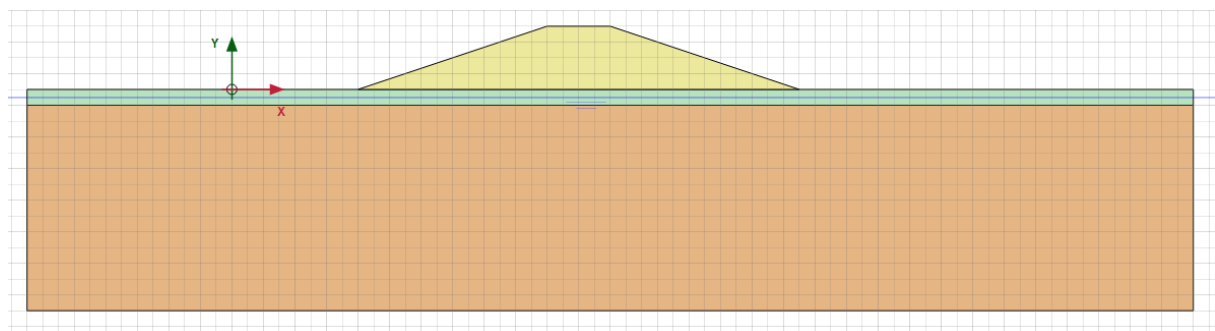


Figure 3-1: Sand Dike (yellow) with 1 meter clay (green) and 13 meter sand layer (orange) (square = 1 by 1 meter).

Hydraulic Conditions

WBN	3.2 meter
-----	-----------

The geometry and hydraulic conditions are made with the agreement of experts within the waterboard. In Appendix A, an overview of all the surface geometries is provided.

Mesh Settings

From the dike geometry, the mesh is constructed. In Plaxis this mesh refinement is set on 'fine'. However, some refinements are made. In the clay sub-soil below the dike, the coarseness factor has been decreased, to create finer mesh locally. This is an important area for the bulge of the phreatic line under daily circumstances. Besides that, the model is not numerical stable in situations with a 1 meter clay layer. The clay dikes got a coarseness factor 0.2.

The 'fine' refinement has been chosen as start position as proposed in the Plaxis tutorials and manuals. Since there are no strange artefacts or other strange situations after modelling. The 'fine' refinement option is a good suitable option. In Figure 3-2, the generated mesh can be seen.

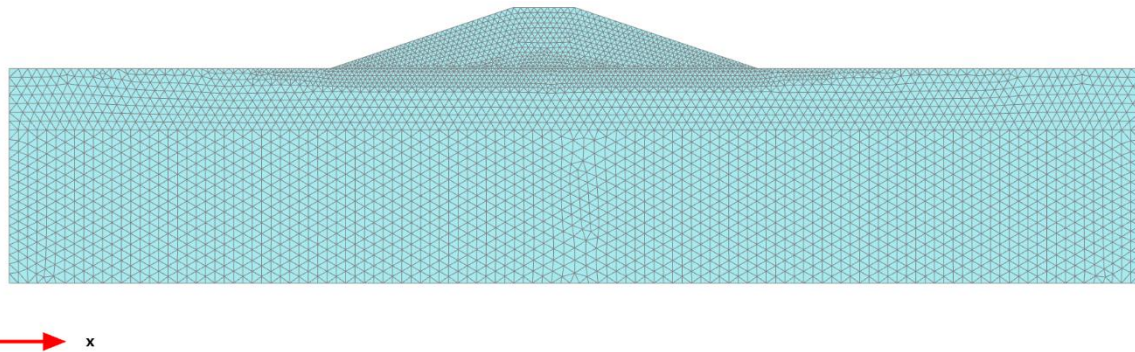


Figure 3-2: Generated Mesh Clay Dike with 4 meter clay sub-soil.

3.2.2 SOIL PARAMETERS

This research covers two different dike types; a homogenous sand dike and a homogenous clay dike. In this section, the soil parameters for the different dike types will be provided and explained. For this research, no soil samples are available and therefore we have to rely on literature and general classification systems. In Table 3, an overview of the different soil types per dike type is given.

Table 3 Soils per layer for different dike types.

Dike Type	Sub-soil	Dike Core
Homogenous Clay Dike	Clay	Clay
Homogenous Sand Dike	Clay	Sand

For simplicity, for both the sub-soil and the dike core, one type of clay material will be specified. In Plaxis, for all the soil layers the soil properties should be specified. However, since the flow only option has been chosen in Plaxis, only the soil parameters affecting the groundwater flow will be used in the calculations. These parameters are the model parameters for the Water Retention Curve and the flow parameters which are the hydraulic conductivity, hydraulic anisotropy, volumetric specific storage.

3.2.2.1 WATER RETENTION CURVES

For the water retention curve, the Van Genuchten model will be used. In Table 4, the Van Genuchten parameters are provided for the clay and sand layer. These parameters are based on the Staring classification. For the clay layer, it is assumed that it is a topsoil light clay (B10). The sand layer is assumed that it is loamy sand (B2) (Wösten et al., 2001). To make the model more stable during the calibration to the starting situation of the model, the Van Genuchten fitting parameter related to the inverse of the air entry suction (g_a) is a little bit altered. During the calibration to get the starting situation of the model, this factor has been made factor 100 lower compared to the literature. This value has no significant influence on the height of the phreatic line,

as can be seen in the figure below (Figure 3-3). The adjustment, however, makes the calculation faster/shorter, and more stable. After starting the situation, for the high water wave analysis and the sensitivity analysis, the original value has been restored.

Table 4: Van Genuchten Fitting Parameters (* = Original value) (Vogel et al., 2000).

Van Genuchten Parameters	Clay (B10)	Sand (B2)
Residual degree of saturation	0,01	0,02
Saturated degree of saturation	0,43	0,42
Measure of the pore-sized distribution (g_n)	1,20	1,491
Inverse of the air entry suction (g_a)	0,0064 (0,64*)	0,0276
Fitting Parameter (g_l)	-3,884	-1,060

For the 10 or 13 meter thick sand aquifer, below the clay layer, the saturated option has been chosen in Plaxis. The assumption has been made that this aquifer is always fully saturated and below the phreatic line.

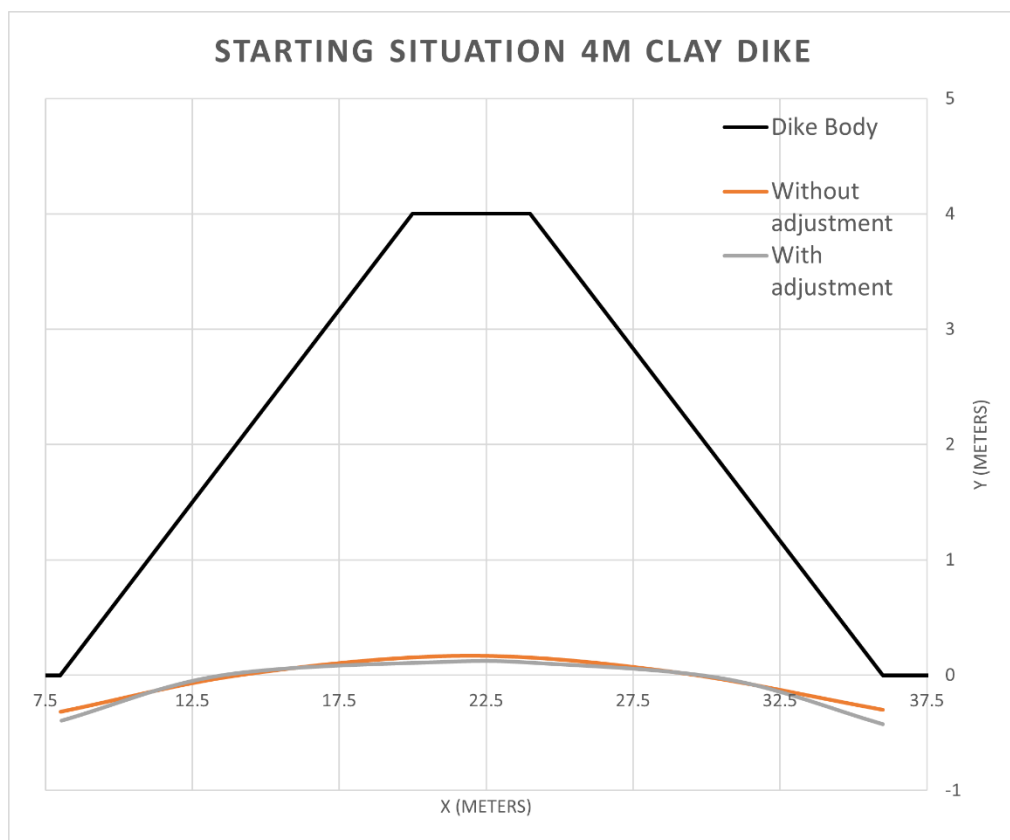


Figure 3-3: Phreatic line after 90 years of precipitation with and without altered Van Genuchten Parameter.

3.2.2.2 HYDRAULIC CONDUCTIVITY

The hydraulic conductivity of the soil is one of the most important parameters. It has an x- and y-direction component. In this way, an-isotropic soil behaviour can be modelled. Due to the nature of the soil, the hydraulic conductivity can vary greatly in both directions. Because there are no soil samples available, the hydraulic conductivity is based on the Staring classification and expert opinions.

Clay

According to the research of van den Akker (2001), it was found that the Staring classification even

underestimates the hydraulic conductivity of clay soils. Oosterbaan & Nijland (1994) show that the range of hydraulic conductivity is even greater. The maximum value is 2 meters per day for well-structured clay, and the lowest value is less than 0,002 meters per day for dense clay.

Table 5: Hydraulic Conductivity Clay.

Horizontal Hydraulic Conductivity (m/day)		Staring (Wösten et al., 2001)	Experts (Dijkteam Zwolle, 2020)	Oosterbaan & Nijland (1994)
Clay	<i>Min</i>	0,007	0,01	< 0,002
	<i>Max</i>	0,14	0,03	2

As can be seen in Table 5, the difference is quite larger. However, for this research, the maximum value for the hydraulic conductivity provided by the experts of Dijkteam Zwolle will be used. This value is in range of the Staring classification and the research provided by Oosterbaan and Nijland (1994).

Hydraulic anisotropy

In the report, *Technisch Rapport Waterspanningen bij Dijklichamen* (Van der Meer et al., 2004), an anisotropy ratio for clay is given of 0,33. In the thesis of De Loor (2018) and Dorst (2019) also an anisotropy ratio of 0,33 is used. However, for the soil deterioration in the top clay layer of the dike, an even higher ratio of 2 is used. This is because of mainly vertical cracks due to plants (de Loor, 2018).

Sand

Sand has a relatively high hydraulic conductivity when compared to clay. The sand types defined in the Staring classification are not 100% sandy and do include some loam, which could cause a lower hydraulic conductivity.

Table 6: Hydraulic Conductivity Sand.

Hydraulic Conductivity (m/day)		Staring (Wösten et al., 2001)	Experts (Dijkteam Zwolle, 2020)	Oosterbaan & Nijland (1994)	Burger & Belitz (1997, p. 1520)
Sand	<i>Min</i>	0,099	1,88	1	1,06
	<i>Max</i>	1,07	2,93	50	4,15

In Table 6, it can be seen that the hydraulic conductivity value of the experts of Dijkteam Zwolle are within line with the values found in literature, and therefore a good starting point.

Hydraulic anisotropy

According to the *Technisch Rapport Waterspanningen bij Dijklichamen* (Van der Meer et al., 2004) sand has an anisotropy of 0,66. Sand compared to clay is a very isotropic material. However, Burger and Belitz (1997, p. 1520) show that the anisotropy ratio of sand can vary between 0,92 up to 2,69. Because in this research an 100% sandy soil will be assumed a hydraulic anisotropy of 1 will be assumed for sand.

Sand Aquifer

To determine the hydraulic conductivity of the sand aquifer the Bortel formation has been used. In the area of the waterboard, another research has been done into the hydraulic conductivity of a sand aquifer. Based on the grains size distribution of soil samples the hydraulic conductivity has been determined (Table 7).

Furthermore, the hydraulic anisotropy has been set to 1. This is based on the fact that the soil already has a very high hydraulic conductivity and differentiating between horizontal and vertical hydraulic conductivity does not have any significant influence.

Table 7: Hydraulic Conductivity Sand Aquifer.

Hydraulic Conductivity (m/day)		Experts (Dijkteam Zwolle, 2020)
Sand Aquifer	Min	24
	Max	24

3.2.2.3 Volumetric Specific Storage

As described in Chapter 2.3, for non-stationary groundwater flow to comply with the law of conservation of mass-specific storage has to occur. There are two types of storage as described in Chapter 2.1.2.1., elastic and phreatic storage. The elastic storage occurs when water pore pressures change but the total soil stresses are constant. As a result, the voids in the soil will be filled by the water change. The volumetric specific storage parameter (S_s) specifies this type of storage, it is the volume of water that will be released when the head drops (Plaxis, 2020)

According to the *Technisch Rapport Waterspanningen bij Dijklichamen* (Van der Meer et al., 2004), the volumetric specific storage in the Netherlands varies between the 10^{-3} and $3 \cdot 10^{-2}$ for sandy soils. The volumetric specific storage cannot be deduced from soil samples. Therefore, it is based on expert judgments. The volumetric specific storages specified in Table 8 will be used for the different soil layers.

Table 8: Volumetric Specific Storage overview.

Soil Layers	Volumetric Specific Storage (1/m)
Clay	0,10
Sand	0,01
Sand Aquifer	0,03

3.2.2.4 OTHER SOIL PROPERTIES

In Plaxis also the soil properties regarding the stiffness and the strength parameters according to the chosen soil model have to be specified. Although these parameters are of no importance for the groundwater flow calculations. These data are mainly based on the following two books; *Unsaturated Soil Mechanics in Engineering Practice* by Fredlund (2006) and *Principles of Geotechnical Engineering* by Das & Sobhan (2016).

Table 9: Other Soil Properties for the different soil layers.

Soil Layer	Clay	Sand	Sand Aquifer
Material Model	Mohr-Coulomb	Mohr-Coulomb	Mohr-Coulomb
Drainage type	Undrained (A)	Drained	Drained
Unsaturated Weight (kN/m ³)	13,0	14,0	18,0
Saturated Weight (kN/m ³)	18,0	19,0	20,0
Effective Young's Modulus (kN/m ²)	2,67	26,67	10000
Effective Poisson's ratio (-)	0,30	0,30	0,33
Effective Cohesion (kN/m ³)	5,0	5,0	0

As the soil material model, the Mohr-Coulomb model has been selected. However, it is of no importance for the groundwater flow calculations since the flow the only option have been chosen. The elastic stiffness parameters (ν' and E') are also not important for the flow the only option. However, these parameters determine indirectly the volumetric specific storage of the soil layer. Therefore, these values are altered to get exactly the volumetric specific storage as described in the previous section.

3.2.3 PRECIPITATION & EVAPORATION DATA

Precipitation and evaporation have an influence on the location and the height of the phreatic line. Therefore, these factors should not be neglected as boundary conditions. Since no exact location of the dike is defined, the daily precipitation minus the evaporation data of the Bilt will be used for modelling. This data is provided by the Dutch Meteorological Institute (KNMI). The rainfall series of the STOWA report (Beersma et al., 2019) is used to model several specific rainfall events during for example a high water wave. In Table 10, the 8-days precipitation volumes are presented. These volumes will be used to simulate rainfall during for example a high water peak. In Appendix B all the exact rainfall time series are available.

In Plaxis precipitation is implemented as infiltration in (m/day) to all the top boundaries of the model. These are the fore- and hinterland, the slopes, and the crest of the dike. Furthermore, a maximum and minimum pore pressure head, relative to the evaluation of the boundaries should be specified ($\psi_{max/min}$). These two parameters need to be specified to simulate ponding and runoff at a specified depth in the dike body. For these parameters, the default values provided by Plaxis are used ($\psi_{max} = -1,0\text{m}$ and $\psi_{min} = 0,03\text{m}$). Only for the sand dikes, the precipitation on the slope had to be removed. Otherwise, some strange ponding occurs on the slopes of the dike due to the relatively high hydraulic conductivity of the sand layer compared to the sub-soil. This is strange, as you might expect that ponding is not a problem on a sand dike due to the high hydraulic conductivity. The consequences of this chose is explained in the discussion.

Table 10: 8-days precipitation volumes (mm) for the different return periods (Beersma et al., 2019, pp. 15–22).

Return Period (Year)	1	5	10	50	100	200	500	1000
Year	79,4	105,1	116,1	141,5	152,3	163,2	177,5	188,3
Winter Period	65,6	89,4	99,1	120,5	129,3	137,7	148,5	156,4

Besides the total volume, a rainfall event has a certain pattern. The STOWA report describes 8 different rainfall patterns. For simplicity for this research, an 8-days uniform rainfall pattern will be used during a high water wave.

3.2.4 WATER LEVELS

In the Plaxis model, the outside and the inner side water levels have to be applied for the starting situation. In all the simulations, it has been assumed that this dike is part of the upper river area in the Netherlands. Therefore, the influence of the sea tide is not noticeable in the calculations. Besides that, the river is mainly discharged dominated. Although in the area of the waterboard near the IJsselmeer, the rivers are also storm dominated.

Under daily circumstances, the inside water level is maintained on 0,5 meter below the surface level. This water level is maintained by pumping and drainage, and therefore has been made constant in the model for the fore- and hinterland. Furthermore, the head of the sandy aquifer is set on the groundwater level under daily circumstances. In case of a high water wave, the head of the sandy aquifer is set to the outside water level in the foreland of the model. This simplification is for thin clay sub-soil layers not conservative, as the effect of a rising head in the sandy aquifer on the top-soil is larger than for a thick clay sub-soil layer.

3.2.5 CALIBRATION

Before different water levels and or precipitation events could be applied to the model. The model should first be calibrated and be warmed up to get the right starting situation of the model for answering the last 3 research sub-questions. With all the settings described above, the starting situation of the model can be constructed.

Without any warm-up period, the dike has the water content as if it just has been constructed. The saturation degree of the soil without any warm-up period is less than 10%. Furthermore, the head for every location is located at polder level (0,5 meters). This is not realistic, because due to daily precipitation there should be a groundwater bulge (phreatic rise) inside the dike due to recharge from precipitation.

Therefore, several years of actual daily precipitation and evaporation data is applied until an equilibrium state has been reached. Another option could be a higher artificial precipitation per day, which could lead to a shorter warm-up period. The effect and consequences of this option will be further explained in the discussion section. For clay dikes, the steady-state is reached after 60 years of annual precipitation data. For sand dikes, this is already reached within 30 years. Due to the relatively high hydraulic conductivity of sand. The resulting starting positions for the four different dike types are shown in the figures below. The colours indicates the effective soil saturation (Red > 90%, Yellow ≈ 60%, Blue < 40%).

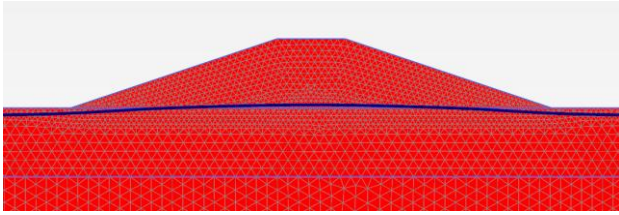


Figure 3-4: Starting situation of the phreatic line (dark blue line) clay dike with 4 meter clay colours indicates the effective saturation.

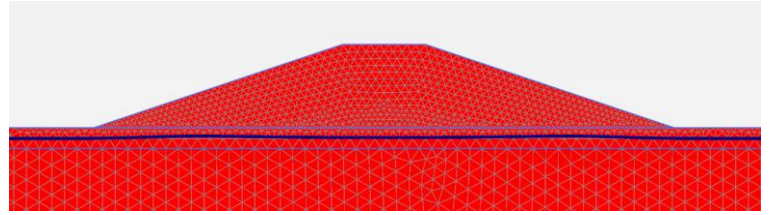


Figure 3-5: Starting situation of the phreatic line (dark blue line) 1 meter clay dike with 1 meter clay colours indicates the effective saturation.

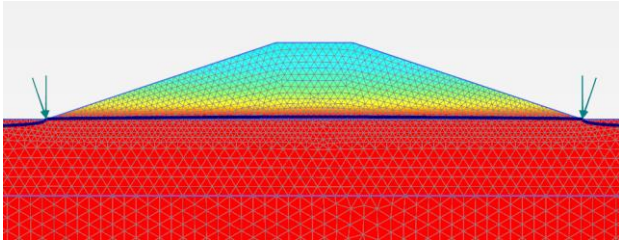


Figure 3-6: Starting situation of the phreatic line (dark blue line) sand dike with 4 meter clay colours indicates the effective saturation.

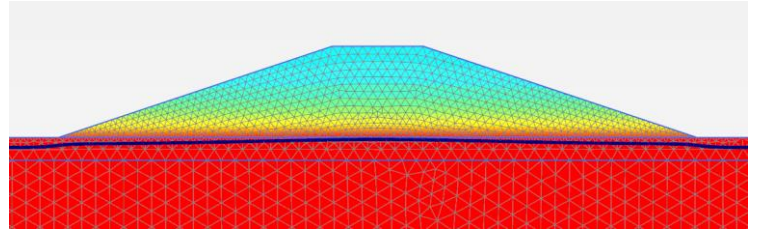


Figure 3-7: Starting situation of the phreatic line (dark blue line) sand dike with 1 meter clay colours indicates the effective saturation.

The warm-up period depends not on the composition of the sub-soil, since the sandy aquifer is assumed to always be saturated zone and the stationary groundwater level is set on 0.5 meters below surface level.

3.3 VALIDATION & RELIABILITY

Verification and validation are the essential procedures required to assess the accuracy and credibility of the numerical Plaxis model. To provide reliable grounds to deviate from the estimated schematisation of the phreatic line, validation of the Plaxis model should be done. Normally, a numerical model will be checked against an analytical model. The strength of analytical models is that the calculation is transparent and thereby provides a method to validate the numerical model. In the TRWD, an analytical model is provided for non-steady groundwater flows. This analytical model is based on the formula of Dupuit and Hooghoudt (Equation 14).

Equation 14

$$h = \sqrt{-\frac{N}{K}x^2 + \left(\frac{\phi_2^2 - \phi_1^2}{L} + \frac{NL}{K}\right)x + \phi_1^2}$$

in which:

h = height of the phreatic surface with reference to the impermeable boundary (m)

N = precipitation (m/s)

K = permeability (m/s)

X = point inside the dike (m)

$\phi_{1,2}$ = Boundary conditions at the sides of the dike, concerning the 'impermeable boundary' (m)

L = width of the dike (m)

However, this analytical formula of Dupuit is not suitable to evaluate the phreatic bulge under daily circumstances in a dike. The formula assumed a well-permeable layer that is bounded at the bottom by an impermeable layer and where no cover is present at the top (unconfined aquifer). However, this is not the case in this modelling study. In this model, the unconfined aquifer is bounded at the top with a relatively poor permeable layer (respectively 4 or 1 meter of clay).

Since there is not a suitable analytical model available to validate this type of dike models. The Plaxis model will be validated based on expert judgement and logical reasoning. According to the formula of Dupuit, the phreatic bulge will become smaller when the permeability increases. In the following graph, the phreatic line progression in the clay dike with 4 meter clay sub-soil for the year 2019 can be seen. The height is maximum of the phreatic bulge measured from the stationary water condition of -0.5 meter below the dike surface.

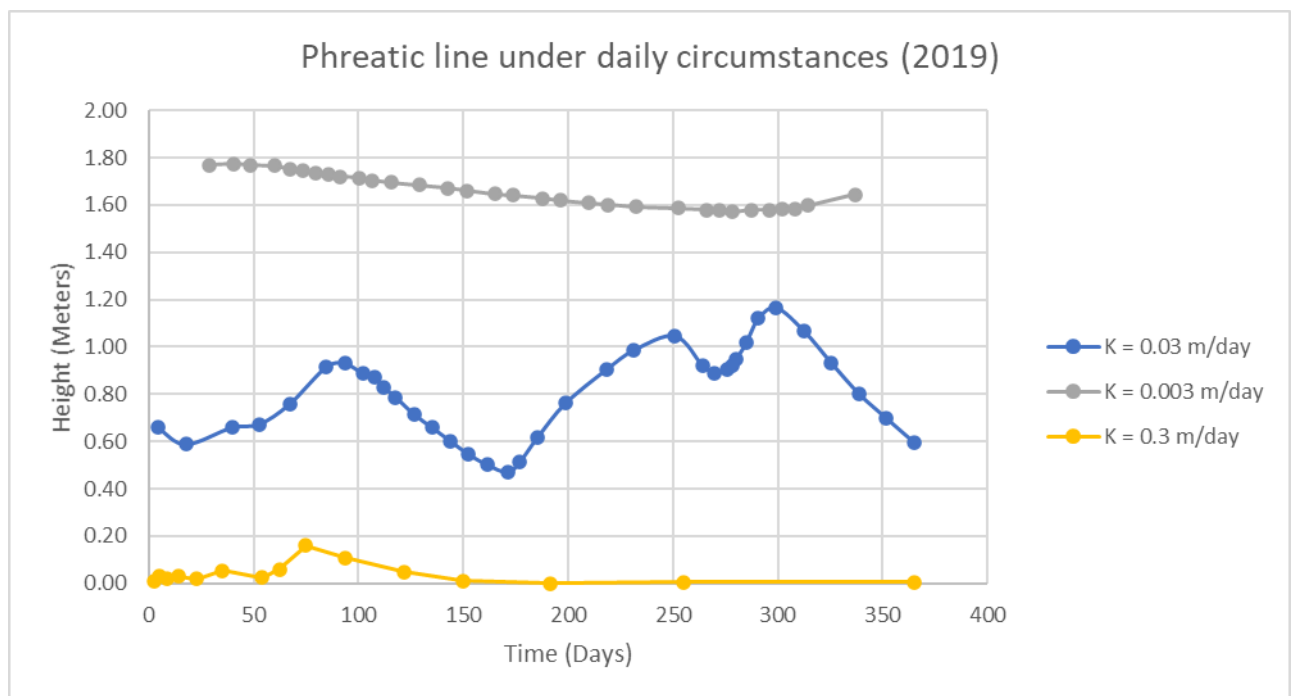


Figure 3-8: Effect of hydraulic conductivity (K) under daily circumstances.

As can be seen in the graph, indeed the lower the hydraulic conductivity of the soil layer the higher the phreatic line under daily circumstances. The same effect is visible when increasing the width of the clay sub-soil, it will cost more time for precipitation to infiltrate to the saturated sandy aquifer. This resulted also in a higher phreatic bulge under daily circumstances as can be seen in Figure 3-9. One note, the data points for the end of the time series of the 6 meter sub-soil variant were not suitable for the analysis, as the results contain unphysical model behaviour such as double phreatic lines in the dike.

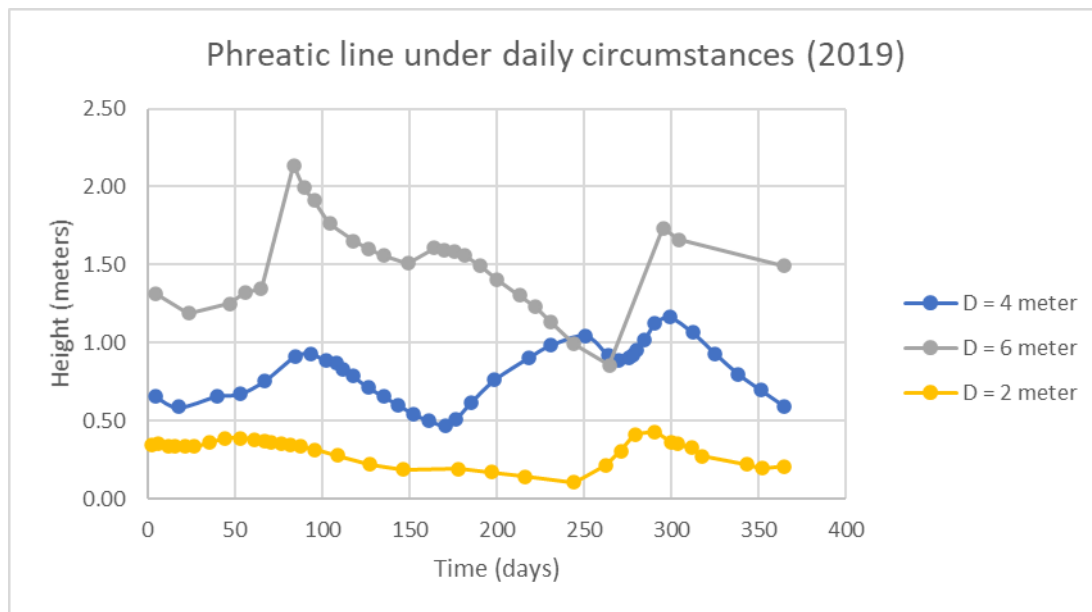


Figure 3-9: Effect of the width of clay sub-soil (D) below the dike under daily circumstances.

Based on both the simulations results it can be said that the Plaxis model behaves accordingly to the analytical formula of Dupuit. This gives a reliable starting position for further simulations to answer the research questions.

3.4 SCHEMATIC OVERVIEW OF THE MODEL

In Figure 3-10, the structure of the model related to the different research question is given. First, the initial model will be calibrated for 30 years (sand dike) or 60 years (clay dike). After which, the daily circumstances will be modelled to answer the 2 and 4 research sub-question. The discharge and storm dominated high water waves are modelled after a start water level as steady-state. The normative water level as a function of time to answer the third research question will start at the peak during the daily circumstances.

More information on the methodology of the last three research sub-questions can be found in the next chapter.

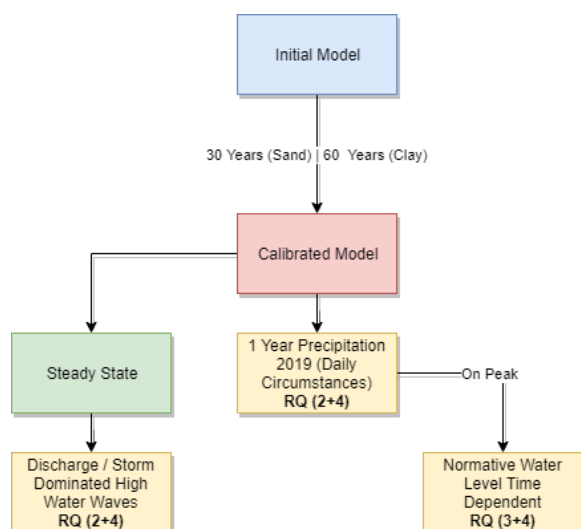


Figure 3-10 Overview of the model setup in relation to the research sub-questions (RQ).

4 METHODOLOGY

Central in this research is the use of a numerical model to simulate the groundwater flow. In the previous chapter, the model set-up for the starting situations has been explained. In this chapter, the methodology for the last 3 research questions will be given. The limitations of the methodology will be discussed in the discussion chapter.

4.1 PHREATIC LINE UNDER DIFFERENT HYDRAULIC CONDITIONS

This section is linked to the second research sub-question; *What are the effects of different hydraulic conditions on the phreatic line?* For this question, different hydraulic realistic situations have to be defined. As explained in the theoretical framework, the phreatic line is mainly depending on the water levels and the precipitation. In Table 11, the 5 different realistic scenarios used in this study can be found. To get insight in the effect of both the rainfall and the high water wave independently, the rainfall events are added in separate scenarios.

Table 11: Overview of different scenarios with different hydraulic conditions.

Scenario	High Water Wave	Rainfall Event
#1	-	2019
#2	Storm High Water Wave	-
#3	Discharge High Water Wave	-
#4	Storm High Water Wave	1/500 8 days
#5	Discharge High Water Wave	1/500 8 days

In the first scenario, the phreatic line under daily circumstances will be simulated without a high water wave over a period of a year. This scenario will provide insight into the progression of the phreatic line bulge over a year, and to see the effect of seasonal weather differences. In the second and third scenario, the effect of two typical different high water waves will be simulated. In the last two scenarios, an 8 day rainfall event is added just before the high water wave peak. This to see the effects of a short severe rainfall event. The results of the modelling scenarios will be compared to the phreatic line estimated schematisations provided in the TRWD and the WC.

4.1.1 WATER LEVEL SCENARIOS

The duration of a high water wave differs for the different river deltas. The peak of the high water wave has been assumed to be the normative water level (WBN) because this research focuses on a fictive location. In this study, we distinguish two types of high water waves: discharge dominated, and storm dominated.

For the discharge dominated high water wave, the high water wave analysis data from Deventer by Gerritsen (2019) has been used. For this location 15 high water waves are available in the period from 1 January 1976 until 7 Augustus 2018. Therefore, the 75%-confidence interval bandwidth is smaller compared to other discharge dominated measurement locations where less high water waves are available. Based on the water height normalized to water levels based on average daily measurements at Deventer, a period of 10 days before the peak till 10 days after the peak is used to model the discharge dominated high water wave in Plaxis.

For the storm dominated scenario, the high water wave analysis data from Kampen has been used (Gerritsen, 2019). For this measurement location 24 high water waves are available in the period from 4 January 1813 until 15 Augustus of 2018. In the data, there are peaks with and without the Afsluitdijk. One of the characteristics of

a storm dominated high water peak is that it is shorter and steeper than a discharge dominated high water wave. The average duration of a high water wave is 2 days.

Based on the characteristics of both the storm and discharge dominated high water level patterns from the high water wave analysis of Gerritsen (2019), both the average high water waves are modelled in Plaxis. In the high water wave analysis, the water height is normalized to the water levels based on average daily measurements based on the peak water level. In this research, the peak has been set on the normative water level (WBN) of 3,2 meter. This results in the following high water wave patterns which will be used in Plaxis (Figure 4-1).

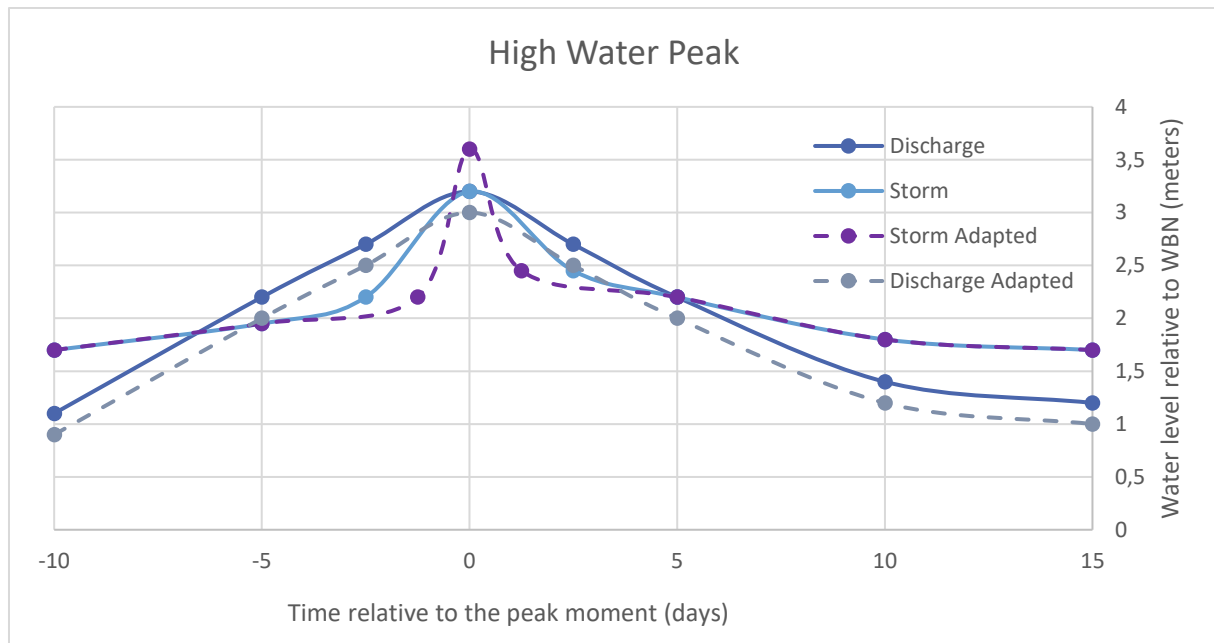


Figure 4-1: The discharge and storm high water waves normalised on the WBN water level.

Because in both the high water wave analysis of Deventer and Kampen, the water height is normalized to the water levels based on average daily measurements based on the peak water level. For both locations, the peak water level is different in height. This leads underestimation of the discharge dominated high water peak compared to the discharge high water wave, because the extremely short duration effect of a storm dominated high water wave becomes less distinct compared to the longer duration of a discharge high water wave. To compensate for this effect, both the peaks are slightly adapted.

The time series of both high water waves are imported in Plaxis. Since this data contains only one high water wave, and it is unknown what the water level just before the beginning of this wave was. To deal with this uncertainty a steady-state with an outside water level of respectively 0.9 meters (discharge dominated) and 1.7 meters (storm dominated) are modelled before the start of the high water wave time series. This is a very conservative assumption because it is very likely that the water level before this wave was shorter than a steady-state situation.

Furthermore, these high water waves times series are based on the average historical measured water levels. To see the effects of extreme events, the upper bound of the 75% confidence interval will also be used. In Figure 4-1, the upper bound of the 75% confidence interval for both the discharge dominated and the storm dominated can be seen. The more accurate 95% confidence interval has not been used, because of the modelling choice to start with a steady state situation before the high water wave.

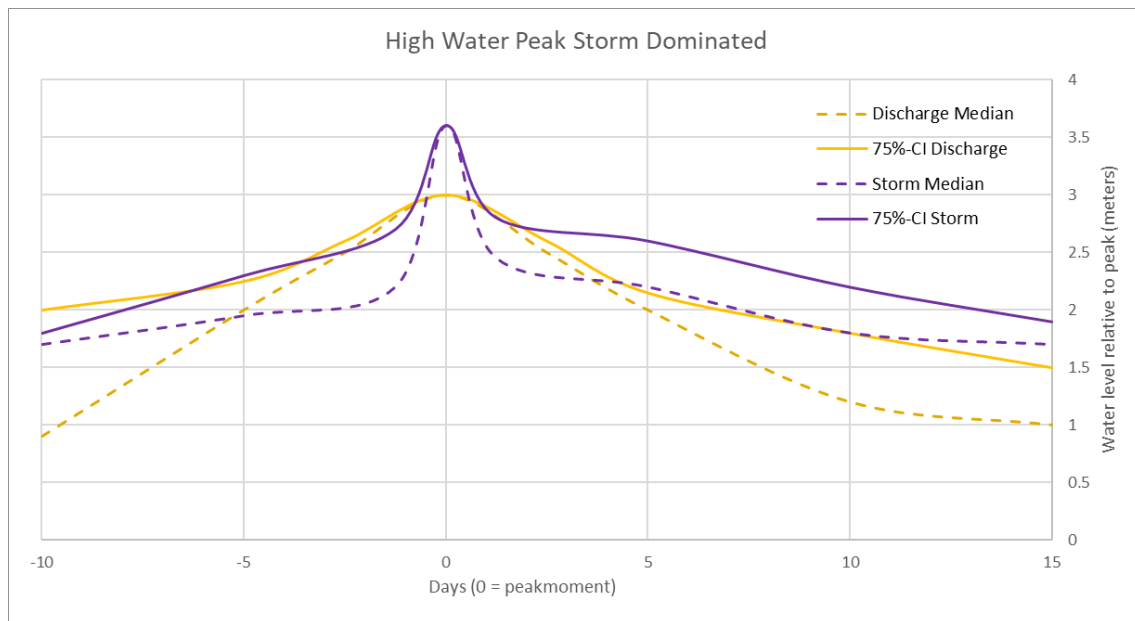


Figure 4-2: The upper bound of the 75% Confidence Interval (solid lines) of the discharge and storm dominated high water waves.

4.1.2 RAINFALL SCENARIOS

As explained in Chapter 3.2.3, the KNMI and STOWA rainfall data will be used. For the first scenario, the daily precipitation data of de Bilt in 2019 will be used. According to the KNMI (2019), this year has one of the wettest winters, and an autumn with a lot of rainfall. This time series has been chosen to see what the effects are of these weather extremes. For the last two scenarios, the 1/500 years 8 days rainfall event will be used to simulate a short severe winter rainfall event. The end of the 8 days rainfall event will coincide with the peak of the high water wave. This to see the effect of a short rainfall event in coincides with a high water peak and to check whether the phreatic line will raise even more because of this rainfall event. However, it is quite hard to determine when exactly the rainwater will reach and influence the phreatic line.

4.1.3 SCHEMATISATION OF THE PHREATIC LINE

In this section, the estimated schematisation of the phreatic line according to the TRWD and the WC is provided. Furthermore, the schematisation of the phreatic line in Plaxis will be explained.

To compare the different hydraulic conditions with the prescribed schematisation of the phreatic line, the prescribed schematic estimation of the phreatic line needs to be determined. In Chapter 2, it is explained that the phreatic line estimation of the TRWD and the WC only depends on the geometry, normative water level and the soil composition of the dike. In Figure 4-3, the phreatic line schematisation based on the WBN of 3.2 for the 4 different dike situations can be found.

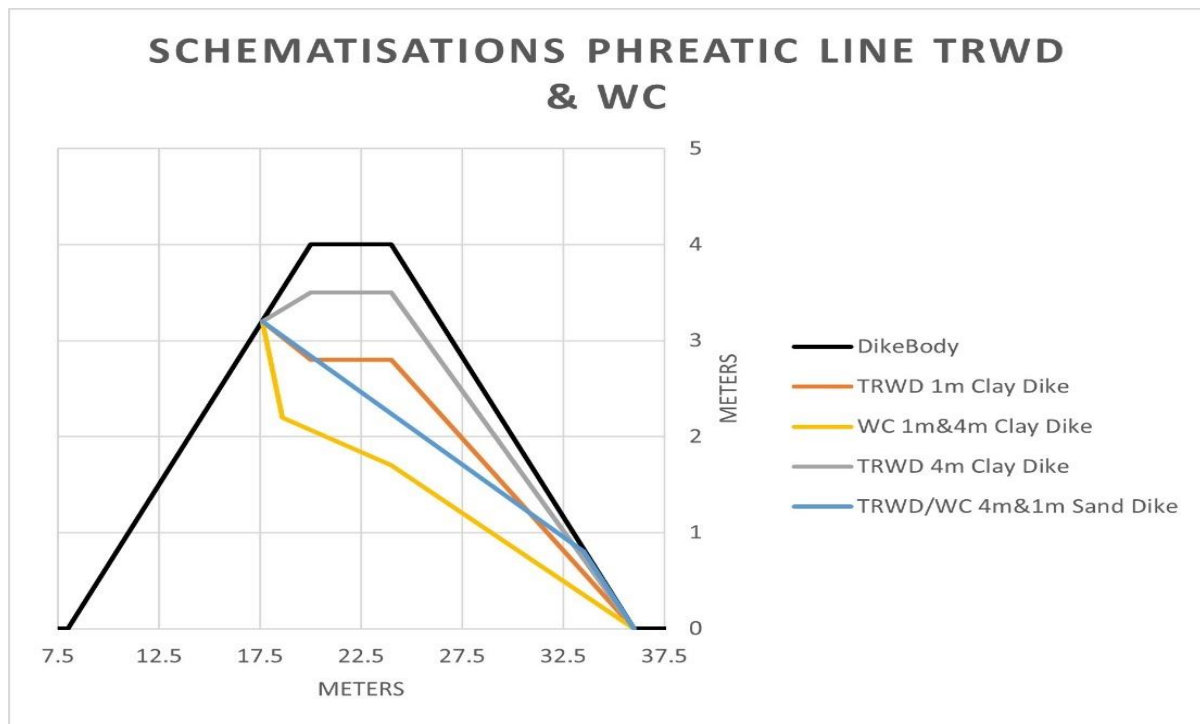


Figure 4-3 The phreatic line schematisations of the four different dike bodies based on the TRWD and WC.

In Plaxis, the schematisation of the phreatic line is plotted for every calculated discrete time step. The coordinates points can be manually extracted to further analysis.

4.2 SITUATIONS LEADING TO PRESCRIBED SCHEMATISATIONS

In this section, the methodology of the second research sub-question (*What different realistic situations lead to the prescribed schematic estimation of the phreatic line?*) is provided. For this sub-question again a modelling study in Plaxis will be performed.

To check what different situation lead to the TRWD and the WC schematic estimation of the phreatic line, different modelling procedures will be followed. First, a steady-state normative water level (WNB) will be modelled on the homogeneous clay and sand dike. This to see how the most conservative phreatic line in the different dike bodies will look like.

Secondly, a time-dependent simulation of the normative water will be evaluated. This is a steady high water level of 3.2 meters (WNB) over a period of 200 days until the steady-state situation has been reached. This method is comparable with the previous research sub-question, however in this simulation the water level is constant.

Furthermore, to check whether or not precipitation has an influence on the progression of the phreatic line an even more extreme scenario will be evaluated. In this scenario, the precipitation data of the winter period December 2019 until February 2020 is added. According to the KNMI weather report (de Wijs, 2020) this was one of the wettest winters ever measured. Besides the added precipitation data, the start of the simulation will be at the moment when there is a maximum phreatic line bulge under daily circumstances. Since the precipitation data contains only 91 days, the series is repeated after its ended in the simulation.

The modelling results of these simulations and the results of the previous sub-question will be used to check which situation will lead to the TRWD or the WC prescribed schematic estimation of the phreatic line.

4.3 SENSITIVITY ANALYSIS

To answer the last sub-question, *Which factors have the most impact on the schematic estimation of the phreatic line?*, a sensitivity analysis will be conducted. For the sensitivity analysis, different scenarios will be evaluated for some of the high water situations of the previous sub-questions (Table 12).

Table 12: The scenarios of the sensitivity analysis based on the previous research sub-questions.

	Scenarios	Research Sub-Question
#1	Phreatic line under daily circumstances	Sub-question 2
#2	Steady-State WBN	Sub-question 3
#3	Time-dependent WBN	Sub-Question 3
#4	Discharge and Storm dominated High Water Wave	Sub-Question 2

In the sensitivity analysis, only the clay and the sand dike with a 4 meter thick clay sub-soil are investigated. Besides that, there is a difference between the parameters and their sensitivity ranges for both dike types. Therefore, the sensitivity analysis is split into two parts.

In Table 13, both the parameters and their sensitivity ranges for the clay dike can be found as well as on which situations a sensitivity analysis has been performed. For the sand dike, it can be found in Table 14. As starting values for the different soil and water retention curve parameters, the results of the literature study for the starting model will be used (See Chapter 3.2.2). The ranges of the parameters for the sensitivity are based on the upper and lower bound found in the literature.

Table 13: Sensitivity analysis for Clay Dike.

Scenario	Description	Applied on situation:
A	10x higher Hydraulic Conductivity of Clay Core	#1,#2,#3 and #4
B	10x lower Hydraulic Conductivity of Clay Core	#1,#2,#3 and #4
C	Less extreme rainfall event (1/200 year return period)	#4
D	More extreme rainfall event (1/1000 year return period)	#4
E	Dike Width of 26 meter	#1
F	Dike Width of 34 meter	#1
G	2x higher Volumetric Specific Storage	#1,#2,#3 and #4
H	10x lower Volumetric Specific Storage	#1,#2,#3 and #4
I	2 meter Depth of clay sub-soil	#1, #2 and #3
J	6 meter Depth of clay Sub-soil	#1, #2 and #3

Table 14: Sensitivity analysis for Sand Dike.

Scenario	Description	Applied on situation:
A	10x higher Hydraulic Conductivity of Clay Core	#2,#3 and #4
B	10x lower Hydraulic Conductivity of Clay Core	#2,#3 and #4
C	Less extreme rainfall event (1/200 year return period)	#4
D	More extreme rainfall event (1/1000 year return period)	#4
G	2x higher Volumetric Specific Storage	#1,#2,#3 and #4
H	10x lower Volumetric Specific Storage	#1,#2,#3 and #4
I	2 meter Depth of clay sub-soil	#1, #2 and #3
J	6 meter Depth of clay Sub-soil	#1, #2 and #3

As can be seen in both the tables, there is not a sensitivity analysis conducted for the first situation, the phreatic line under daily circumstances, for the sand dike. Since there is no phreatic bulge over time visible under a sand dike, due to the relatively high hydraulic conductivity. Furthermore, the scenario I & J are not evaluated for the two typical high water waves since the effect of the depth of the sub-soil will also become clear in the time-dependent WBN level.

5 MODEL RESULTS

In this chapter, the results of the Plaxis simulations are presented and the answers for the last three sub-questions are given. The results are grouped per research for the last three sub-questions. At the end of each section, a short conclusion will be drawn for that research question. The overall conclusion of the main research questions can be found in Chapter 7.

5.1 SCHEMATISATION OF THE PHREATIC LINE UNDER DIFFERENT HYDRAULIC CONDITIONS

In this section, the second sub-question will be answered; *What are the effects of different hydraulic conditions on the phreatic line?* The goal of this question is to provide insight into the progression of the phreatic line over time. This sub-question consists of 4 scenarios as explained in the Methodology. In the first scenario, the phreatic line under daily circumstances with the precipitation and evaporation data of 2019 has been calculated. In the second and third scenario, the phreatic line progression during a storm and discharge high water wave has been simulated. In the last two scenarios, an 8-day rainfall event with a 1/500 years returns period has been added on top of the high water wave.

5.1.1 DAILY CIRCUMSTANCES 2019

In this scenario, the daily circumstances for the sand dike and the clay dike has been simulated. This is a simulation of typical winter dike, only depending on precipitation for most of the year. The precipitation data of 2019 has been applied on the dike. This is a year with a wet second half of the summer and autumn and a relatively drier winter.

In Figure 5-1, the results of the simulation of the clay dikes (1 meter sub-soil and 4 meter sub-soil) can be found. The height is measured from the top of the phreatic bulge in the centre of the dike relative to the stationary groundwater conditions of 0.5 meter below surface level. For the sand dikes, it became clear that the effect of the phreatic bulge under daily circumstances was too small to be measured and therefore neglected.

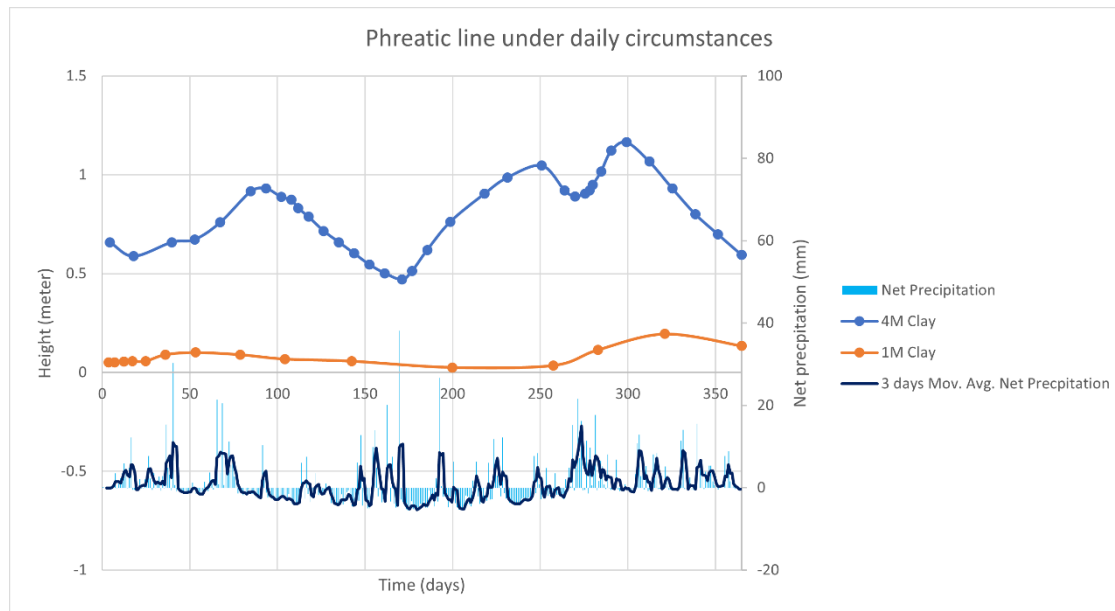


Figure 5-1: The phreatic line over the year 2019 together with the net precipitation of 2019 and the 3 days moving average net precipitation.

It is clear to see that both lines follow the same pattern. However, in case of the 1 meter clay sub-soil situation, the phreatic bulge is more subdued than the situation with a 4 meter clay sub-soil. This is due to the fact that it is for precipitation is harder to flow out through a thicker layer of the relatively high impermeable clay layer to the sandy aquifer. In the figure, it can be seen that the relative drought period between day 100 and 150 lead to a decrease of the phreatic line on both clay dikes. Around 150 days, the rainfall peaks lead to increase of the phreatic line only on the clay dike with a 4 meter thick sub-soil. Furthermore, the peaks in the end of the time series lead for both clay dikes to a decrease of the phreatic line, this hydrological process causing this effect is still unknown.

Furthermore, the graph shows that the phreatic line can vary because of the precipitation around 0.7 meters throughout the year in case of a clay dike with 4 meter thick sub-soil. For the clay dike with a 1 meter thick this variation is less than 0.2 meters. Therefore, it is important to take the daily circumstances into consideration when choosing a starting position for further modelling such as high water waves.

5.1.2 STORM AND DISCHARGE HIGH WATER WAVE

In these two scenarios, the two typical storm and discharge high water waves for the IJsseldelta have been simulated as described in Chapter 4.1.1.

In Figure 5-2, several time steps (days) of the discharge and storm dominated high water wave can be seen in related to the WC and the TRWD estimation of the phreatic line. As can be seen, that is not in a single time step the WC nor the TRWD schematic estimation of the phreatic line is reached over the whole dike section. Only at the inner toe during a storm high water wave, the WC estimation is reached. This could be the cause due to the steady-state water level of 1.7 meter before the actual time-dependent high water wave starts.

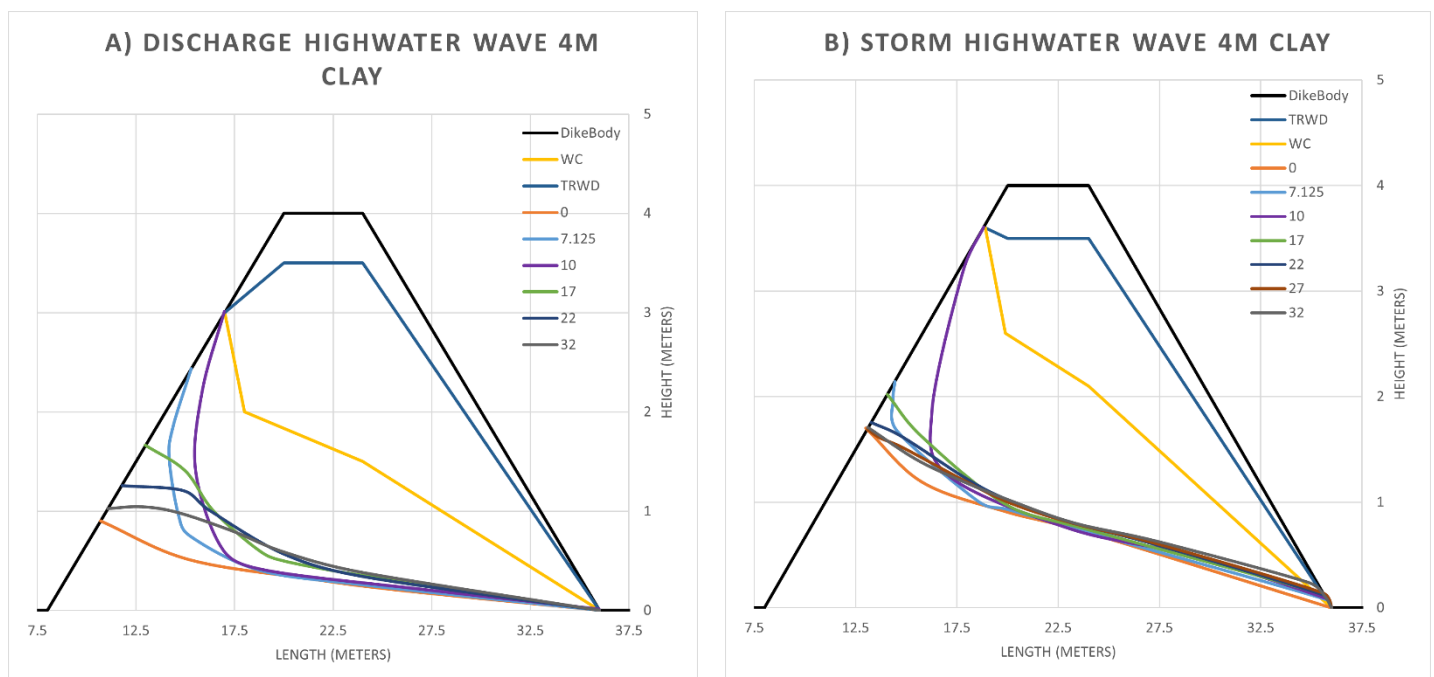


Figure 5-2: The phreatic line at different time steps in days together with the dike body and the schematizations of the WC and TRWD for a clay dike with a 4 meter clay sub-soil for: (a) the discharge dominated high water wave, (b) the storm dominated high water wave.

In Figure 5-3, the discharge and storm dominated high water wave are simulated on the clay dike with a sub-soil of 1 meter. According to the TRWD, the phreatic line should be lower with a thinner sub-soil. This effect is not noticeable in the simulation results. However, during the discharge high water wave at the inner toe, there

is a higher phreatic line modelled compared with the situation with a 4 meter thick sub-soil layer. This is in contradiction with the guidelines provided in the TRWD and theory on groundwater flow because a thinner clay layer should make drainage to the stationary groundwater level at 0.5 meter easier as in line with the differences between the phreatic bulge under daily circumstances for a 1.0 and 4 meter thick sub-soil.

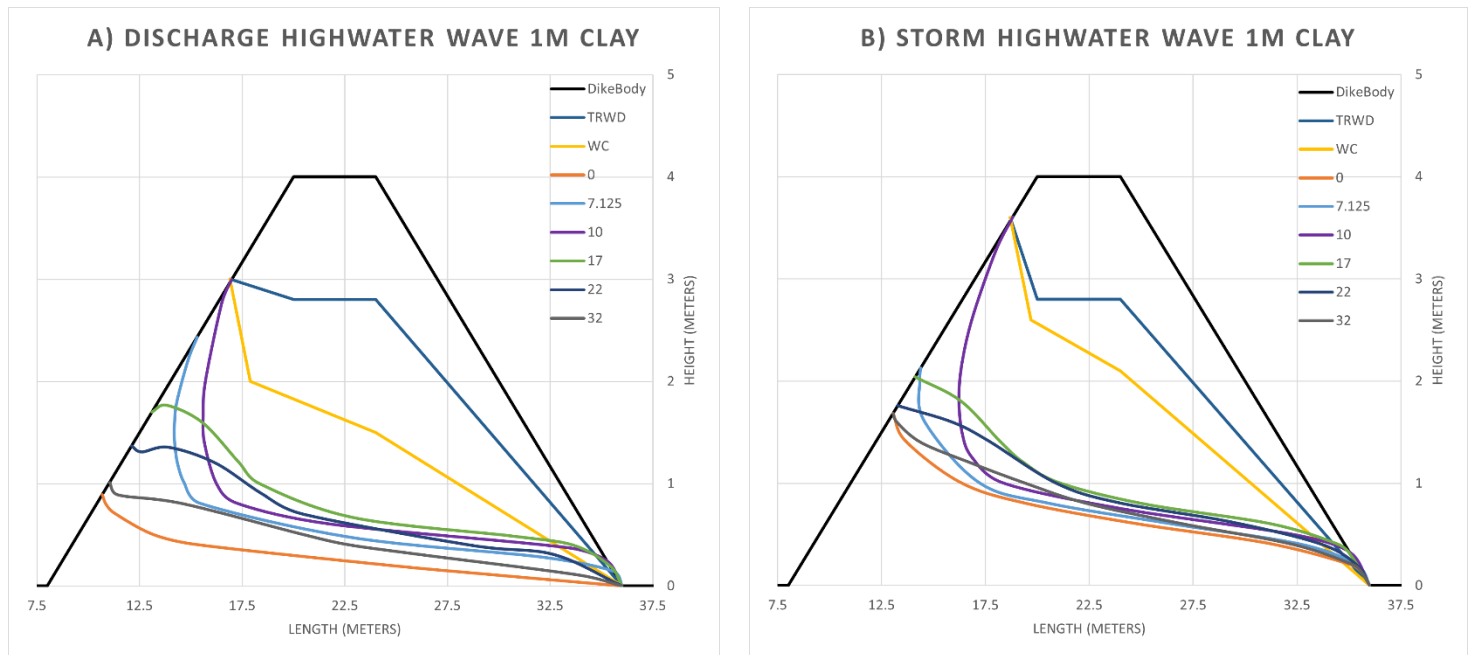


Figure 5-3: The phreatic line at different time steps in days together with the dike body and the schematizations of the WC and TRWD for a clay dike with a 1 meter clay sub-soil for: (a) the discharge dominated high water wave, (b) the storm dominated high water wave.

In Figure 5-4 and Figure 5-5, the results of the high water waves on the sand dikes with a 1 and 4 meter thick clay sub-soil layer can be seen. Due to the relative higher permeability of sand, the lines have a smaller curve. The TRWD and the WC schematic estimation of the phreatic line will never be reached in the Plaxis model. It can be seen that the height of the phreatic line does not depend on the thickness of the clay sub-soil. This is in according with the guidelines of the TRWD. Even at the inner toe of the dike, the guideline of $0.25 \times$ the height of the higher water wave will never be reached.

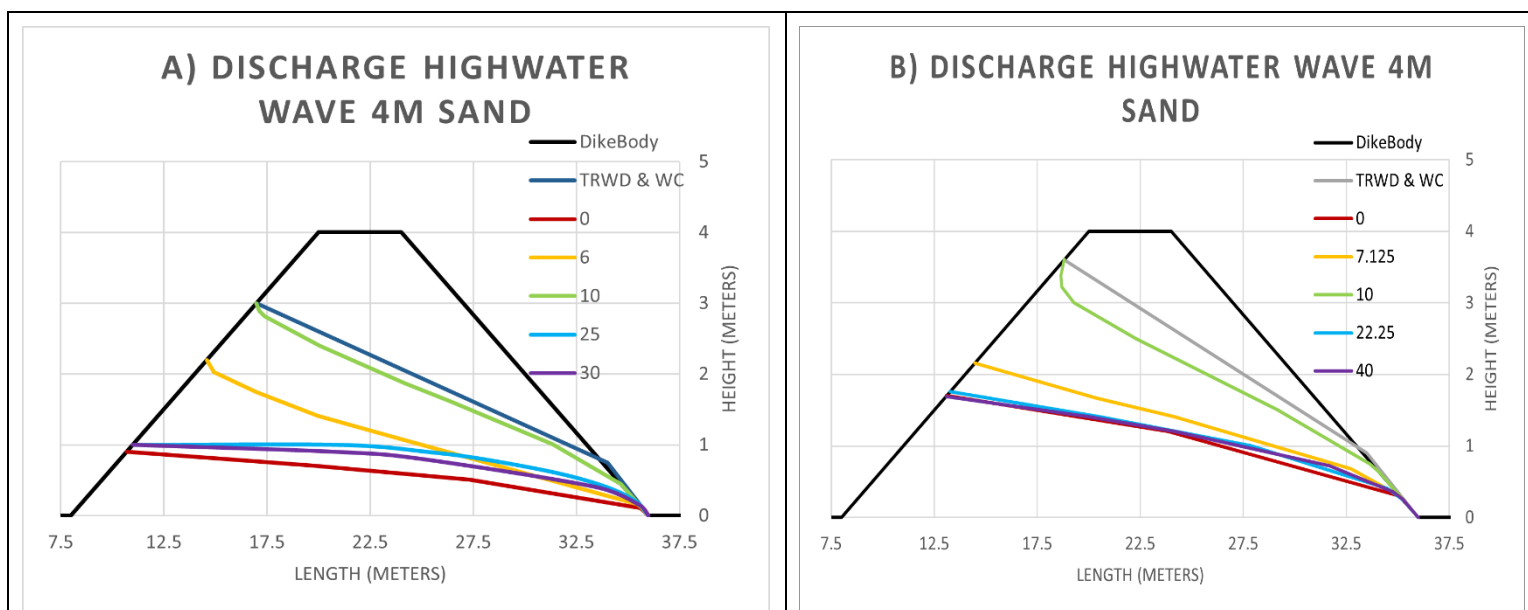


Figure 5-4: The phreatic line at different time steps in days together with the dike body and the schematizations of the WC and TRWD for a sand dike with a 4 meter clay sub-soil for: (a) the discharge dominated high water wave, (b) the storm dominated high water wave.

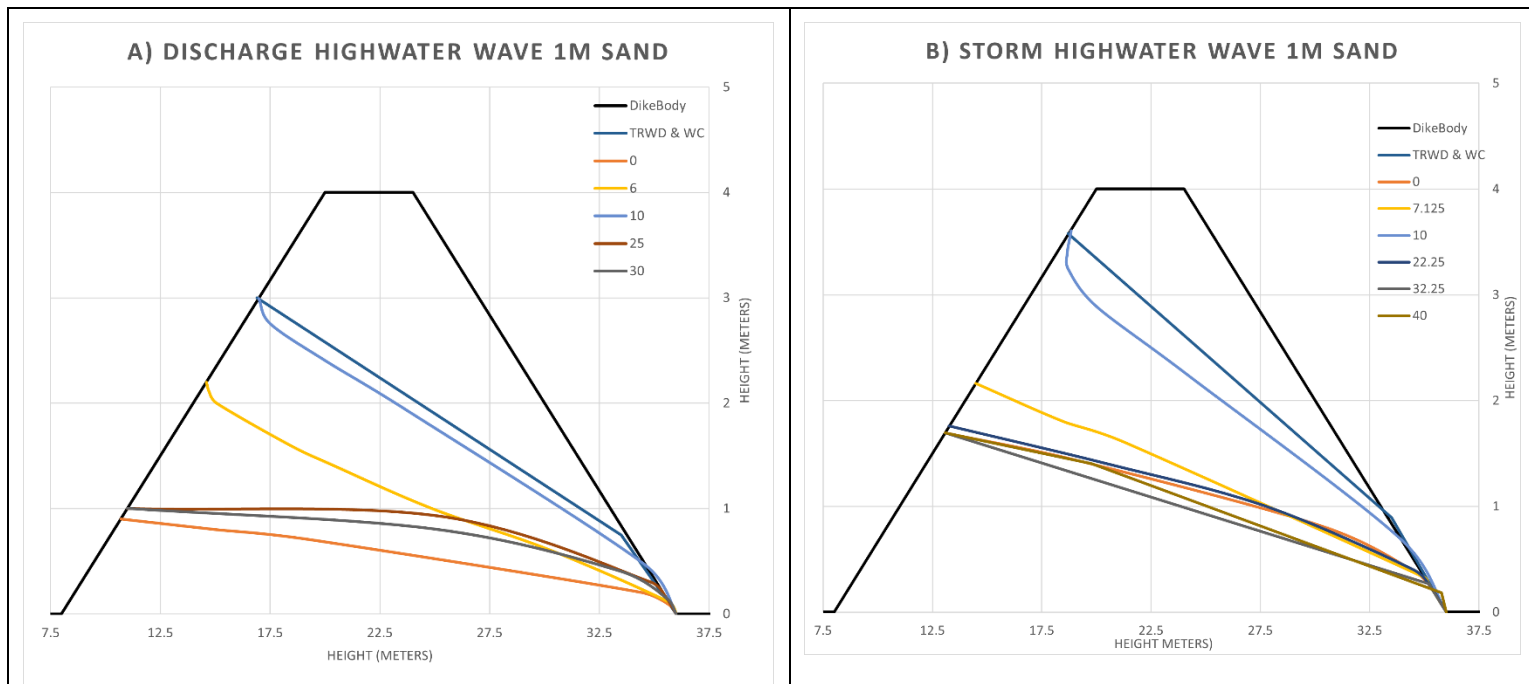


Figure 5-5: The phreatic line at different time steps in days together with the dike body and the schematizations of the WC and TRWD for a sand dike with a 1 meter clay sub-soil for: (a) the discharge dominated high water wave, (b) the storm dominated high water wave.

To conclude, it can be seen in all the results the TRWD and the WC schematic estimation of the phreatic line will never be reached. For the clay dikes, the difference between the simulated phreatic line and the WC and TRWD estimation of the phreatic line is much larger than for the sand dikes. Furthermore, in all the clay dike simulations a (slightly) higher phreatic line is measured at the inner toe of the dike compared to the WC and TRWD estimated schematisation of the phreatic line (Figure 5-2 and Figure 5-3).

Lastly, the results of the 75% confidence interval for the clay dikes can be found in Appendix C.

5.1.3 RAINFALL

In these two scenarios and 8-days uniform rainfall event is added. The rainfall event has a return period of 1 in 500 years and is characterised as an extreme rainfall event (Beersma et al., 2019). As the rainfall event starts at day 0 and ends at day 10, more focus will be on these timesteps.

In Figure 5-6, the simulation results for the clay dike with a 4 meter thick clay sub-soil layer can be found. It is interesting to see that the effects due to the rainfall event are clearly visible in the phreatic bulge at the area below the inner crest of the dike. Even 10 days after the rainfall period ended, the phreatic line rise because of the rainfall is still visible. The WC schematic estimation of the phreatic line is in both the discharge and storm dominated high water wave exceeded at the inner toe.

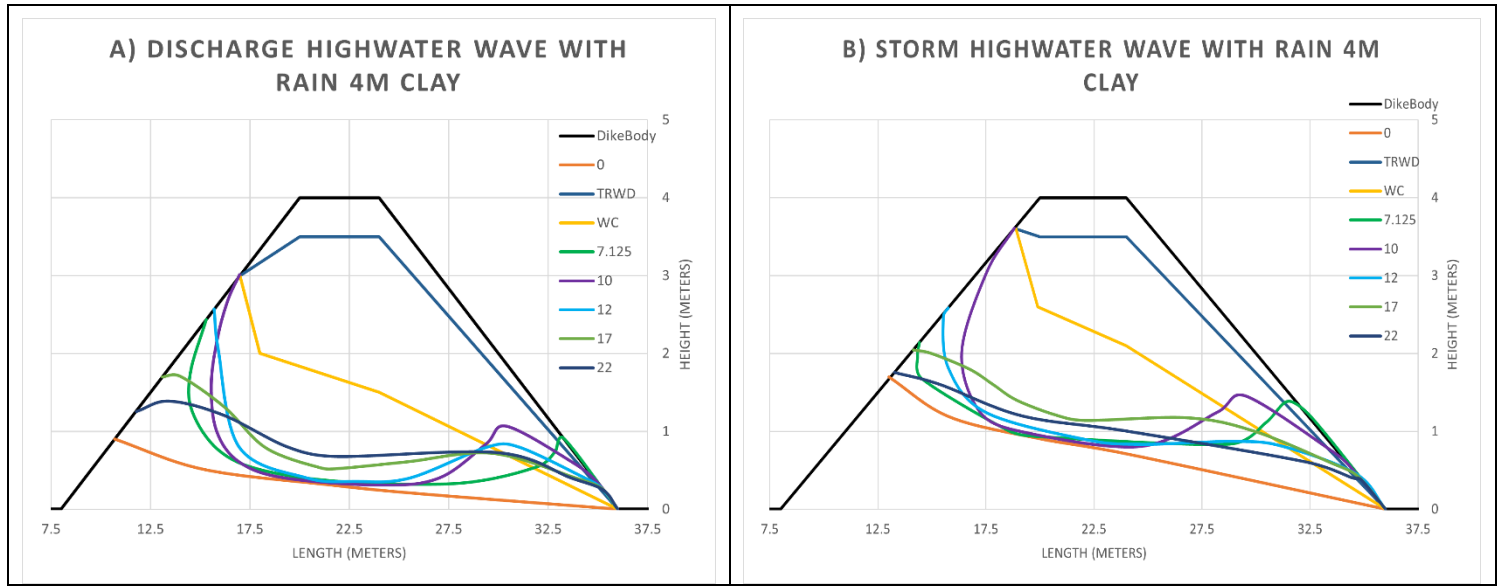


Figure 5-6: The phreatic line at different time steps in days together with the dike body and the schematizations of the WC and TRWD for a clay dike with a 4 meter clay sub-soil for: (a) the discharge dominated high water wave with a 1/500 year rainfall event, (b) the storm dominated high water wave with a 1/500 year rainfall event.

In Figure 5-7, the simulation results of the same high water waves and the rainfall on a clay dike with a 1 meter thick clay subsoil can be seen. It can be seen that the phreatic line is in higher in case of a 1 meter thick sub-soil compared to a 4m thick sub-soil. This is the case in both the simulations with and without rainfall.

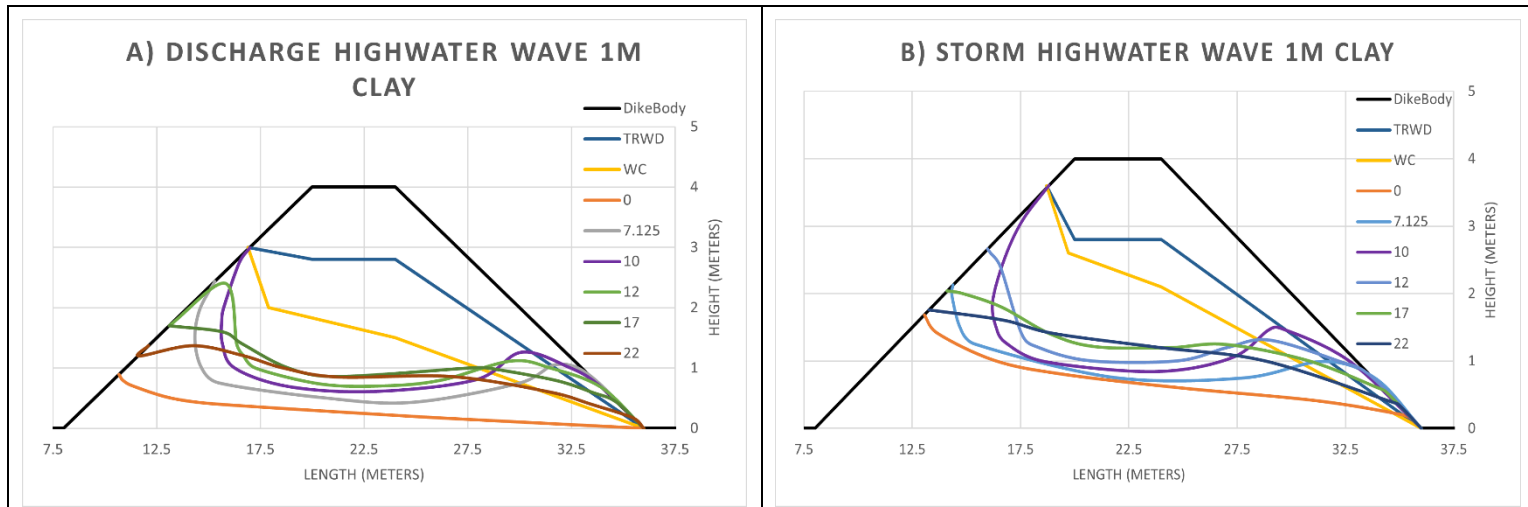


Figure 5-7: The phreatic line at different time steps in days together with the dike body and the schematizations of the WC and TRWD for a clay dike with a 1 meter clay sub-soil for: (a) the discharge dominated high water wave with a 1/500 year rainfall event, (b) the storm dominated high water wave with a 1/500 year rainfall event.

In Figure 5-8 and Figure 5-9, the results of the high water waves with the 8 days rainfall event on the sand dikes with a 1 and 4 meter thick sub-soil layer can be found. To make the small effect of rainfall on a sand dike visible, the high water wave graphs with rainfall and without rainfall are being combined. The full version of the progression over time for the discharge and storm high water waves can be found in Appendix D. As can be seen, the phreatic line with rainfall is from the inner crest inwards higher located than the phreatic line without rainfall. This effect is relatively larger at the peak moment (time = 10 days) of the high water wave. However, the TRWD and the WC schematisation of the phreatic line will never be exceeded.

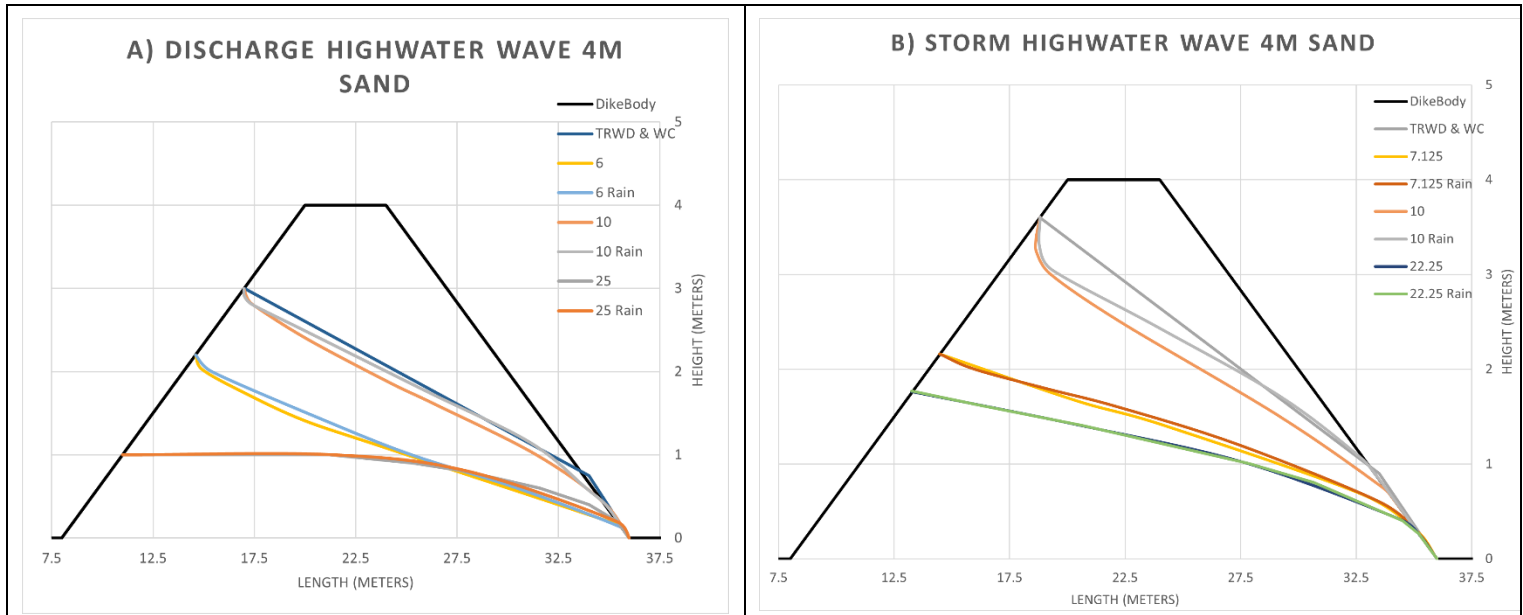


Figure 5-8: The phreatic line at different time steps in days together with the dike body and the schematizations of the WC and TRWD for a clay dike with a 4 meter clay sub-soil for: (a) the discharge dominated high water wave with and without 1/500 year rainfall event, (b) the storm dominated high water wave with and without a 1/500 year rainfall event.

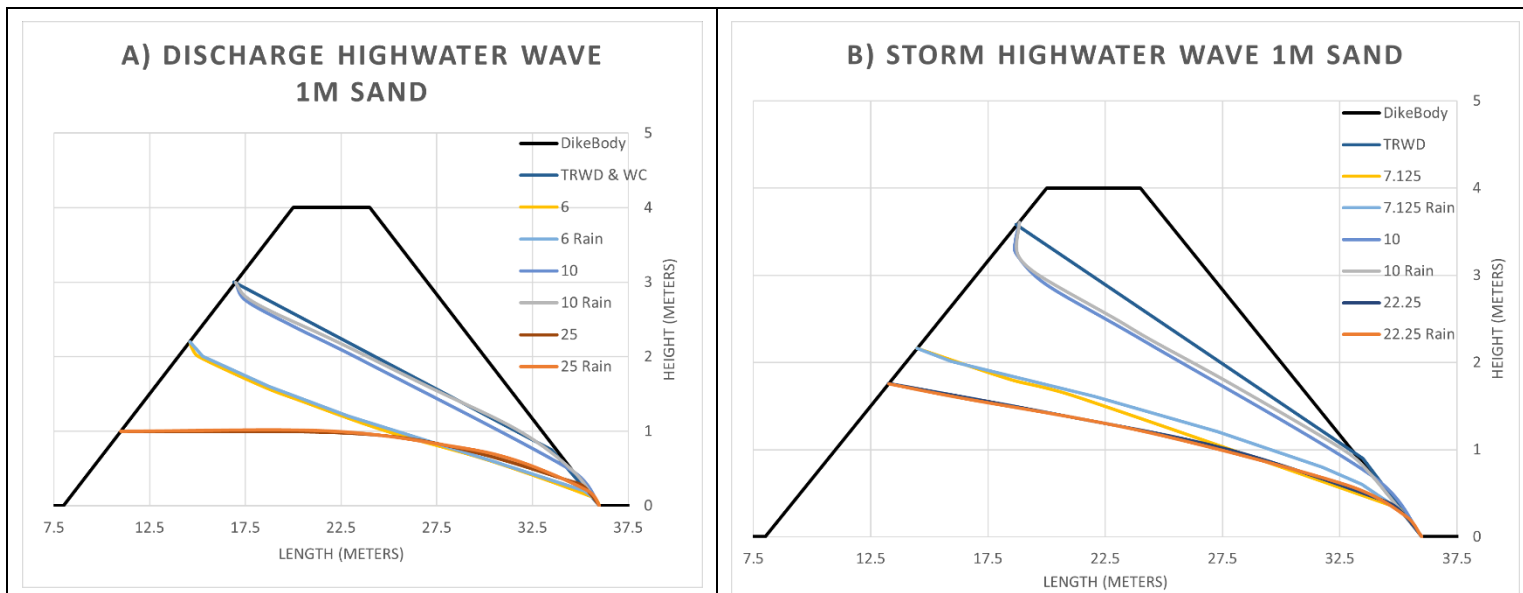


Figure 5-9: The phreatic line at different time steps in days together with the dike body and the schematizations of the WC and TRWD for a clay dike with a 1 meter clay sub-soil for: (a) the discharge dominated high water wave with and without 1/500 year rainfall event, (b) the storm dominated high water wave with and without a 1/500 year rainfall event.

5.2 SITUATIONS LEADING TO THE PRESCRIBED SCHEMATIC ESTIMATION OF THE PHREATIC LINE

In this section, the third sub-question will be answered; *What different situations lead to the prescribed schematic estimation of the phreatic line, and how realistic are those situations?* As explained in the Methodology, first a steady-state normative water level (WBN) will be modelled on the homogenous clay and sand dike. Then, a time-dependent simulation of the normative water level will be evaluated. These two simulation results are combined in one graph.

5.2.1 TIME-DEPENDENT NORMATIVE WATER LEVEL

In Figure 5-10, the normative water level wave as function of time has been plotted. It can be seen that after 135 days not even the steady-state point has been reached. This shows how conservative a calculation with a steady-state is. Below the outer crest of the dike, the WC estimated schematisation is reached after 60 days. At the inner toe area of the dike, the WC estimated schematisation is already reached after 40 days. The TRWD situation will never be reached since it is located higher than the steady-state situation.

From day 20 onwards the phreatic line at the inner toe is increasing above the WC. This is an important area for the stability of the inner slope. This simulation also shows that WC underestimates the phreatic line in this area, as was also seen in Figure 5-2 and Figure 5-3.

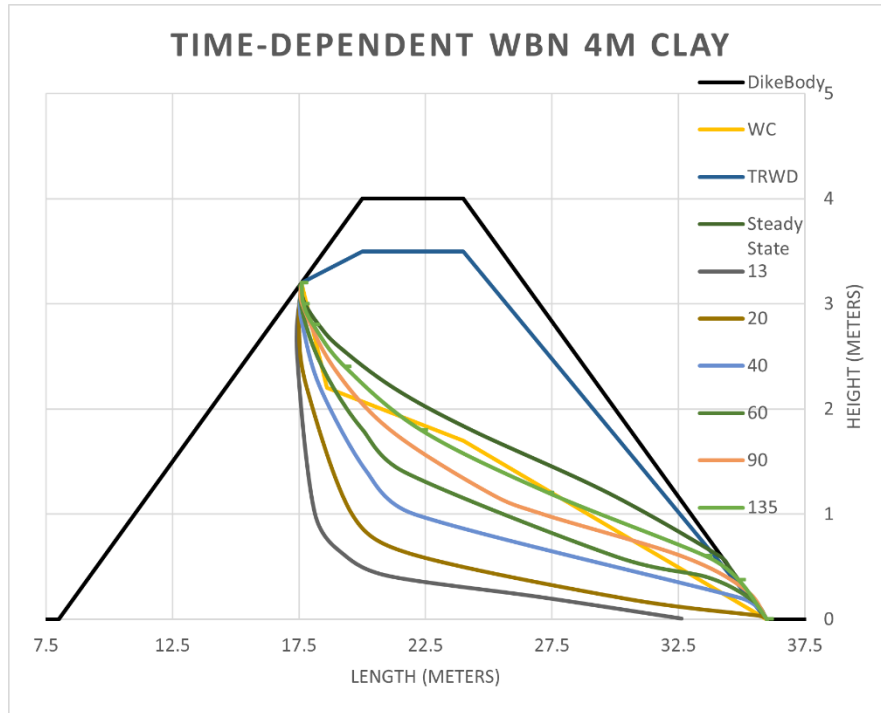


Figure 5-10: The phreatic line for a normative water level at different time steps in days together with the dike body and the schematizations of the WC and the TRWD for a clay dike with a 4 meter sub-soil.

In Figure 5-11, the normative water level wave overtime for a clay dike with a sub-soil of 1 meter can be found. Noticeable is that the steady-state is already reached around the 90 days. Moreover, the WC line is already touched after 12 days at the inner toe. Besides that, the phreatic line is higher at the inner toe for a sub-soil of 1 meter compared to a sub-soil of 4 meters.

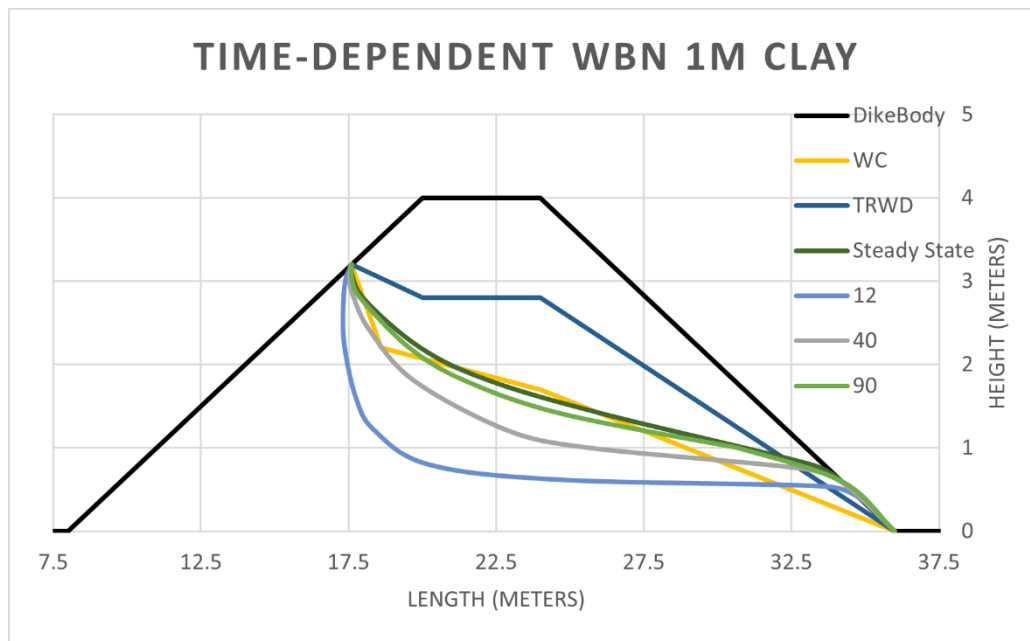


Figure 5-11: The phreatic line for a normative water level at different time steps in days together with the dike body and the schematizations of the WC and the TRWD for a clay dike with a 1 meter sub-soil.

In Figure 5-12, the normative water level as function of time for a sand dike with a 4 meter thick clay sub-soil is given. As already could be seen in the previous research sub-question, the steady-state phreatic line is located higher compared to the TRWD and the WC schematic estimation of the phreatic line. Furthermore, due to the relatively high permeability of sand, the wave progressed very fast in time towards its steady-state condition. In less than 8 days the TRWD and the WC schematic estimation of the phreatic line have been reached.

For a sand dike with a clay sub-soil of 1 meter, the results are the same as for a sand dike with a sub-soil of 4 meters. This is in accordance with the guidelines of the TRWD that the height of a phreatic line in a sand dike is not depending on the sub-soil conditions. Therefore, the normative water level as function of time for the sand dike with a 1 meter thick clay sub-soil can be found in Appendix E.

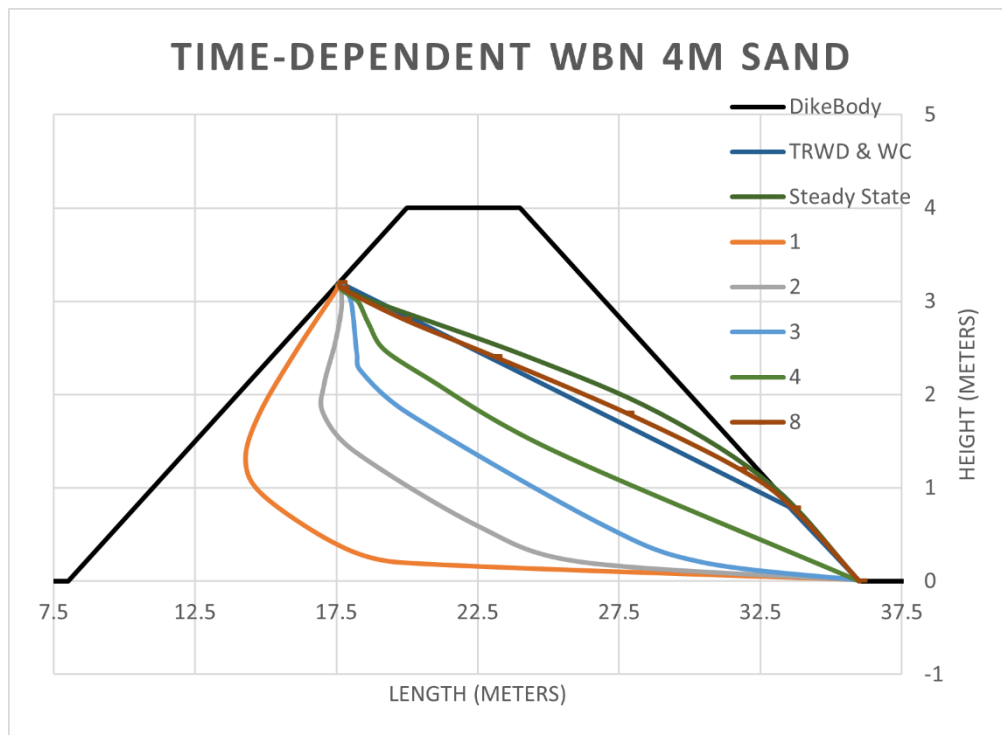


Figure 5-12: The phreatic line for a normative water level at different time steps in days together with the dike body and the schematizations of the WC and the TRWD for a sand dike with a 4 meter sub-soil.

5.2.2 RAINFALL

In Figure 5-13, the normative water level over time with and without precipitation and evaporation data of the winter 2019-2020 can be seen. Over the full length of the dike, there is an increase in the height of the phreatic line. For the rainfall should be taken into account that the net precipitation can differ per day due to the fact that natural real data has been used. This could cause local variation in individual timesteps.

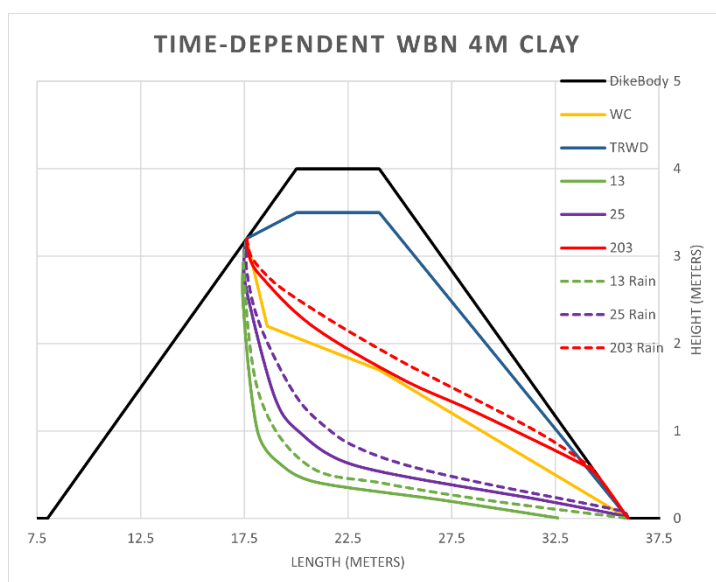


Figure 5-13: The phreatic line for a normative water level with winter rainfall at different time steps in days together with the dike body and the schematizations of the WC and the TRWD for a clay dike with a 4 meter sub-soil.

As can be seen in Figure 5-14, the effect of precipitation on a clay dike with a sub-soil of 1 meter is lower. This has two reasons; due to smaller clay layer the dike can drainage faster to the sandy aquifer, and the phreatic bulge under daily circumstances is much lower for the clay dike with a 1 meter thick sub-soil.

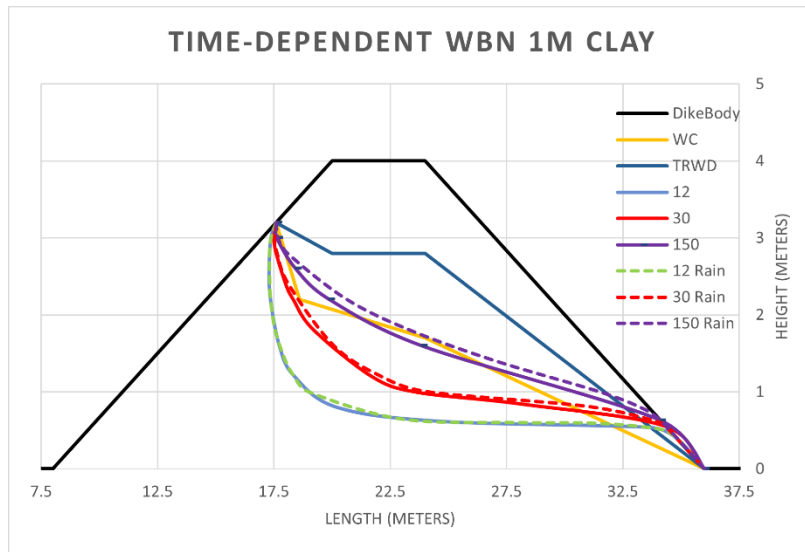


Figure 5-14: The phreatic line for a normative water level with winter rainfall at different time steps in days together with the dike body and the schematizations of the WC and the TRWD for a clay dike with a 1 meter sub-soil.

To summarize, the effect of precipitation on a dike with a thicker sub-soil is larger than a dike on a thin or good permeable sub-soil. In both cases, the steady-state would be reached earlier due to precipitation.

5.3 SENSITIVITY ANALYSIS

In this section, the results of the sensitivity analysis are given. In the sensitivity analysis, different situations are analysed based on the previous research sub-questions. First, the sensitivity analysis on the phreatic line under daily circumstances will be provided. After which, the steady-state and time-dependent normative water level will be analysed. Lastly, a sensitivity analysis will be performed on the discharge and storm dominated high water wave.

5.3.1 PHREATIC LINE UNDER DAILY CIRCUMSTANCES

For the phreatic line under daily circumstances. The rainfall and precipitation data of 2019 has been used. The height is measured from the stationary groundwater level of 0.5 meters below surface area until the highest point of the phreatic line under the dike. For the phreatic line-height under daily circumstances, only the clay dike has been considered, this because a sand dike has not a raised phreatic level throughout the year.

In Figure 5-15, the effect of the different hydraulic conductivity for the clay core is displayed. It can be seen that the effect of a smaller hydraulic conductivity leads to a higher phreatic level in the dike. Besides that, a smaller conductivity also leads to a lower variation throughout the year. This mainly because a lower hydraulic conductivity leads to a slower process before the rainwater reaches the phreatic line, and the water can drain through the clay layer. Furthermore, it can be seen that some rainfall peaks in the 3 days moving average of the net precipitation can be related to the rise and drop of the phreatic line.

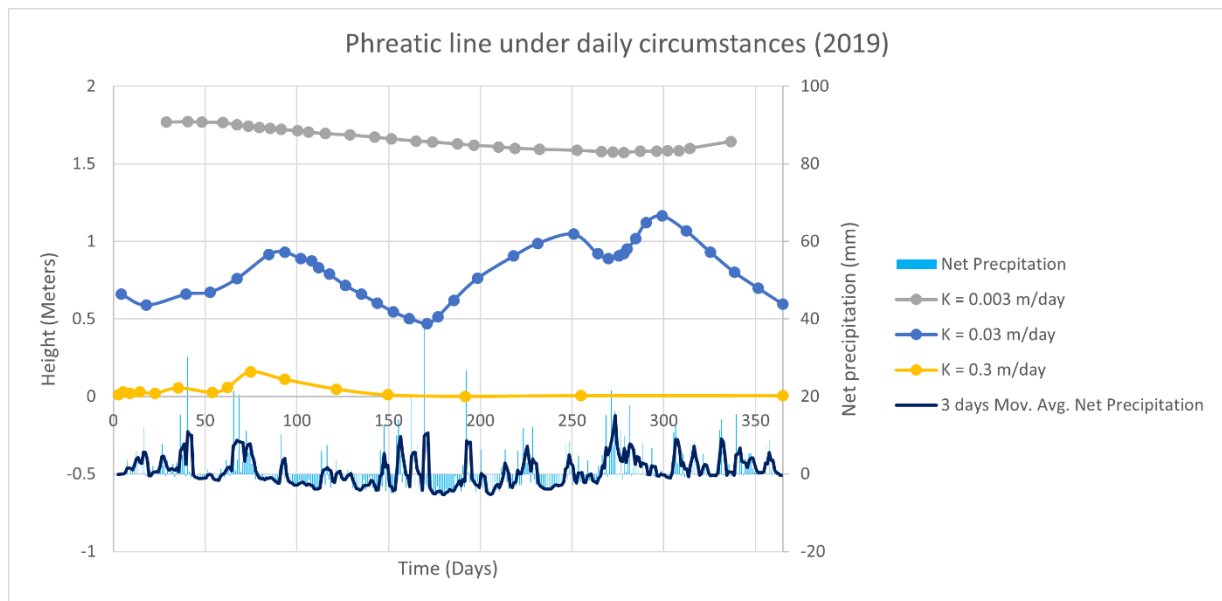


Figure 5-15: The effect of different hydraulic conductivity (K) on the phreatic line over the year 2019 together with the net precipitation of 2019 and the 3 days moving average net precipitation.

The volumetric storage capacity is a parameter which is hard to be validated. It cannot be measured based on soil samples, and literature values are quite different. In Figure 5-16, the effects of different volumetric storage capacity on the phreatic line under daily circumstances becomes visible. It can be seen that a lower volumetric storage capacity gives a more distorted phreatic line progression over time. This is because the soil is reacting to a drop in the head and realising more water.

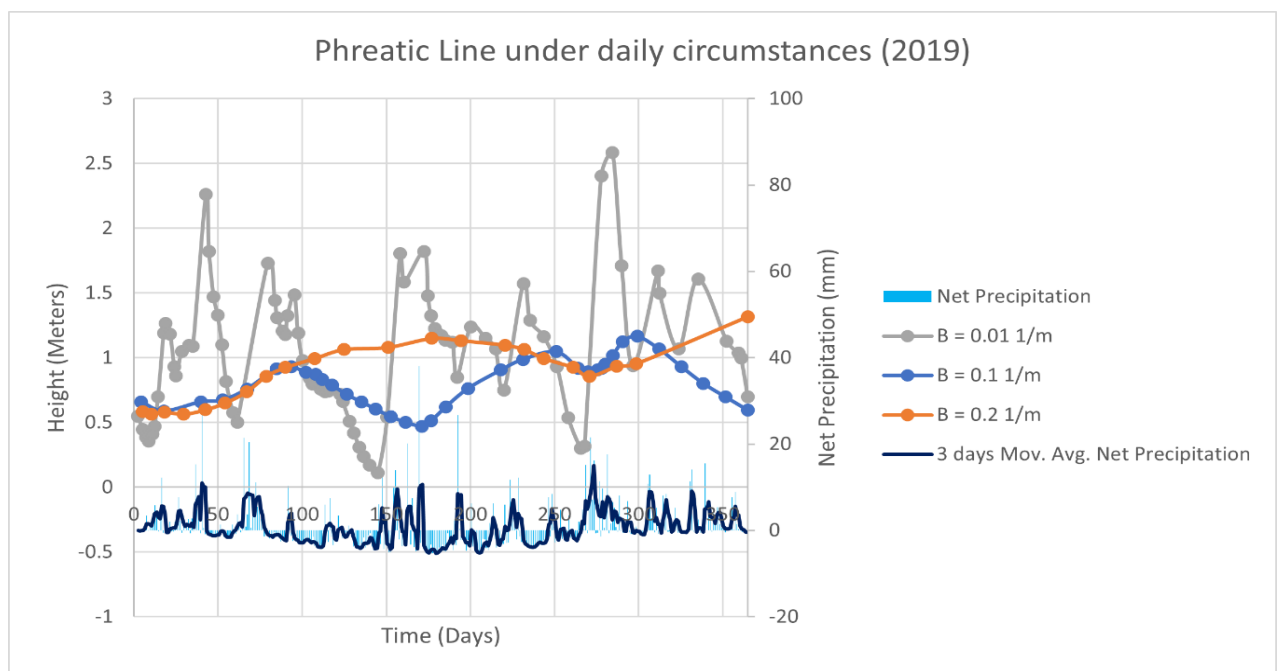


Figure 5-16: The effect of different Volumetric Storage Capacity (B) on the phreatic line over the year 2019 together with the net precipitation of 2019 and the 3 days moving average net precipitation.

According to the TRWD, the thickness of the sub-soil determines the height of the phreatic line. In Figure 5-17, it can be seen that this statement is correct. However, after 250 days something strange happens in the

situation with a sub-soil thickness of 6 meters. In Plaxis a lot of timesteps after day 250 contains artefacts such as floating water and double phreatic lines in the dikes. Therefore, these points are neglected in the sensitivity analysis.

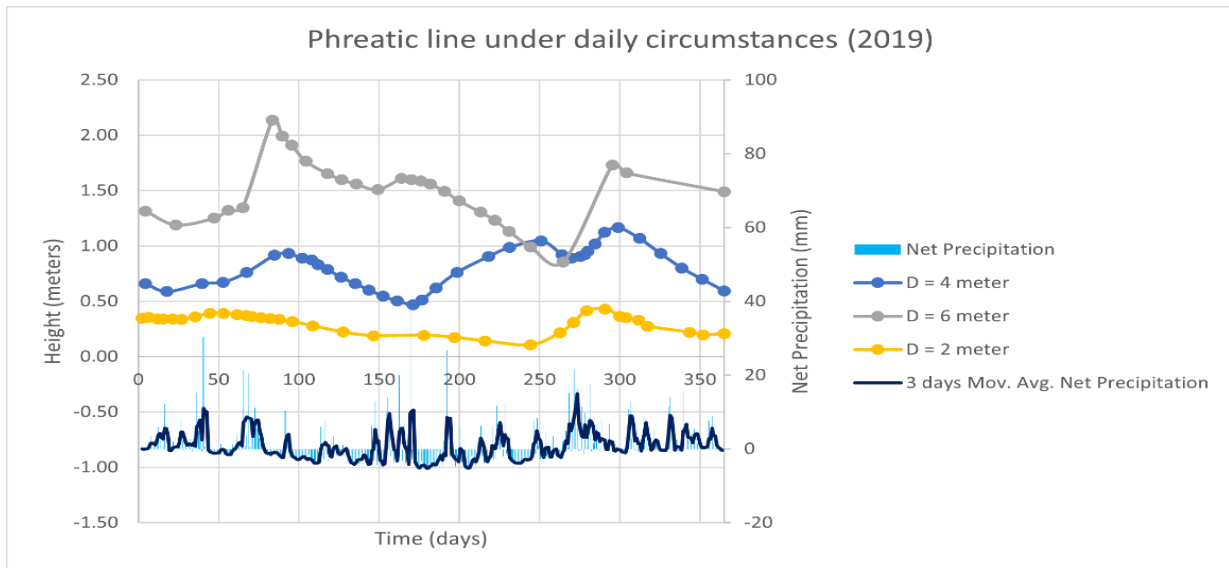


Figure 5-17: The effect of different clay sub-soil thickness (D) on the phreatic line over the year 2019 together with the net precipitation of 2019 and the 3 days moving average net precipitation.

Besides the thickness of the sub-soil layer also the width of the dike has been considered. In Figure 5-18, it can be seen that a wider dike body has a higher phreatic line than a smaller dike. Furthermore, the graph is also a bit distorted in the time since a wider dike has more storage capacity. Therefore, it costs more time to drain or refill the dike.

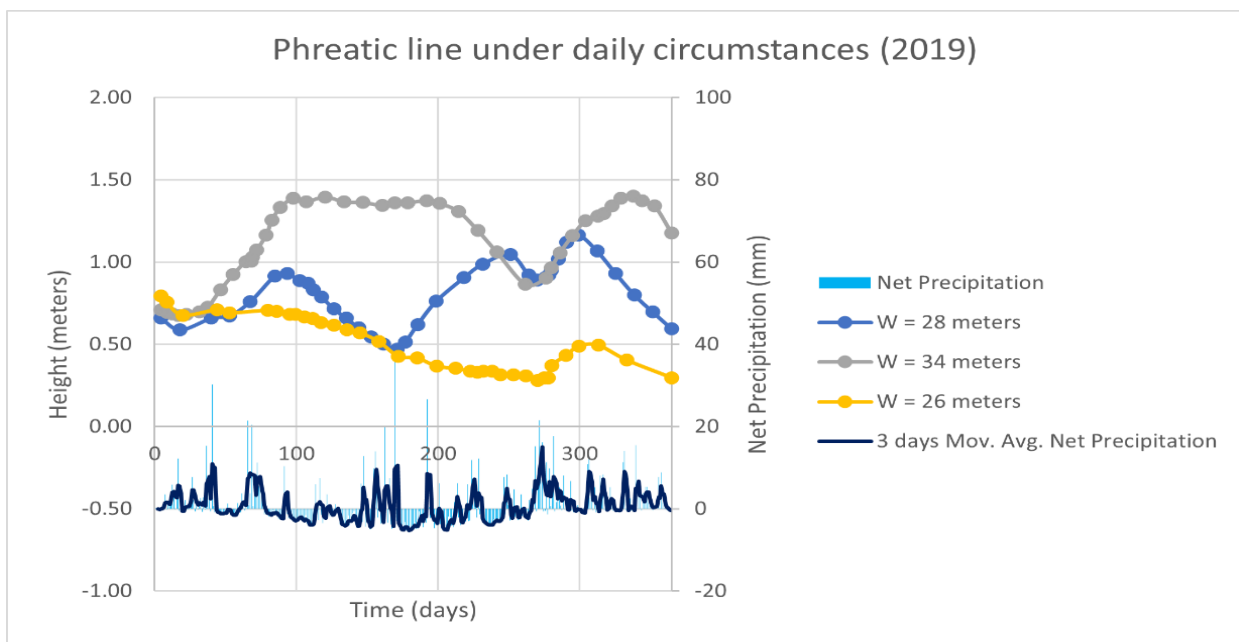


Figure 5-18: The effect of different clay dike widths (W) on the phreatic line over the year 2019 together with the net precipitation of 2019 and the 3 days moving average net precipitation.

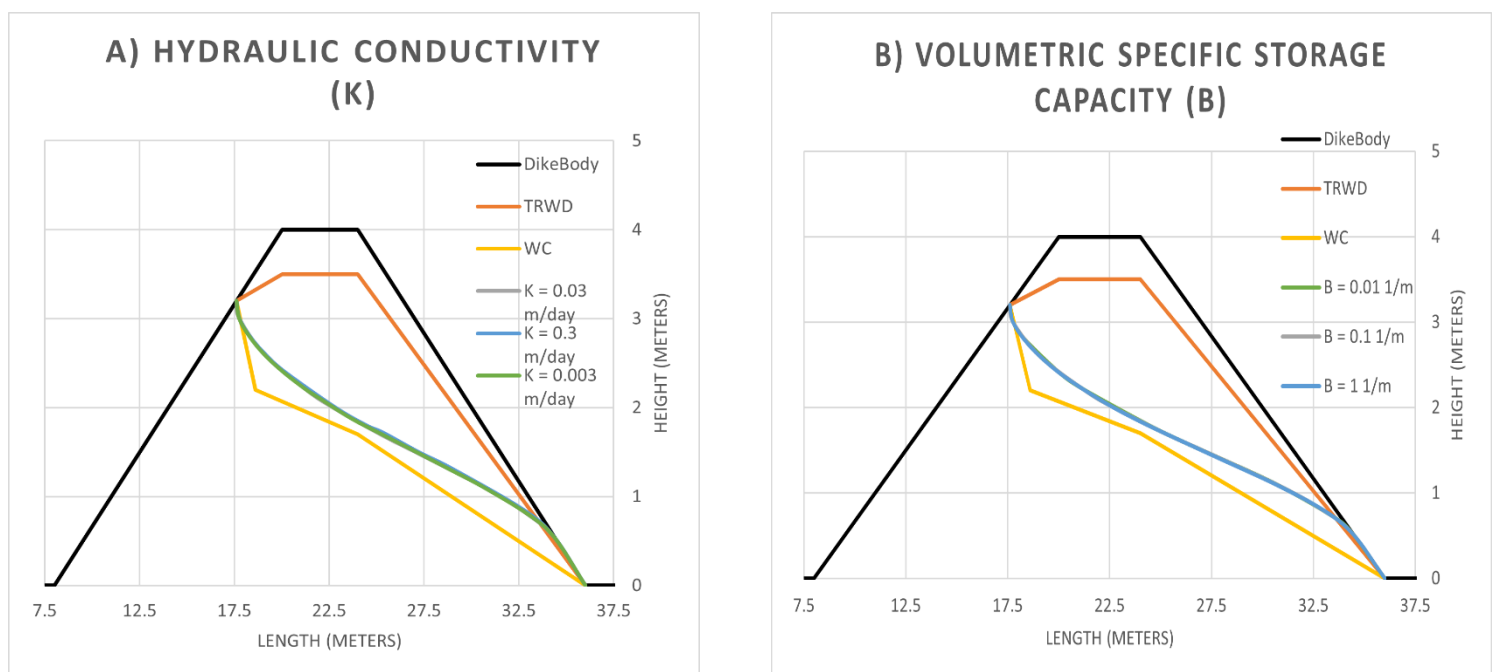
To sum up, when considering the parameters above it becomes clear that all these parameters influence the height of the phreatic line when simulating the phreatic line over a year. From all parameters, it is interesting to the effects of different volumetric specific storage parameter values as the simulated results are quite diverse.

5.3.2 STEADY-STATE & TIME-DEPENDENT NORMATIVE WATER LEVEL

In this section, the steady-state and time-dependent analysis of the normative water level is provided. As explained in the methodology, the normative water level is set on 3,2 meter above the surface level.

5.3.2.1 STEADY-STATE ANALYSIS

In this section, the results of the steady-state and time-dependent normative water level sensitivity analysis will be given. In Figure 5-19, the steady-state situations on a clay dike with a 4 meter sub-soil are given. It can be seen that only the depth of the sub-soil has a small impact on the phreatic line.



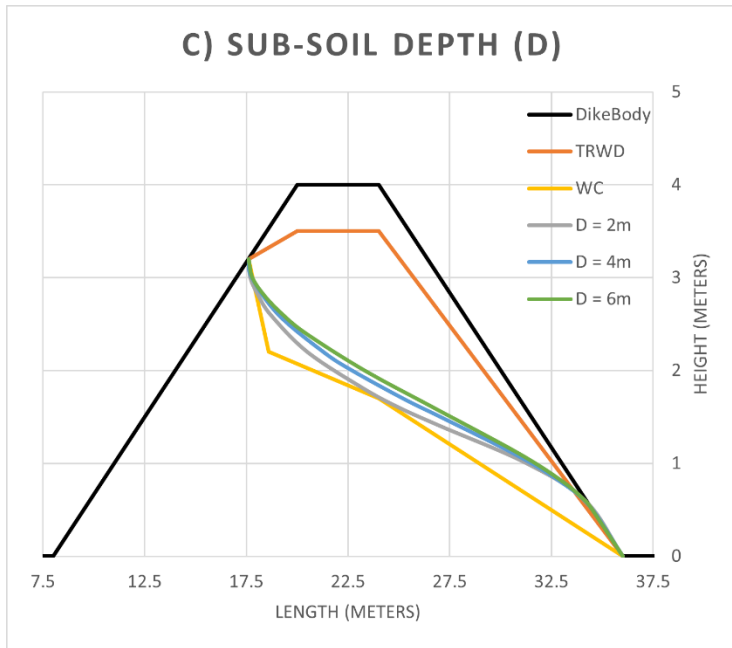
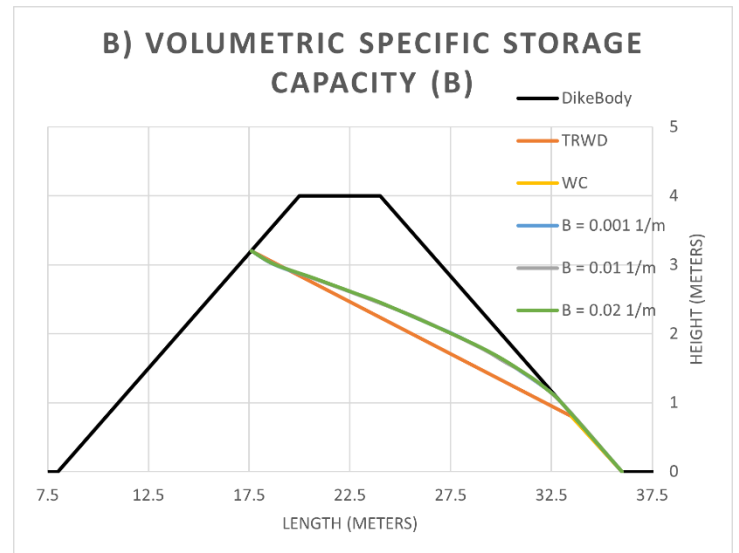
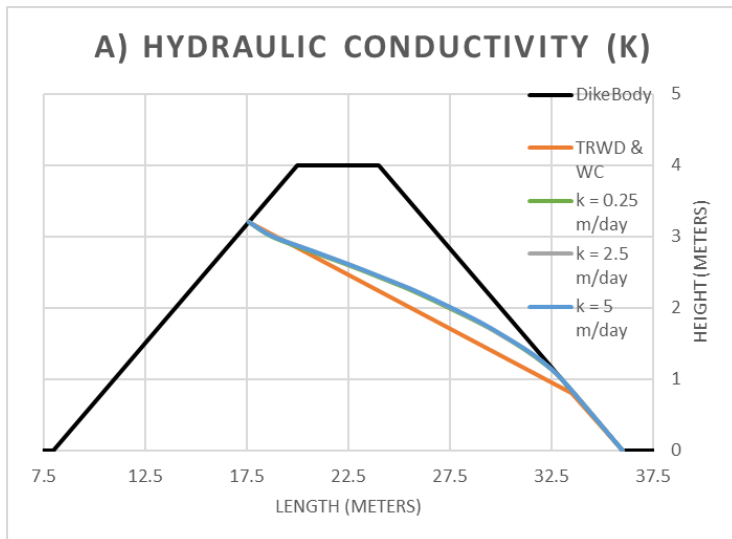


Figure 5-19: The phreatic line during a steady-state simulation with the dike body and the schematizations of the WC and TRWD for a clay dike with a 4 meter clay sub-soil for: (a) different hydraulic conductivities, (b) different volumetric specific storage capacities, (c) different sub-soil thicknesses.

The results of the steady-state sensitivity of the sand dike (Figure 5-20) are in line with the results given in the previous sub-question. The effect of the sub-soil under the dike has no impact on the height of the phreatic line. This is in accordance with the TRWD guidelines, in which there is no relation between the sub-soil in a sand dike and the height of the phreatic line.



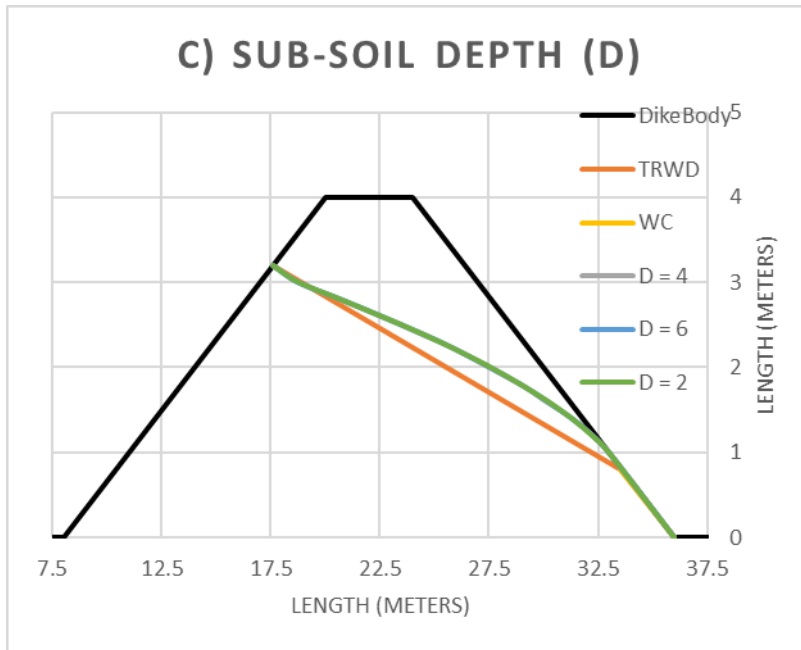


Figure 5-20: The phreatic line during a steady state simulation with the dike body and the schematizations of the WC and TRWD for a sand dike with a 4 meter clay sub-soil for: (a) different hydraulic conductivities, (b) different volumetric specific storage capacities, (c) different sub-soil thicknesses.

5.3.2.2 TIME-DEPENDENT ANALYSIS

In this section, the time-dependent normative water level sensitivity analysis can be found. In all the following figures, the colour intensities show the progression over time, with a constant parameter. The colour and line pattern groups the situations with the same parameter value.

In Figure 5-21, it can be seen that a higher soil hydraulic conductivity leads to a straighter phreatic line than a lower hydraulic conductivity. However, it is interesting to see that there is a point at which a low hydraulic conductivity will raise a higher phreatic line at the inner side of the dike. This is due to the fact that a lower conductivity leads to a higher phreatic bulge under daily circumstances. It can be seen that the red dotted lines are higher located blue straight lines.

In case of the volumetric storage capacity, it can be seen in Figure 5-22 that 10x smaller volumetric storage capacity (0.01 1/m) leads to the same effect as a 10x larger (0.03 m/day) hydraulic conductivity. Due to the very small volumetric storage capacity of the soil, the dike reacts very fast to a water load, this can be seen to the fact that the green dotted lines are close together for the different time steps. It is unknown what the effect is of combining both a 10x smaller volumetric specific storage capacity and 10x larger hydraulic conductivity.

In Figure 5-23, the soil depth is varied. Again, the same strange thing happens that a soil layer of 2 meter has a higher simulated phreatic line than a thicker soil layer at the same time step. Although the phreatic line of the 6 meters sub-soil variant is higher located than the 4 meters variant, which is in line with the theory provided in the TRWD.

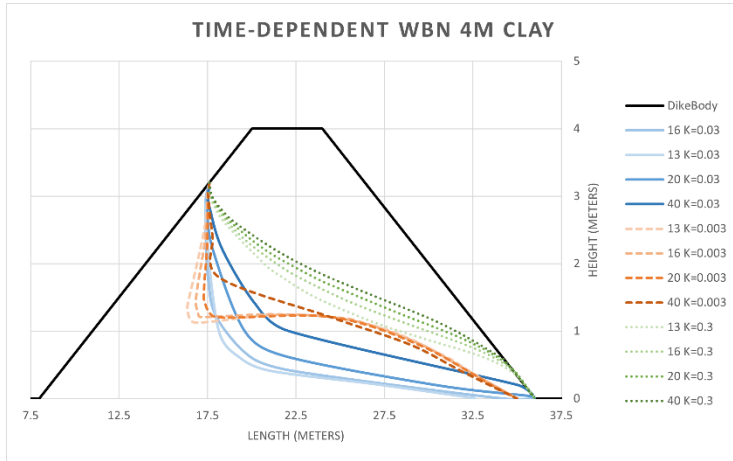


Figure 5-21: The phreatic line for a normative water level with different hydraulic conductivities at different time steps in days together with the dike body and the schematizations of the WC and the TRWD for a clay dike with a 4 meter sub-soil.

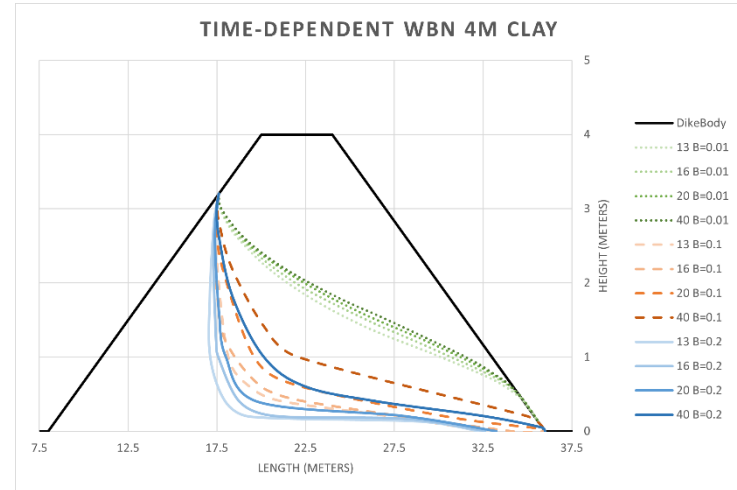


Figure 5-22: The phreatic line for a normative water level with different volumetric specific storage capacity at different time steps in days together with the dike body and the schematizations of the WC and the TRWD for a clay dike with a 4 meter sub-soil.

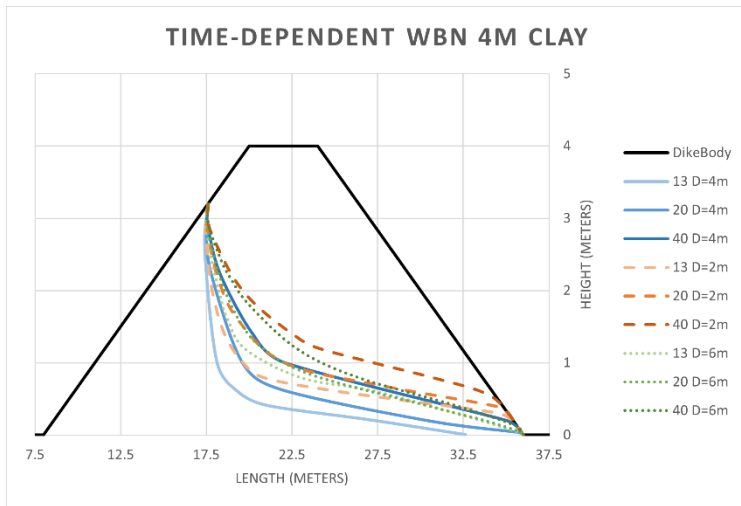


Figure 5-23: The phreatic line for a normative water level with different sub-soil thickness at different time steps in days together with the dike body and the schematizations of the WC and the TRWD for a clay dike with a 4 meter sub-soil.

In the next part, the sand dike with a sub-soil of 4 meter clay is considered. Compared to the clay dike, it can be seen that the effect of the phreatic bulge during daily circumstances is not noticeable in a sand dike. In Figure 5-24, it can be seen that the effect of a smaller or larger hydraulic conductivity has mainly an effect from the outer toe inwards.

In Figure 5-25, it can be seen that the effect different volumetric specific storage on a sand dike is much smaller than on the same variation on a clay dike. This could be due to the fact that the sand is a relatively better permeable than clay. Lastly, the effect of different sub-soil thickness for sand is negligible small as can be seen in Figure 5-26.

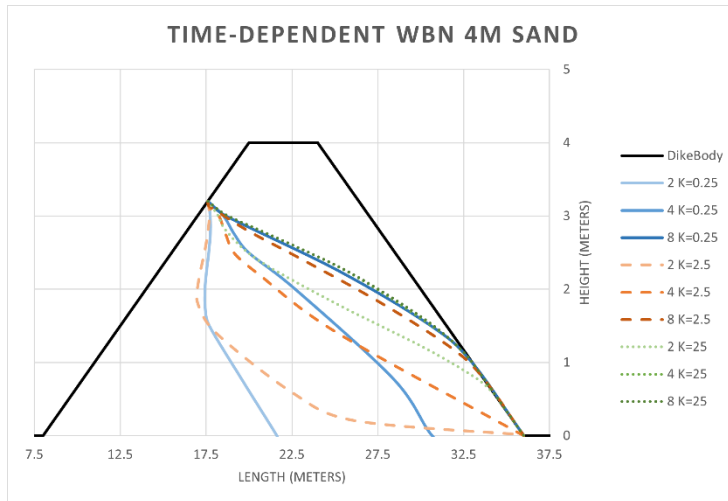


Figure 5-24: The phreatic line for a normative water level with different hydraulic conductivities (unit m/day) at different time steps in days together with the dike body and the schematizations of the WC and the TRWD for a sand dike with a 4 meter sub-soil.

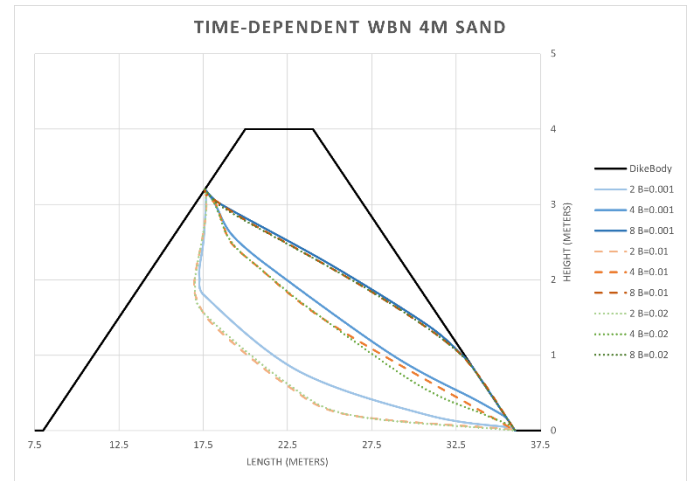


Figure 5-25: The phreatic line for a normative water level with different volumetric storage capacity (unit 1/m) at different time steps in days together with the dike body and the schematizations of the WC and the TRWD for a sand dike with a 4 meter sub-soil.

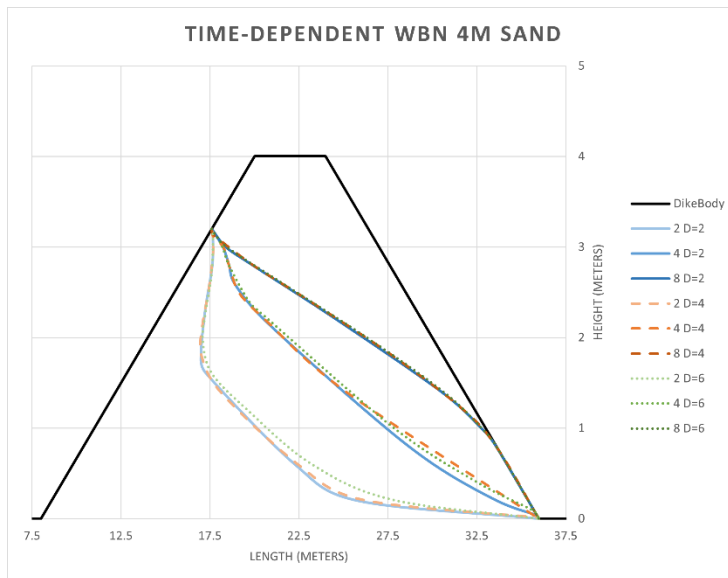


Figure 5-26: The phreatic line for a normative water level with different sub-soil thickness (unit meter) at different time steps in days together with the dike body and the schematizations of the WC and the TRWD for a sand dike with a 4 meter sub-soil.

To summarise, when performing a steady-state analysis, the exact parameter determination is not that important. Since the sensitivity analysis shows that the effect of varying the parameters is neglectable small. For sand dikes, the hydraulic conductivity seems an important variable as the model results are quite different for the different literature values for the hydraulic conductivity of sand. For clay dikes, the specific volumetric storage capacity and the hydraulic conductivity are the parameters which have the most impact on the height of the phreatic line.

5.3.3 DISCHARGE AND STORM DOMINATED HIGH WATER WAVES

In this section, the results of the sensitivity analysis on the discharge and storm dominated high water waves is provided.

Based on the results of the previous sub-section, in which the clay dike the hydraulic conductivity and the specific volumetric storage and for the sand dike only the hydraulic conductivity seems to be the important parameters. Furthermore, for both the clay and sand dike, an analysis on the effect of a more severe (1/1000 years 8 days rainfall event) and a less more extreme rainfall event (1/200 years 8 days rainfall event) will be evaluated. Only for these parameters and the two dike bodies the results will be discussed in this section. The sensitivity analysis for the other parameters can be found in Appendix F.

5.3.3.1 CLAY DIKE

Based on the results of scenario 2 & 3 in the first research sub-question (Figure 5-2), the timesteps 10 and 17 days have been chosen. These timesteps are the peak of the high water wave and 7 days after the peak.

In Figure 5-27 and Figure 5-28, the effect of different hydraulic conductivities is visible on the two different high water waves. It can be seen that a 10x larger hydraulic conductivity simulates a higher located phreatic line compared to a 10x smaller hydraulic conductivity. Only at the inner toe of the dike the WC and the TRWD estimated schematisations of the phreatic line have been reached.

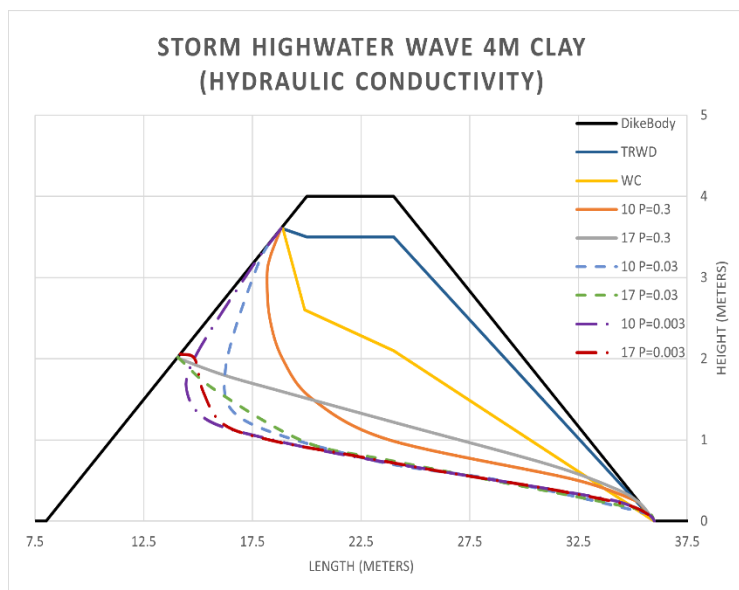


Figure 5-27: The phreatic line for a discharge highwater wave with different hydraulic conductivities (unit m/day) at different time steps in days together with the dike body and the schematisations of the WC and the TRWD for a clay dike with a 4 meter sub-soil.

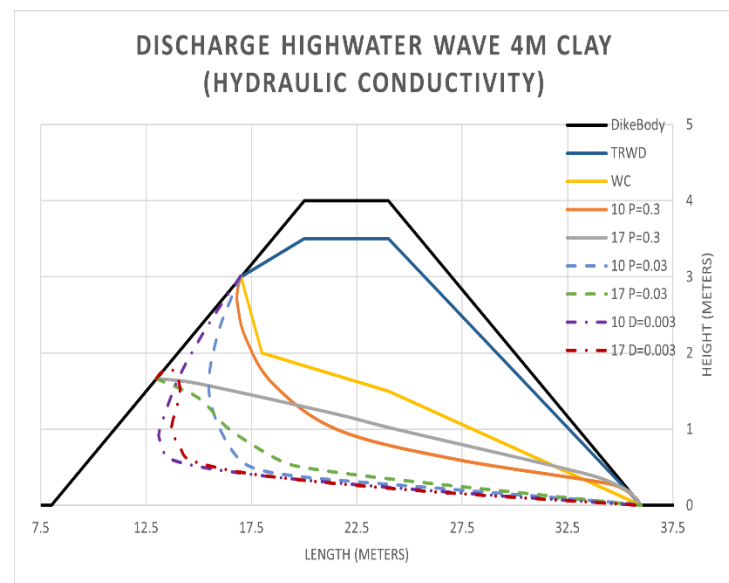


Figure 5-28: The phreatic line for a storm highwater wave with different hydraulic conductivities (unit m/day) at different time steps in days together with the dike body and the schematisations of the WC and the TRWD for a clay dike with a 4 meter sub-soil.

The next parameter, which will be evaluated is the specific volumetric storage. It can be seen that a smaller specific volumetric storage has the same effect higher hydraulic conductivity.

In Figure 5-29 and Figure 5-30, it can be seen that that difference between a 0.1 and 0.2 1/m specific volumetric storage on the phreatic line is nearly neglectable. Only in case of a 10x smaller specific volumetric storage at the inner toe the TRWD and WC estimated schematisation has been reached.

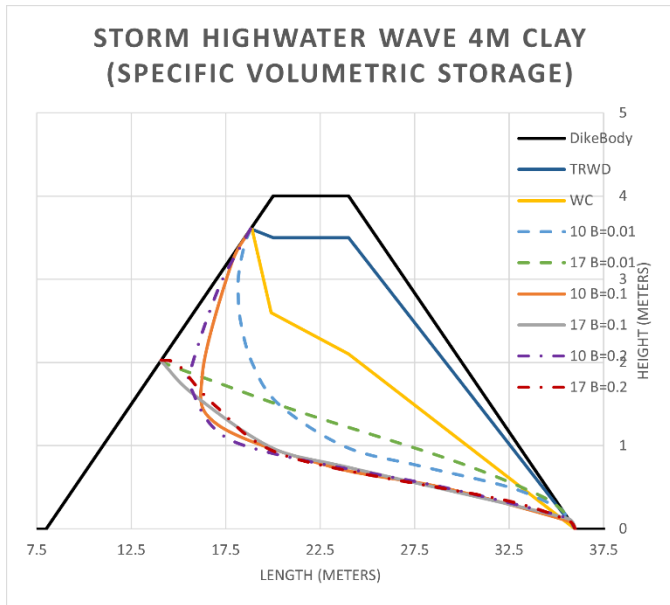


Figure 5-29: The phreatic line for a discharge highwater wave with different specific volumetric storage capacities (unit 1/m) at different time steps in days together with the dike body and the schematizations of the WC and the TRWD for a clay dike with a 4 meter sub-soil.

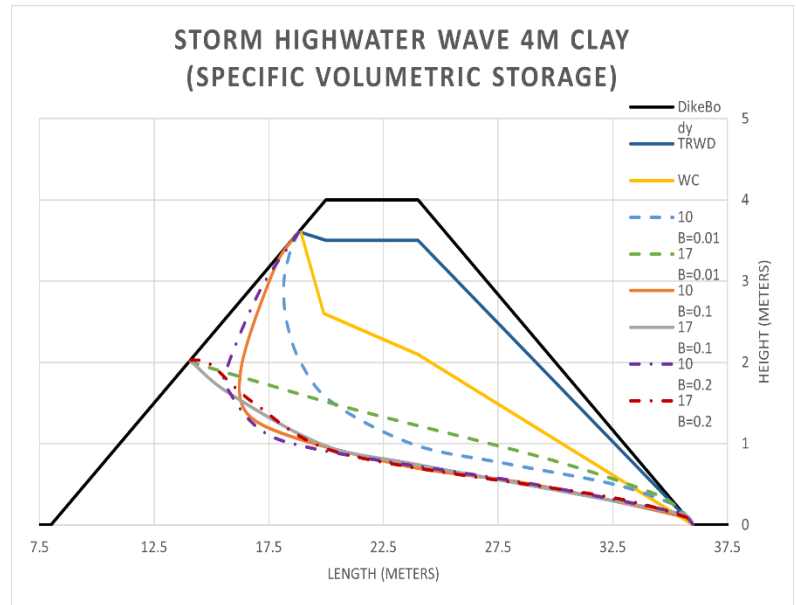


Figure 5-30: The phreatic line for a storm highwater wave with different specific volumetric storage capacities (unit 1/m) at different time steps in days together with the dike body and the schematizations of the WC and the TRWD for a clay dike with a 4 meter sub-soil.

Next, the intensities of the 8-days rainfall events are varied. In the normal scenario, an 8 days uniform rainfall event with a return period of 1/500 years have been used. Now, the rainfall intensities of 1/200 and 1/1000 years have been considered. In Figure 5-32 and Figure 5-33, it can be seen that the effect of a more extreme rainfall event has no influence on the height of the phreatic line during a high water wave.

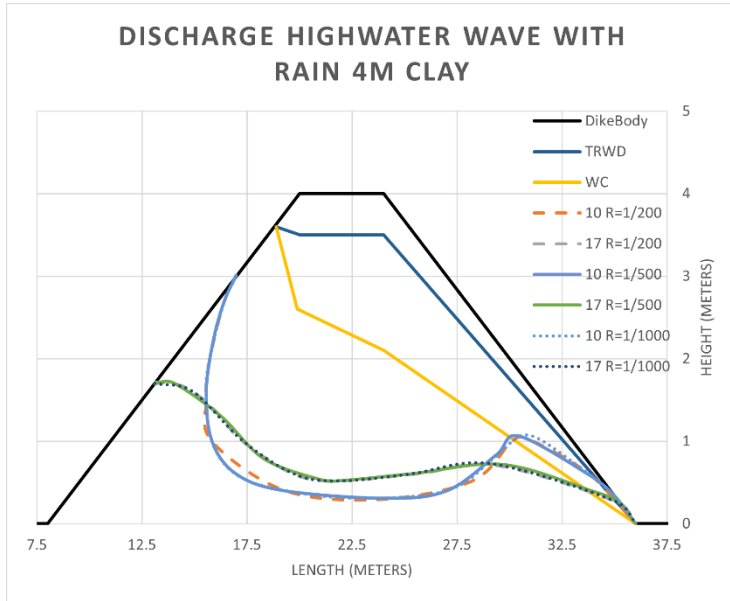


Figure 5-31: The phreatic line for a discharge highwater wave with different rainfall intensities (R = return period 1/... year) at different time steps in days together with the dike body and the schematizations of the WC and the TRWD for a clay dike with a 4 meter sub-soil.

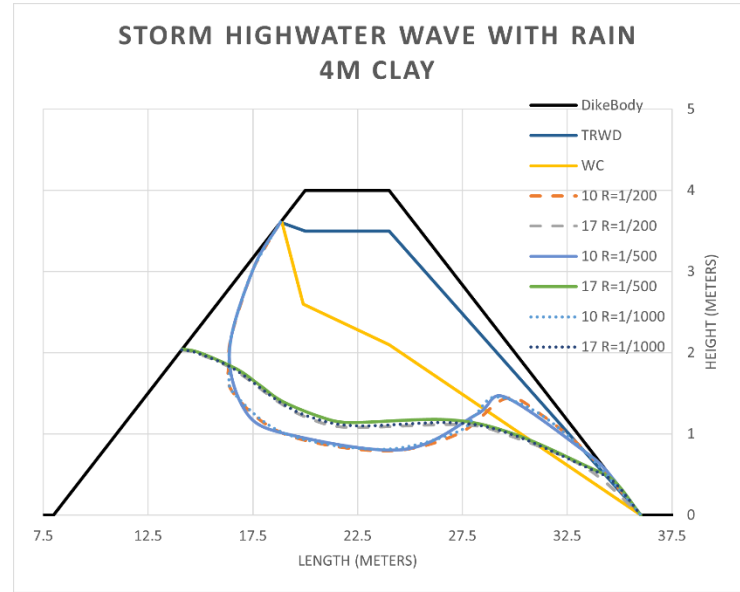


Figure 5-32: The phreatic line for a storm highwater wave with different rainfall intensities (R = return period 1/... year) at different time steps in days together with the dike body and the schematizations of the WC and the TRWD for a clay dike with a 4 meter sub-soil.

5.3.3.2 SAND DIKE

For the sand dike, only the hydraulic conductivity and the rainfall intensities are incorporated in the sensitivity analysis. Since the effects of the time-dependent sensitivity analysis on the normative water levels have shown that the effect of the other parameters on the phreatic line is very small.

In Figure 5-33 and Figure 5-34, the effect of the different hydraulic conductivities on the phreatic line during a discharge and storm high water wave can be found. Interesting to see that a 10x higher hydraulic conductivity gives a higher phreatic line. For all the different hydraulic conductivities the phreatic line is at the same height at the inner toe of the dike.

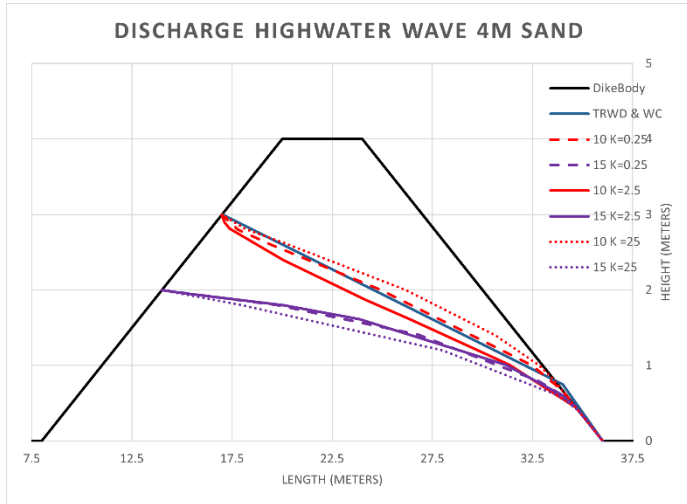


Figure 5-33: The phreatic line for a discharge highwater wave with different hydraulic conductivities (unit m/day) at different time steps in days together with the dike body and the schematizations of the WC and the TRWD for a sand dike with a 4 meter sub-soil.

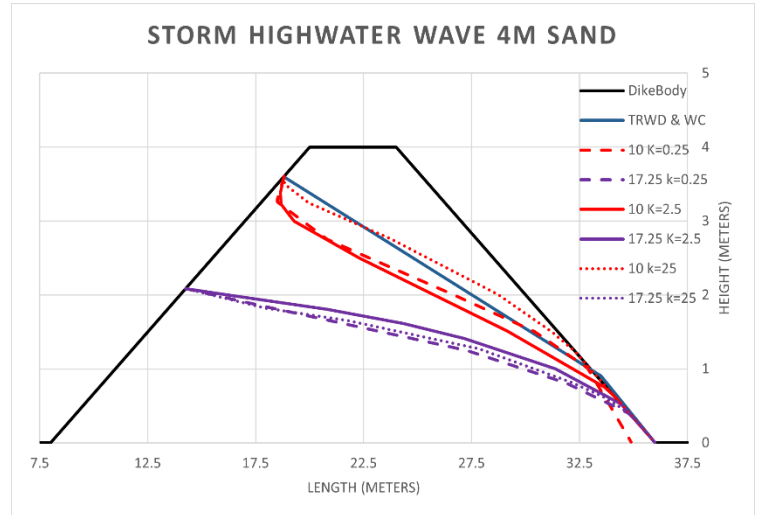


Figure 5-34: The phreatic line for a storm highwater wave with different hydraulic conductivities (unit m/day) at different time steps in days together with the dike body and the schematizations of the WC and the TRWD for a sand dike with a 4 meter sub-soil.

In the last two figures (Figure 5-35 and Figure 5-36), the intensities of the 8 days rainfall event are varied. It can be seen that also the effect of a more extreme rainfall event on the phreatic line in a sand dike is very small.

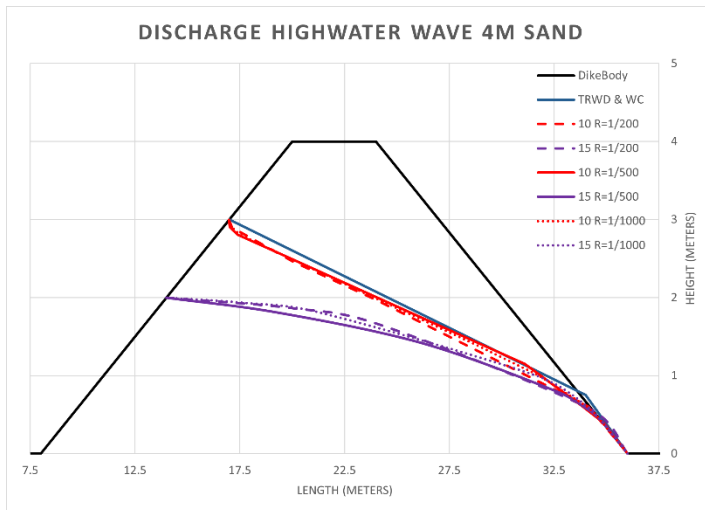


Figure 5-35: The phreatic line for a discharge highwater wave with different rainfall intensities (R = return period 1/... year) at different time steps in days together with the dike body and the schematizations of the WC and the TRWD for a sand dike with a 4 meter sub-soil.

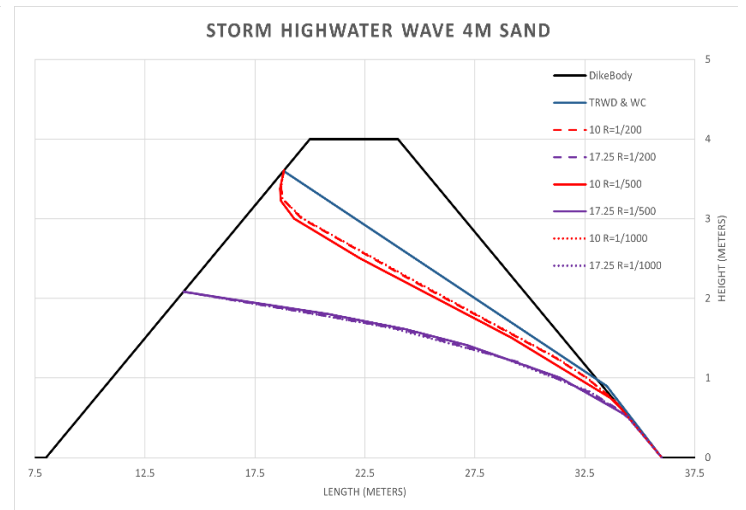


Figure 5-36: The phreatic line for a storm highwater wave with different rainfall intensities (R = return period 1/... year) at different time steps in days together with the dike body and the schematizations of the WC and the TRWD for a sand dike with a 4 meter sub-soil.

6 DISCUSSION

In the first part of this chapter, the modelling choices and assumptions that have been made will be discussed. In the second part, the model results will be discussed. In the end, a comparison between the model results and schematisations will be provided.

6.1 MODELLING CHOICES

The first limitation of this study is that the finite element method is not validated against an analytical model or field measurements. Because of the fictive location and simple dike schematisation, no field measurements are available to validate the model on. Furthermore, no suitable analytical model is available for the phreatic bulge under daily circumstances in dikes, other analytical models assume a constant water level with drainage construction. Therefore, more information on the water height or the groundwater head is needed to validate the model on. This information could be gathered by conducting a physical experiment on a scale model of the dike schematisations used in this research. For example, Al-Janabi et al. (2020, p. 2490) have conducted a physical experiment to validate the numerical model on a silty sand dike with a drainage construction.

For this modelling study, the flow only option has been chosen in Plaxis in order to reduce the computation time. This method treats the soil as a rigid structure and only calculates the (ground)water flow through it. The effect of soil deformation is neglected in this research. Since the soil body does not change over time, this means that the calculation is only valid for stable situations. Therefore, the water forces from a certain high water wave will not affect dike stability. For example, macro instability or piping failure and the effect of these failure mechanisms on the phreatic line will not be simulated and evaluated.

Furthermore, for this study a fully homogeneous dike profile has been chosen. The effect of different sub-soils could lead to local differences in the height of the phreatic line. Besides this, the head of the sandy aquifer has been set to 0.5 meter below the surface level. This is a simplification of reality, as during a high water wave there is an increase in the head of the sandy aquifer, which could cause an increase in the height of the phreatic line.

Next, the water levels of the discharge and storm dominated high water waves have to be normalised on a given water level, because a fictive dike location within the IJssel delta has been chosen. First, the peak of both waves have been normalised on the normative water level. Followed by a slight adaptation to make the contrast between both peaks larger. Therefore, it should be taken into account that the water levels during a high water wave are not absolute values for the IJssel delta. Furthermore, in the high water wave data of Kampen both the peaks with and without the Afsluitdijk have been used. Of course, the peaks in the time period without the Afsluitdijk lead to an overestimation of the overall peak height of the high water waves.

Another option to calibrate the model, could be considered instead of applying several years of actual daily precipitation and evaporation data until an equilibrium state has been reached as was done in this study. A larger amount of artificial precipitation could be applied until a steady-state has been reached. Nevertheless, this option leads to more numerical unstable and unphysical results, such as double phreatic lines. The choice to not use an artificial amount of precipitation does not affect the simulation results but only increases the time until the model has reached an equilibrium state.

For the third research sub-question, the normative water level has been plotted as function of time. It is important to consider that this way of modelling is overestimating high water waves in reality. Normally, a high water wave has a gradual increase in height and starts not directly at its peak (normative water level). Because of this modelling choice, the phreatic line will be located lower in this study compared to a more realistic situation when there is a gradual increase of water height to the normative water level.

For the 8-days rainfall simulations, the precipitation on the inner slope of the sand dikes had to be removed. This to avoid strange ponding results on the inner slope. Of course, removing precipitation from the slope of the sand dike is a simplification of reality and has effects on the model results. Therefore, the results of the precipitation on a sand dike are underestimated compared to reality.

Furthermore, an 8 day uniform distributed rainfall event has been used. In reality, there are more types of rainfall patterns. The choice for the uniform distributed event is because of simplicity and the scope of the research. Also, the ponding parameters ($\psi_{max/min}$) are set to the Plaxis standard and it is unsure whether or not these parameters could have a significant impact on the height of the phreatic line. More research in the effects and the validity of these parameters should be done to find the best way to represent a rain event in the Plaxis model.

6.2 MODEL RESULTS

In the results, it can be seen that there is an increase in phreatic line height at the inner toe of the dike in the high water simulations. The phreatic line height increase at the inner toe could be the effect of first modelling a steady-state water level before the actual high water wave is simulated. This is a conservative modelling approach, because it is unknown how long there is an increased water level in front of the dike before the high water wave starts. More analysis could be done into the exact progression of a high water wave and the effect on the phreatic line at the inner side of the dike.

Furthermore, when simulating the normative water level on a clay dike with and without rainfall as function of time, the results show that the phreatic line is higher located in case of a 1 meter thick sub-soil (Figure 5-10) compared to a 4 meter thick sub-soil (Figure 5-11). The same behaviour is seen in the sensitivity analysis when comparing the 2 meter thick sub-soil with the 4 or 6 meter thick sub-soil (Figure 5-23). However, when comparing the 4 meter thick sub-soil with the 6 meter thick sub-soil the effect is not visible. According to the model results, the phreatic line decreases with an increase in the sub-soil thickness for a thickness smaller than 4 meters, contrary to the TRWD guideline that suggests an increase in the phreatic line with increasing sub-soil layer thickness.

In the sensitivity analysis, variation in the volumetric specific storage soil parameter gives diverse results (Figure 5-16). When doubling only this soil parameter, the peaks and the valleys of the phreatic line are inversed compared to the original situation. As the other parameters were constant in these simulations, the cause of this effect should be the volumetric specific storage capacity of the soil. More research should be done into the effect and importance of the volumetric specific storage parameter.

6.3 COMPARISON PLAXIS MODEL AND SCHEMATISATIONS

The main goal of this research is to provide insight into the phreatic line schematisations provided in the TRWD and the WC. In this section, the comparison and differences between the model results and the schematisations will be discussed.

The TRWD schematisation shows that for a thicker clay sub-soil layer the phreatic line will be higher located in the dike for clay dikes (Figure 4-3). In the model results, this effect is visible in the phreatic line under daily circumstances (Figure 5-1) and in the sensitivity analysis with different sub-soil thickness (Figure 5-23). However, the results of the normative water levels show that the steady-state on a clay dike with a 1 meter clay sub-soil will be reached earlier compared to the clay dike with a 4 meter sub-soil (Figure 5-10, Figure 5-11). Furthermore, the high water wave simulations on a clay dike with a 1 meter sub-soil show an increase of the phreatic line at the inner toe of the dike, this is in contradiction with the theory suggested in the TRWD about the sub-soil thickness.

Because of the results of the sensitivity analysis and the normative water levels on a 1 meter thick sub-soil, it could be that in the situation with a 1 meter thick clay sub-soil layer other hydrological mechanisms dominate, therefore more research should be conducted on the exact effect of sub-soil on the phreatic line. Furthermore, the TRWD schematisation shows an increase of the phreatic line below the dike crest for some dike geometries and water levels. In none of the simulations, this effect is measured.

In research of Al-Janabi et al. (2020, p. 2490), an experimental and numerical analysis of the phreatic line has been conducted on a silty sand dike. The hydraulic conductivity of this material is comparable with the hydraulic conductivity of the clay dike in this research. The results of both the experimental and numerical analysis show that there is an even larger increase of the phreatic line at the inner toe of the dike than in this research. However, the experimental and simulation conditions are not exactly identical, which have an influence on the height of the phreatic line. In the research of Al-Janabi et al. (2020 p. 2490), a steady-state water height is applied and there is a drainage construction in the inner toe of the dike. Furthermore, the volumetric specific storage capacity of silty sand is much smaller than clay. All these characteristics lead to a higher phreatic line compared to this research.

The WC schematisation for clay dikes is not depending on the geometry and sub-soil thickness, but suggest a phreatic line drop of 1 meter around the inner crest line of the dike. In the high water waves simulations, it can be seen that the phreatic line drop is larger than 1 meter.

The results of the sand dikes are more in line with the schematisations provided by the TRWD and the WC. The exit point as provided in both the TRWD and the WC schematisations at $0.25 \cdot$ the outer water level relative to the surface level is in none of the simulation results exceeded. Furthermore, the effect of the clay sub-soil thickness is neglectable for sand dikes as shown in the simulation results and provided in the guidelines of the TRWD.

7 CONCLUSION

In this section the conclusions from this research and the answers of the research (sub-)questions are present. Following the conclusions is the recommendations for further research.

In this study, the aim was to provide insights into what degree the estimated schematisation of the phreatic line approximation, as currently stipulated in the *Technisch Rapport Waterspanning bij dijklichamen* (Van der Meer et al., 2004) and provided by the *Waternet Creator* (Van der Meij, R., 2020), are conservative approximations. These insights can help the waterboard to decide whether they can deviate from this prescribed standard for the dike assessments.

To achieve this aim, the following main research question was posed:

Can the current phreatic line schematisation be improved to provide a more realistic safety factor for the inner macro stability?

This main research question has been divided into four sub-questions as presented in Chapter 1. The answers for each of these sub-questions will be provided, followed by the conclusion of the main research question.

1. What are the main factors influencing the phreatic line?

Based on the literature research of the first sub-question, the main influencing factors on the phreatic line are the variation in water levels, precipitation and evaporation. The water levels have the largest influence on the position of the phreatic line, as the inner and outer water levels determine the entry and exit point of the phreatic line in the dike. Next, precipitation and evaporation are important parameters, as they could cause a phreatic line to rise 0.5 to 1.0 meter during extreme rainfall events. This was also found in the simulations where the phreatic line in case of a situation with rainfall is around 1 meter higher at the inner crest area of the dike compared to a situation without rainfall.

The factors affecting the phreatic line are the soil characteristics. Especially the hydraulic conductivity and the specific volumetric storage of the soil have a larger influence on the progression of the phreatic line through the dike. As soil is often anisotropic, the hydraulic conductivity differs in the horizontal and vertical direction. The horizontal component of the hydraulic conductivity is more important for the height of the high water wave, as the flow of a high water wave is mostly horizontal. However, the vertical component is more important for precipitation as rainfall has to infiltrate in the vertical direction to the phreatic line. Furthermore, the effect of the relative low permeable sub-soil above the sandy aquifer is also related to the vertical hydraulic conductivity.

Both the volumetric specific storage capacity of the soil and the hydraulic conductivity have an impact on how fast the dike reacts to a high water wave. A relative small volumetric specific storage leads to a more horizontal progression of the phreatic line through the dike similar to a relatively high hydraulic conductivity.

2. What are the effects of different hydraulic conditions on the phreatic line?

During the simulation of the phreatic line under daily circumstances, in which only the precipitation and evaporation data of 2019 has been incorporated, it appears that a thicker sub-soil layer on a clay dike results in a higher located and more variation in the phreatic line over time. Therefore, it is important to consider the daily circumstances when choosing a start position for further modelling, for example, the high water waves.

When simulating a storm and discharge dominated high water wave (Figure 5-2 & Figure 5-3), it becomes clear that there is an increased phreatic line at the inner toe of the clay dike compared to the phreatic line

schematisations provided in the TRWD and the WC. This location is important for the stability of the dike slope as a higher phreatic line could lead to a saturated soil at that location which could affect the macro stability of the dike slope. For the sand dikes (Figure 5-4 & Figure 5-5), the simulated phreatic line at the inner toe does not exceed the TRWD and the WC phreatic line schematisations.

Lastly, the rainfall has been incorporated in the high water waves simulations. The effects of precipitation on a clay dike is compared to a sand dike. For the clay dikes, the effects of rainfall on the height of the phreatic line is largest at the inner side of the dike. The phreatic line has raised around 0.5 meters during the peak of the high water wave compared to the high water wave simulation without rainfall, exceeding both the TRWD and the WC estimation at the inner side of the dike (Figure 5-6 & Figure 5-7). For sand, the effect of rainfall is relatively low. The TRWD and the WC phreatic line estimated schematisation will not be exceeded and can be used as a safe approximation during the simulated high water wave and rainfall events dikes (Figure 5-8 & Figure 5-9).

3. What different realistic situations lead to the prescribed schematic estimation of the phreatic line?

The simulations with different hydraulic conditions showed that the prescribed schematic estimation of the phreatic line provided by the TRWD and the WC is reached but not exceeded during a high water wave with and without rainfall on a sand dike. For the clay dikes, the prescribed schematic estimation of the TRWD and the WC have been exceeded at the area below the inner crest of the dike and at the inner toe of the dike. One exception is the discharge high water wave on a 4 meter thick sub-soil. For the clay dikes, the prescribed schematic estimation of the TRWD and the WC have been exceeded in all simulations below at the inner toe of the dike (Figure 5-2 & Figure 5-3). One exception is the discharge high water wave on a 4 meter thick sub-soil.

In the simulations with the normative water level as function of time, it became clear that for a clay dike with a sub-soil of 4 meter already after 20 days the phreatic line at the inner toe has exceeded the WC and the TRWD prescribed schematic estimation (Figure 5-10). When the sub-soil thickness has decreased from 4 meter to 1 meter, the WC and the TRWD estimation of the phreatic line is already exceeded after 12 days at the inner toe (Figure 5-11). The effect of precipitation on a clay dike with a thicker sub-soil layer is larger compared to a dike on with a thin or a better permeable sub-soil. In both cases, the TRWD and the WC estimation would be reached earlier due to precipitation compared to the situations without rainfall (Figure 5-13 & Figure 5-14).

For the sand dikes, the phreatic line during steady-state conditions is higher located than the TRWD and the WC schematic estimation. The steady-state is already reached around 8 days. Furthermore, it can be seen that the height of the phreatic line does not depend on the sub-soil thickness, which is in line with the guidelines provided in the TRWD.

Finally, it can be concluded that the TRWD and the WC prescribed estimation of the phreatic line is not conservative enough for the clay dikes. Even when taking precipitation into account the WC schematisation will be reached faster. The simulated phreatic line is especially higher at the inner toe compared to the schematisation in the guidelines. Based on these simulations, it would be recommended to take the exit point of the phreatic line at the inner toe of the dike at a height of $0.25 \cdot$ the peak of the high water wave. The same concept as has been provided in the TRWD guidelines for the schematisation of the phreatic line for sand dikes.

Furthermore, the phreatic line schematisation under the crest of the clay dike is in both the TRWD and the WC schematisations overestimated compared to the simulation results of the high water waves. Based on these results, the heights of points A & B of TRWD schematisation and the Boffset of the WC schematisation could be lowered to provide a less conservative phreatic line schematisation. However, to get the exact heights of these points and to provide a reliable safety margin in the schematisations more research should be done.

4. Which factors have the most impact on the schematic estimation of the phreatic line?

A few conclusions can be drawn based on the results of the sensitivity analysis conducted to answer this research question. First of all, when simulating the phreatic line with precipitation over a year, a decrease in hydraulic conductivity leads to a higher phreatic line, however the variation in height over time will decrease (Figure 5-15).

Next, a relatively low specific volumetric storage leads to more variation in the phreatic line over time under daily circumstances (Figure 5-16). Furthermore, when performing a steady-state simulation in Plaxis (Figure 5-19 & Figure 5-20), the exact determination of the soil parameters is not extremely important, as the differences in the progression of the phreatic line are negligible small. Besides that, it became clear in the sensitivity analysis on the time-dependent simulation of the normative water level that the hydraulic conductivity and the specific volumetric storage capacity are important parameters for a homogeneous clay dike (Figure 5-21 & Figure 5-22). Especially, the hydraulic conductivity parameter as both a decrease and increase of permeability leads to a higher phreatic line (Figure 5-21), because a decrease of permeability leads to a higher phreatic line under daily circumstances. In case of a sand dike, only the hydraulic conductivity is an important parameter for the schematisation of the phreatic line (Figure 5-24).

Lastly, it can be concluded that both an intensification and a de-intensification of the 8-days rainfall event on clay and sand dikes do not lead to a rise or drop in the phreatic line during a discharge and storm dominated high water wave (Figure 5-31, Figure 5-32, Figure 5-35 and Figure 5-36).

Main Research Question

The research sub-questions above served to answer the main research question, which is the following question: *Can the current phreatic line schematisation be improved to provide a more realistic safety factor for the inner macro stability?*

The research has shown the effect of different hydrological conditions, soil parameters and sub-soils on the progression of the phreatic line during different hydraulic conditions (e.g., high water waves). From the simulations, it becomes that clear that for clay dikes, the phreatic line at the inner side of the dike is underestimated by the TRWD and the WC schematisations compared to the simulation results. Based on these simulations it would be recommended to take the exit point of the phreatic line at the inner toe of the dike at a height of $0.25 \cdot$ the peak of the high water wave relative to the surface level. The same concept as has been provided in the TRWD guidelines for the schematisation of the phreatic line for sand dikes.

The model simulations show that the height of the phreatic line increases when the clay sub-soil thickness increases. The TRWD states that the height of the phreatic line is depending on the sub-soil thickness. The WC schematic estimation of the phreatic line has not incorporated this effect. Therefore, it would be recommended to incorporate the thickness of the clay sub-soil layer in the schematisation of the phreatic line, as the simulation results show that the height of the phreatic line increases when the clay sub-soil thickness increases.

For the sand dike, the difference between the simulated phreatic line and the TRWD and WC estimated schematisations is not significantly larger. The TRWD and WC estimated schematisations are not overestimating nor underestimating the phreatic line, therefore no adaptations have to be made for sand dikes.

8 RECOMMENDATIONS

Based on the results of this study, a few recommendations for further study and for the use of application of FEM models to simulate the phreatic line are done.

One of the main limitations of this research, as already stated in the discussion, is the fact that the results of this finite element method could not be validated against an analytical model nor field measurements. Therefore, the credibility of these types of models is still unknown. It would be a good idea to validate this type of numerical models with field data. Physical lab experiments are only recommended for simple dike geometries to validate different analytical solutions or numerical models.

There is an increase in the phreatic line height at the inner toe of the dike in the simulation results of the high water wave on a clay dike. The cause of this effect is still unknown and in contradiction with the guidelines provided in the TRWD and the WC. However, especially the validity of the model has to be checked at the inner toe of the dike. Therefore, it is recommended to investigate the cause of this higher phreatic line at the inner toe of the dike in more detail. When it turns out that the model results are indeed correct, the TRWD and WC phreatic line schematisations of the clay dikes have to be altered.

As already explained in the conclusion, based on the simulation results it would be recommended to take the exit point of the phreatic cline at the inner toe of the dike at a height of $0.25 \cdot \text{peak of the high water wave}$ relative to the surface level. In this proposed exit point height, an extra margin is incorporated on top of the simulation results. The same concept as has been provided in the TRWD guidelines for the schematisation of the phreatic line for sand dikes.

Furthermore, when limited (ground)water pressure measurements are available then the waterboard have to rely on the TRWD and the WC schematisation to estimate the phreatic line. Based on the simulation results of the sand dike, the TRWD and WC schematisations are a good approximation when no field measurements are available. However, for clay dikes it is not recommended to use the TRWD nor the WC schematisation of the phreatic line, because in almost all simulations the schematic estimations have been exceeded at the inner side of the dike and therefore the schematisations underestimate the height of the phreatic line. It would be recommended to do the phreatic line analysis in a Finite Element Method in Plaxis for clay dikes. In this analysis, it is important to incorporate a realistic and extreme rainfall time series and high water waves scenarios.

In this research, the effects of individual rainfall peaks in the daily net precipitation could not always be correlated to a rise or drop of the phreatic line over time. To get more insight into the effect of weather conditions on the phreatic line, more extensive research could be carried out with different types of precipitation events.

Lastly, as the height of the phreatic line varied over time, it is a good approach to first simulate the phreatic line under daily circumstances with actual precipitation and evaporation data to see what the maximum phreatic bulge under the daily circumstances is. This maximum could then be the starting point for further modelling such as high water waves.

BIBLIOGRAPHY

Al-Janabi, A. M. S., Ghazali, A. H., Ghazaw, Y. M., Afan, H. A., Al-Ansari, N., & Yaseen, Z. M.

(2020). Experimental and Numerical Analysis for Earth-Fill Dam Seepage.

Sustainability, 12(6), 2490. <https://doi.org/10.3390/su12062490>

Assaad, F. A., LaMoreaux, J. W., & Hughes, T. (2004). *Field Methods for Geologists and Hydrogeologists*. Springer Publishing.

Beersma, J., Hakvoort, H., Jilderda, R., Overeem, A., & Versteeg, R. (2019). *Neerslagstatistiek en -reeksen voor het waterbeheer 2019* (Vol. 19). Kruyt Grafisch Adviesbureau.

<https://www.stowa.nl/sites/default/files/assets/PUBLICATIES/Publicaties%202019/S TOWA%202019-19%20neerslagstatistieken.pdf>

Billen, M. (2020). *UCD GEL 56 - Introduction to Geophysics*.

[https://geo.libretexts.org/Courses/University_of_California_Davis/UCD_GEL_56 - Introduction to Geophysics](https://geo.libretexts.org/Courses/University_of_California_Davis/UCD_GEL_56_-_Introduction_to_Geophysics)

Bootsma, J. (2019). *Optimalisatie van de faalkanseis en de schematisatie van het faalmechanisme macrostabiliteit buitenwaarts* (Bachelor's thesis, University of Twente). <http://purl.utwente.nl/essays/80175>

Brinkgreve, R. B., & Wendy, M. S. (2008). Possibilities and limitations of the finite element method for geotechnical applications. *Delft University of Technology, Faculty of Civil Engineering and Geo-sciences, Geo-engineering Section*.

https://www.gidhome.com/archive/GiD_Convention/2008/papers/p98.pdf

- Burger, R. L., & Belitz, K. (1997). Measurement of anisotropic hydraulic conductivity in unconsolidated sands: A case study from a shoreface deposit, Oyster, Virginia. *Water Resources Research*, 33(6), 1515-1522. <https://doi.org/10.1029/97WR00570>
- Chbab, E. H. (2019). *Basisstochasten WBI-2017 Statistiek en statische onzekerheid*. Technical Report 1209433-012, Deltares, Delft, The Netherlands.
<https://www.helpdeskwater.nl/onderwerpen/waterveiligheid/primaire/beoordelen/@205816/basisstochasten/>
- Das, B. M., & Sobhan, K. (2016). *Principles of geotechnical engineering*. Nelson Education.
- de Loor, D. A. (2018). *An Analysis of the Phreatic Surface of Primary Flood Defences* (Master's thesis, Delft University of Technology). <http://resolver.tudelft.nl/uuid:0c0b9178-bebe-4a7e-95a0-a619fba82fe6>
- de Raadt, W. S., Jaspers Focks, D. J., Van Hoven, A., & Regeling, E. (2015). *How To Determine the Phreatic Surface in a Dike during Storm Conditions with Wave Overtopping: A Method Applied to the Afsluitdijk*. <https://doi.org/10.3233/978-1-61499-580-7-509>
- de Wijs, Y. (2020) *Winter 2019-2020: (december, januari, februari)* (in Dutch). Koninklijk Nederlands Meteorologisch Instituut, De Bilt, The Netherlands.
<https://www.knmi.nl/nederland-nu/klimatologie/maand-en-seizoensoverzichten/2020/winter>
- Dorst, P. H. (2019). *Modelling the phreatic surface in regional flood defences* (Master's Thesis, Wageningen University & Research). <http://resolver.tudelft.nl/uuid:269046f2-bf32-4b97-bdf2-e5b81d53c4d8>

- Expertisenetwerk waterveiligheid. (2009). *Technisch Rapport Actuele sterkte van dijken* (in Dutch). Technical Report.
- https://www.helpdeskwater.nl/publish/pages/144724/trasd_technischrapportactuelesterktevandijken.pdf
- Fanchi, J. (2010). *Integrated reservoir asset management: principles and best practices*. Gulf Professional Publishing.
- Fredlund, D. G. (2000). The 1999 R.M. Hardy Lecture: The implementation of unsaturated soil mechanics into geotechnical engineering. *Canadian Geotechnical Journal*, 37(5), 963–986. <https://doi.org/10.1139/t00-026>
- Fredlund, D. G. (2006). Unsaturated soil mechanics in engineering practice. *Journal of geotechnical and geoenvironmental engineering*, 132(3), 286-321.
- [https://doi.org/10.1061/\(ASCE\)1090-0241\(2006\)132:3\(286\)](https://doi.org/10.1061/(ASCE)1090-0241(2006)132:3(286))
- Dijkteam Zwolle (2020). *Stadsdijken Zwolle Plaxis Analyse – Freatische lijn (STBU)* (in Dutch). Internal Report, Waterschap Drents Overijsselse Delta. Unpublished.
- Gerritsen, G. H. (2019). *Hoogwater Analyse IJsseldelta* (in Dutch). Internal Report, Waterschap Drents Overijsselse Delta. Unpublished.
- ‘t Hart, R., De Bruijn, H., & de Vries, G. (2016). *Fenomenologische beschrijving* (in Dutch). Technical Report 1220078-000, Deltares, Delft, The Netherlands.
- https://www.helpdeskwater.nl/publish/pages/144669/fenomenologische_beschrijving.pdf

Helpdesk Water. (n.d.). *Wat gaat er veranderen in WBI voor wat betreft macrostabiliteit?* (in Dutch).

<https://www.helpdeskwater.nl/onderwerpen/waterveiligheid/primaire/beoordelen/vragen/macrostabiliteit/macrostabiliteit/gaat-veranderen-wbi/>

Helpdesk Water. (2017). *Beoordelingsinstrumentarium (WBI2017)* (in Dutch).

<https://www.helpdeskwater.nl/onderwerpen/waterveiligheid/primaire/beoordelen/beoordelingsinstrumentarium-wbi2017-0/>

Kanning, W., Huber, M., Krogt Mvd, S. T., & Teixeira, A. M. (2015). *Derivation of the semi-probabilistic safety assessment rule for inner slope stability*. Technical Report 1230086-009, Deltares, Delft, The Netherlands.

<https://www.helpdeskwater.nl/publish/pages/157096/1220080-003-zws-0018-derivationofthesemi-probabilisticsafetyassessmentruleforinnerslopestability.pdf>

Lind, B. B., & Lundin, L. (1990). Saturated hydraulic conductivity of Scandinavian tills. *Hydrology Research*, 21(2), 107-118.

Ministerie van Infrastructuur en Waterstaat. (2019). *Schematiseringshandleiding macrostabiliteit* (in Dutch).

<https://www.helpdeskwater.nl/onderwerpen/waterveiligheid/primaire/beoordelen/@205756/schematiseringshandleiding-macrostabiliteit/>

Oosterbaan, R. J., & Nijland, H. J. (1994). 12 Determining the Saturated Hydraulic Conductivity.

Planbureau voor de Leefomgeving. (2014). *Kleine kansen - grote gevolgen* (in Dutch).

<https://www.pbl.nl/publicaties/kleine-kansen-grote-gevolgen>

Plaxis. (2020). *Reference Manual*.

<https://communities.bentley.com/products/geotech-analysis/w/plaxis-soilvision-wiki/46137/manuals---plaxis>

Kremer, R. H. J., Van der Meer, M. T., Niemeijer, J., Koehorst, B. A. N., & Calle, E. O. F. (2001).

Technisch Rapport Waterkerende Grondconstructies; Geotechnische aspecten van dijken, dammen en boezemkaden (in Dutch). *TR19-prepared by GeoDelft*.

<http://resolver.tudelft.nl/uuid:e9533009-c1e1-4f06-bd19-d79538822fbe>

Technisch Adviescommissie voor de Waterkeringen. (1996). *Clay for Dikes*. Technical Report,

Technische Adviescommissie voor de Waterkeringen.

<http://resolver.tudelft.nl/uuid:76d7502e-1519-449f-874f-fcd70f12c221>

Thusyanthan, N. I., & Madabhushi, S. P. G. (2003). Scaling of seepage flow velocity in

centrifuge models. *CUED/D-SOILS/TR326*, 1-13.

Tuller, M., Or, D., & Hillel, D. (2004). Retention of water in soil and the soil water

characteristic curve. *Encyclopedia of Soils in the Environment*, 4, 278-289.

Van den Akker, J. J. H. (2001). *Een inventarisatie van bodemfysische materiaalmodellen zoals*

toegepast in het landbouwkundig onderzoek (in Dutch).

Van der Meer, M. T., Niemeijer, J., Post, W. J., & Heemstra, J. (2004). *Technisch rapport*

waterspanningen bij dijken Waterkeringen (TAW) (in Dutch). *TR26-DWW-2004-057*.

<https://www.helpdeskwater.nl/onderwerpen/waterveiligheid/primaire/technische-leidraden/zoeken-technische/@192510/technisch-rapport-0/>

Van der Meij, R. (2020). *D-Stability installation manual*. User Manual D-Stability, Deltares, Delft, The Netherlands. <https://www.deltares.nl/app/uploads/2019/06/User-manual-D-Stability-2020.03.3.pdf>

Vogel, T., Van Genuchten, M. T., & Cislerova, M. (2000). Effect of the shape of the soil hydraulic functions near saturation on variably-saturated flow predictions. *Advances in water resources*, 24(2), 133-144.

Warmink, J. J. (2019). *Syllabus Hydraulic Engineering*. University of Twente. Unpublished.

Wösten, J. H. M., Veerman, G. J., de Groot, W. J. M., & Stolte, J. (2001). *Waterretentie- en doorlatendheidskarakteristieken van boven- en ondergronden in Nederland: de Staringreeks; vernieuwde uitgave 2001* (in Dutch). (Alterra-rapport 153). Alterra. <https://edepot.wur.nl/43272>

APPENDICES

A SURFACE GEOMETRIES

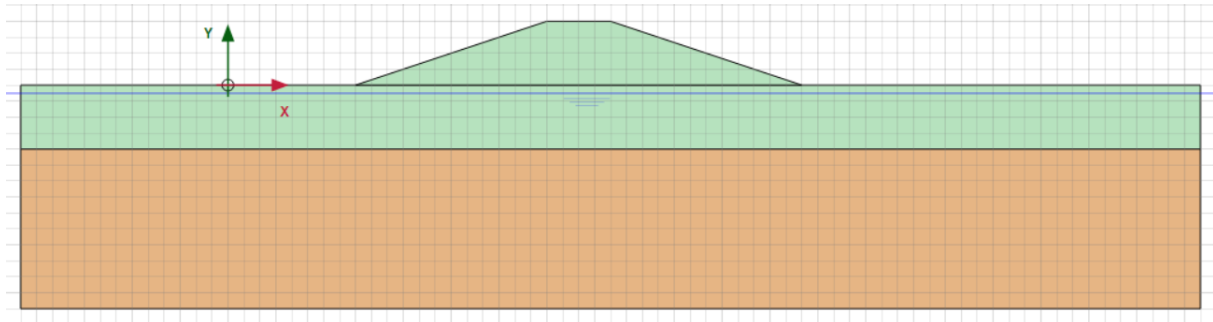


Figure A-1: Clay Dike (green) with 4 meter clay (green) and 10-meter sand layer (orange) (square = 1 by 1 meter).

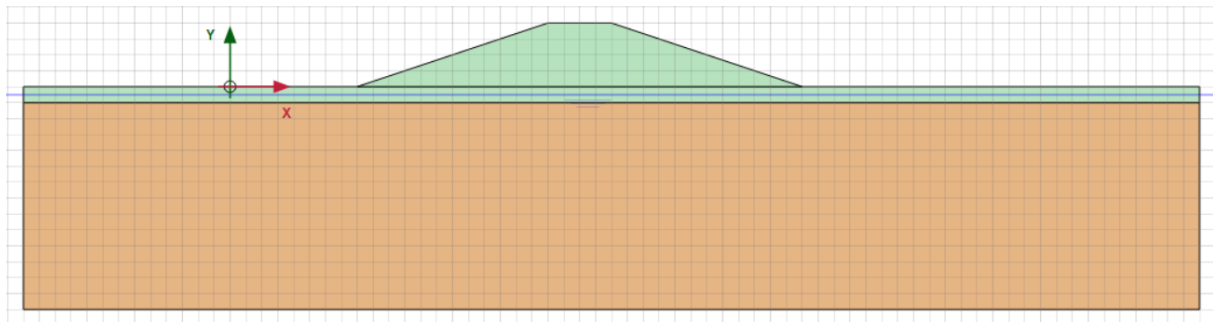


Figure A-2: Clay Dike (green) with 1 meter clay (green) and 13 meter sand layer (orange) (square = 1 by 1 meter).

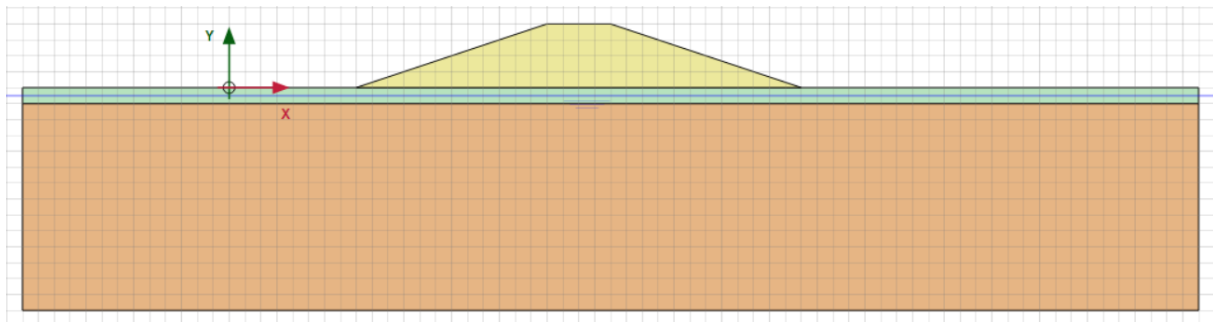


Figure A-3: Sand Dike (yellow) with 1 meter clay (green) and 13 meter sand layer (orange) (square = 1 by 1 meter).

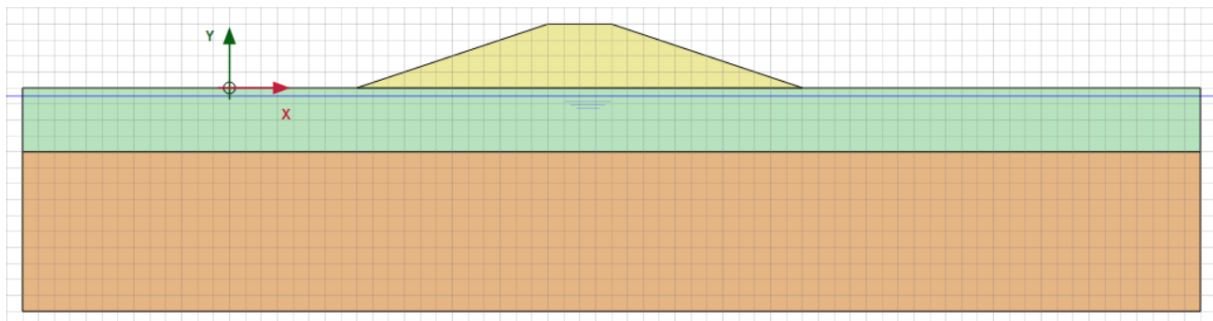


Figure A-4: Sand Dike (yellow) with 4 meter clay (green) and 10-meter sand layer (orange) (square = 1 by 1 meter).

B RAINFALL TIME SERIES

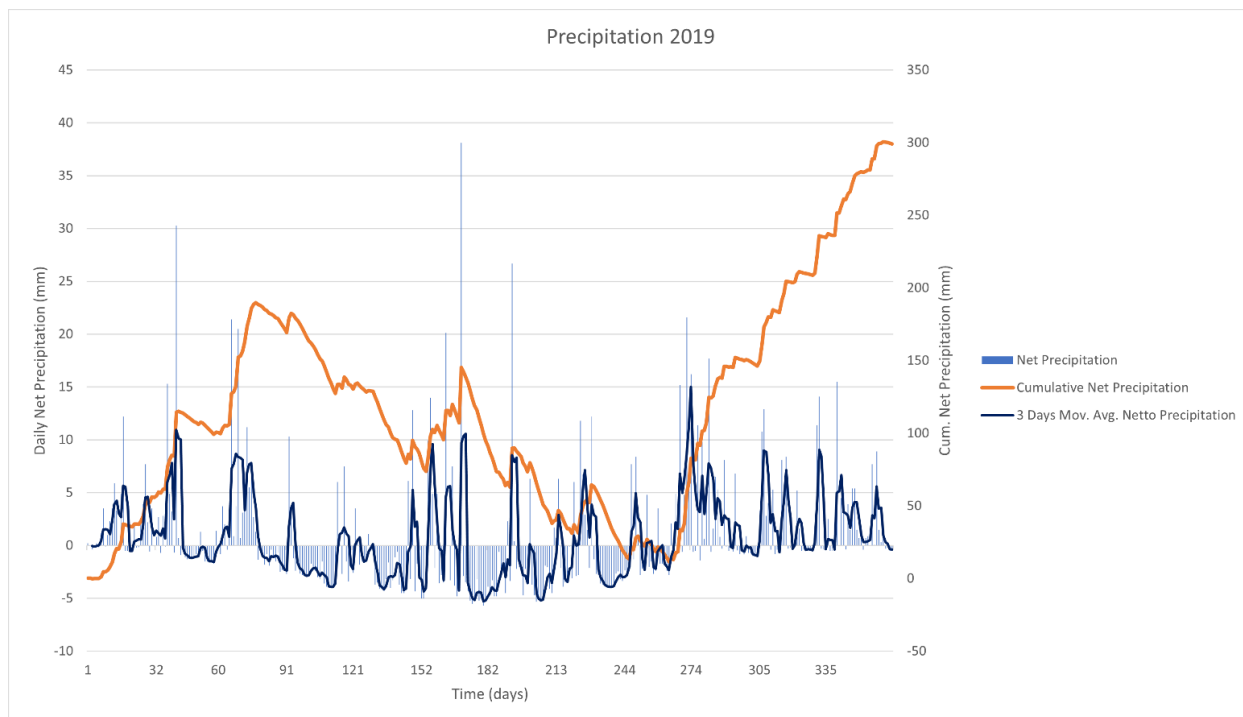


Figure A-5: The daily precipitation of 2019 on the left vertical axis as function over the time in days (blue columns) with the 3 days moving average (dark blue solid line). Orange line indicates the cumulative net precipitation over time (right vertical axis).

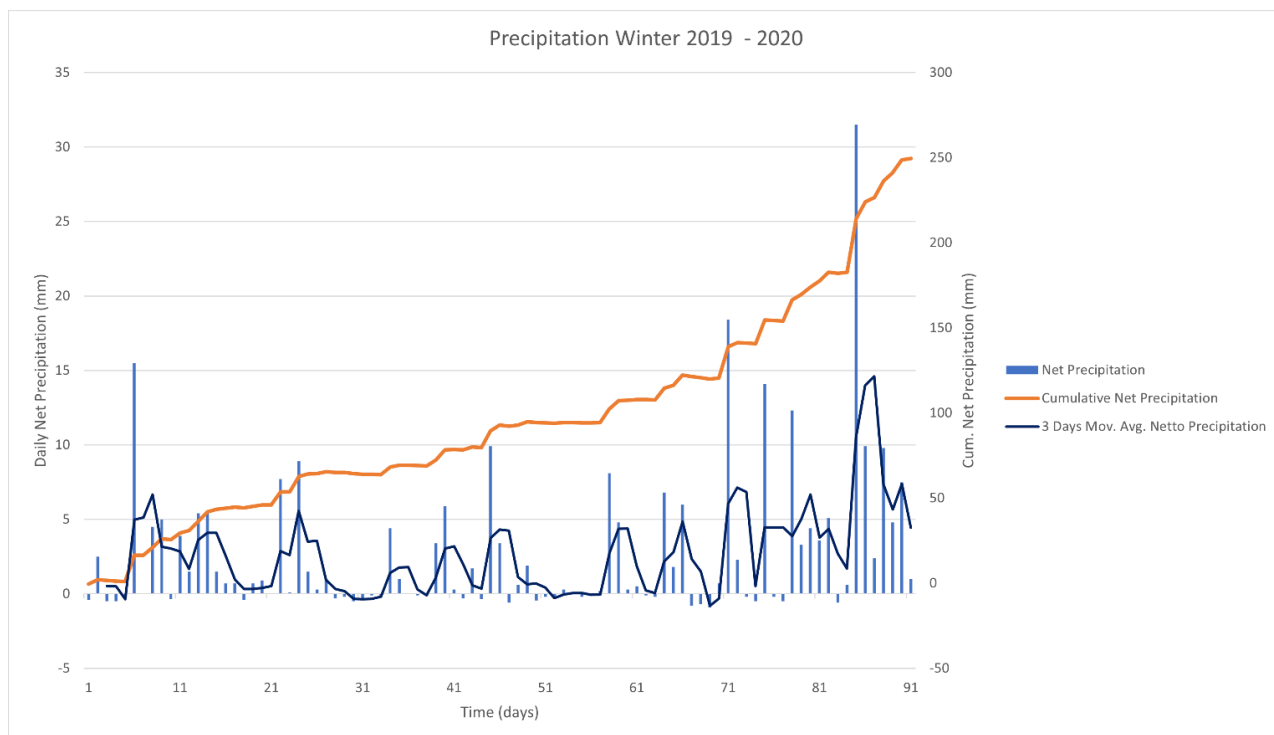


Figure A-6: The daily precipitation of winter 2019-2020 on the left vertical axis as function over the time in days (blue columns) with the 3 days moving average (dark blue solid line). Orange line indicates the cumulative net precipitation over time (right vertical axis).

C 75% CONFIDENCE INTERVAL DISCHARGE/STORM HIGH WATER WAVE

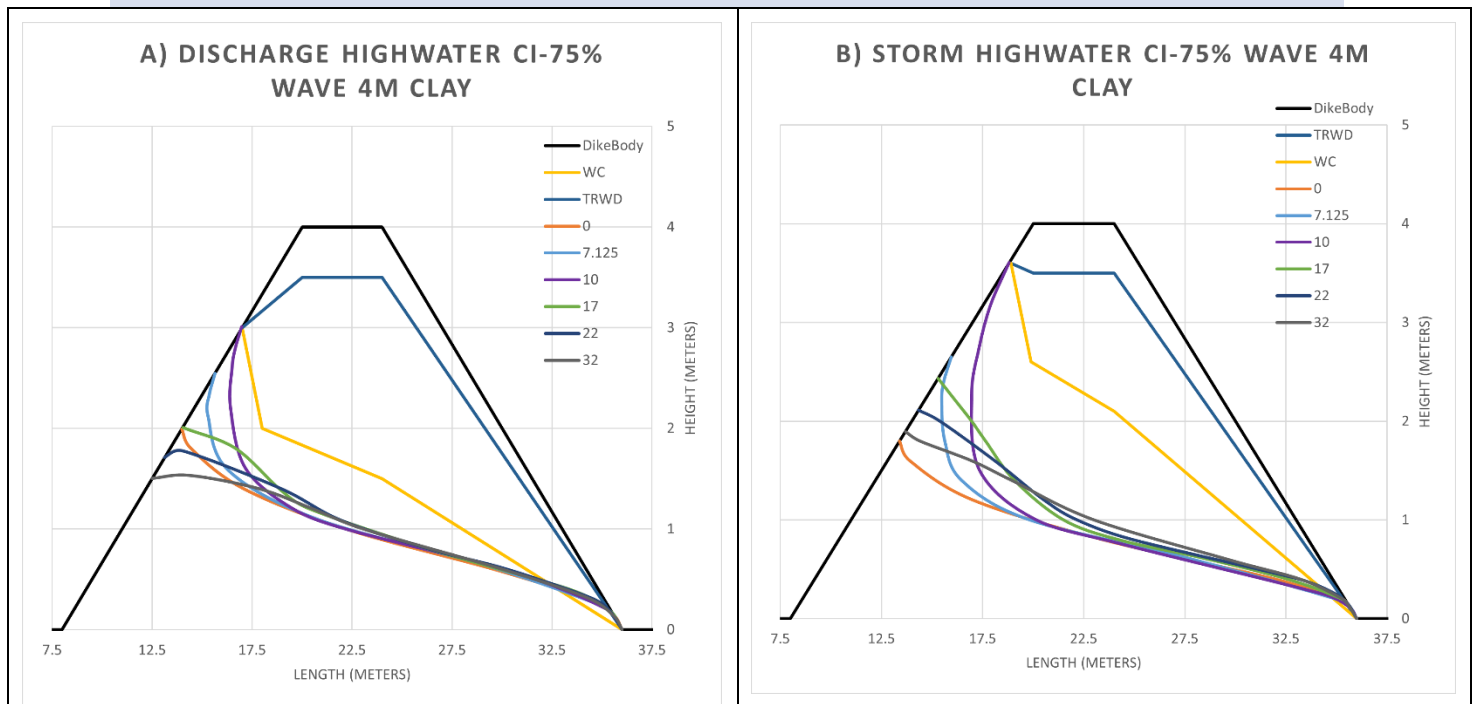


Figure A-7: The phreatic line at different time steps in days together with the dike body and the schematizations of the WC and TRWD for a clay dike with a 4 meter clay sub-soil for: (a) the 75%-Confidence upper bound discharge of the dominated high water wave, (b) the 75%-Confidence upper bound of the storm dominated high water wave.

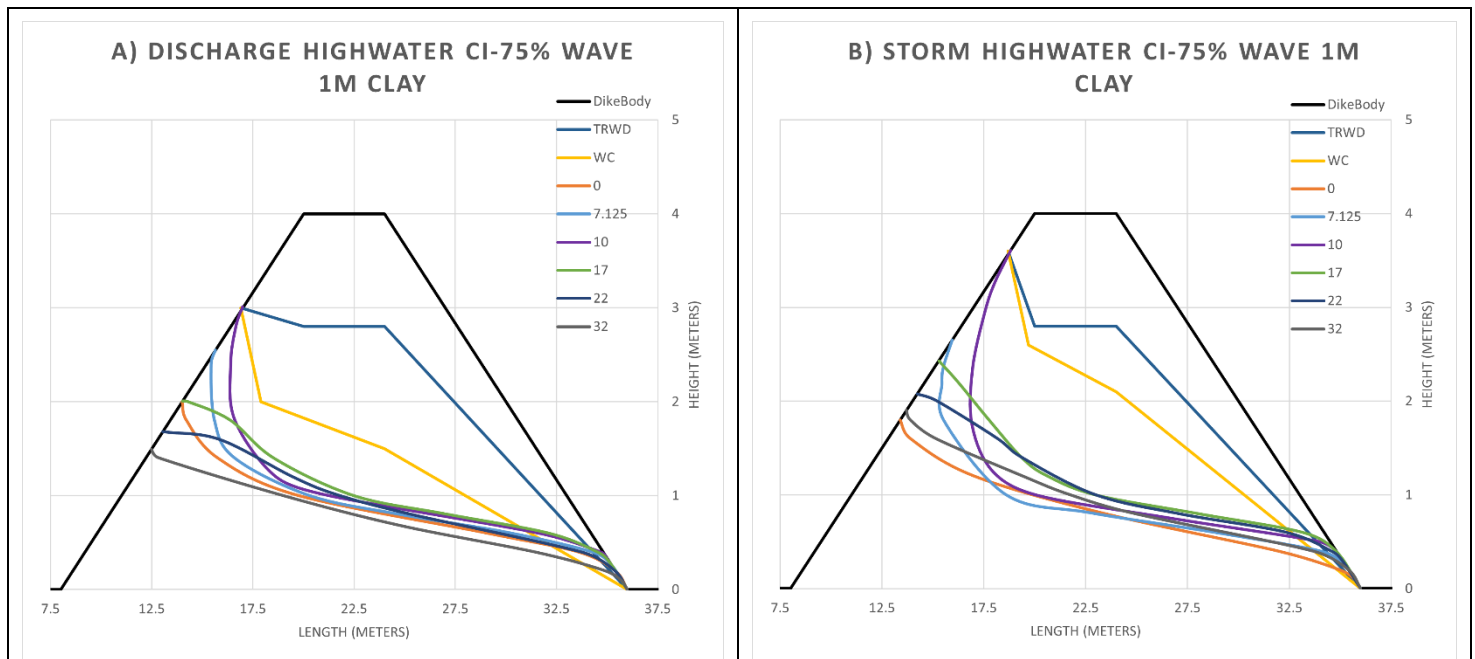


Figure A-8: The phreatic line at different time steps in days together with the dike body and the schematizations of the WC and TRWD for a clay dike with a 1 meter clay sub-soil for: (a) the 75%-Confidence upper bound discharge of the dominated high water wave, (b) the 75%-Confidence upper bound of the storm dominated high water wave.

D DISCHARGE AND STORM HIGH WATER WAVES FULL TIME-SERIES

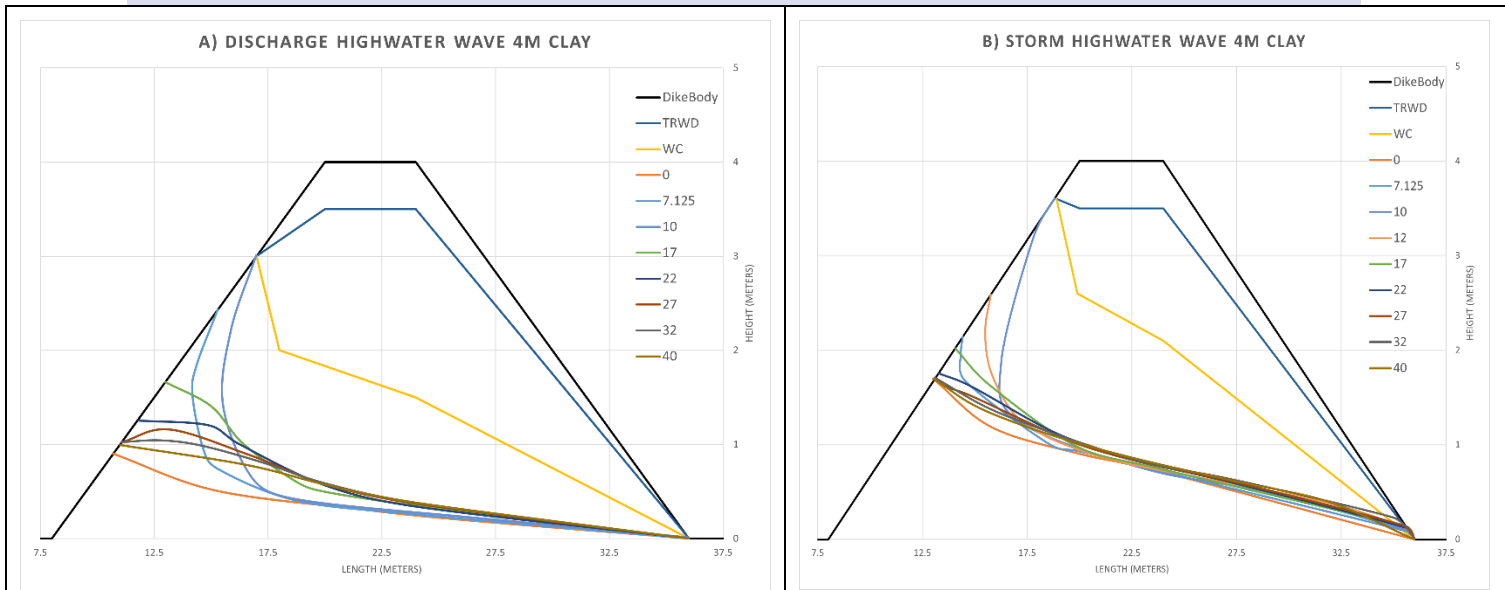


Figure A-9: The phreatic line at different time steps in days together with the dike body and the schematizations of the WC and TRWD for a clay dike with a 4 meter clay sub-soil for: (a) the discharge dominated high water wave, (b) the storm dominated high water wave.

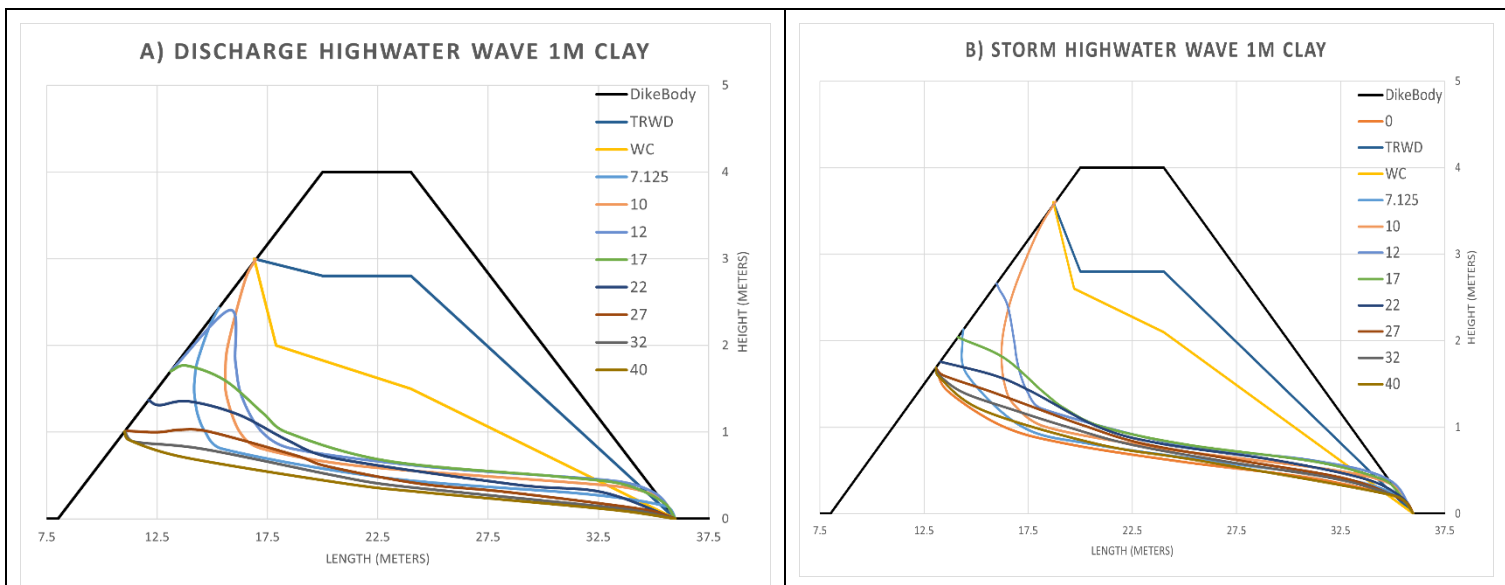


Figure A-10: The phreatic line at different time steps in days together with the dike body and the schematizations of the WC and TRWD for a clay dike with a 1 meter clay sub-soil for: (a) the discharge dominated high water wave, (b) the storm dominated high water wave.

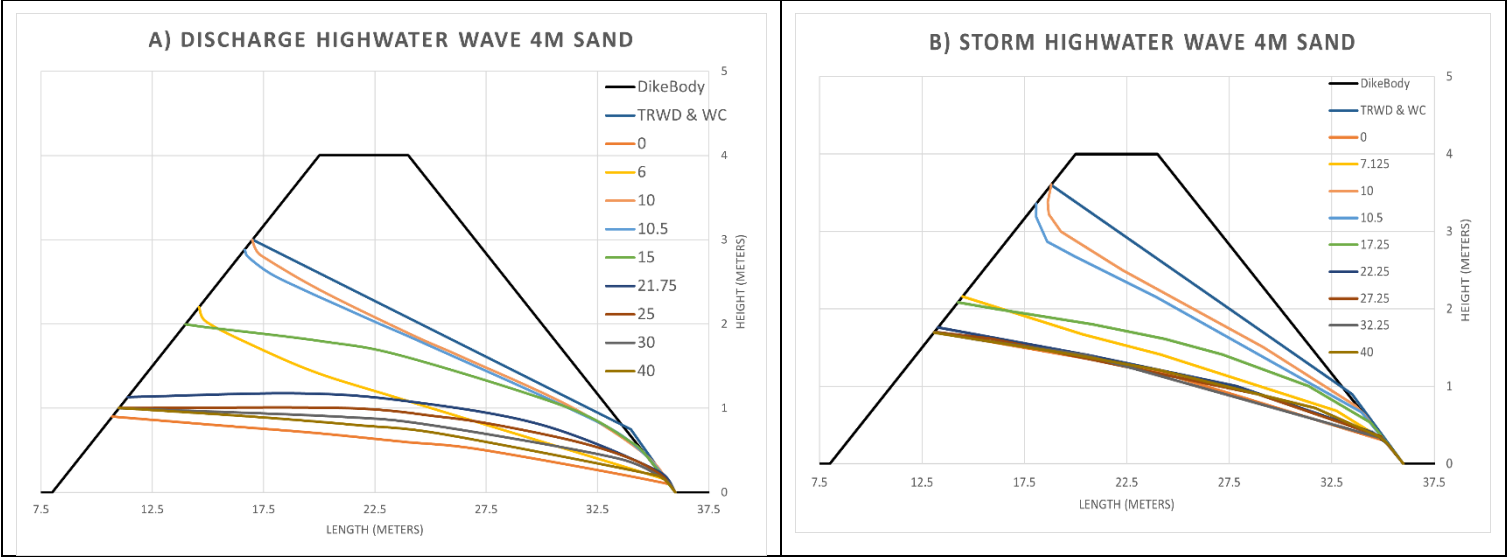


Figure A-11: The phreatic line at different time steps in days together with the dike body and the schematizations of the WC and TRWD for a sand dike with a 4 meter clay sub-soil for: (a) the discharge dominated high water wave, (b) the storm dominated high water wave.

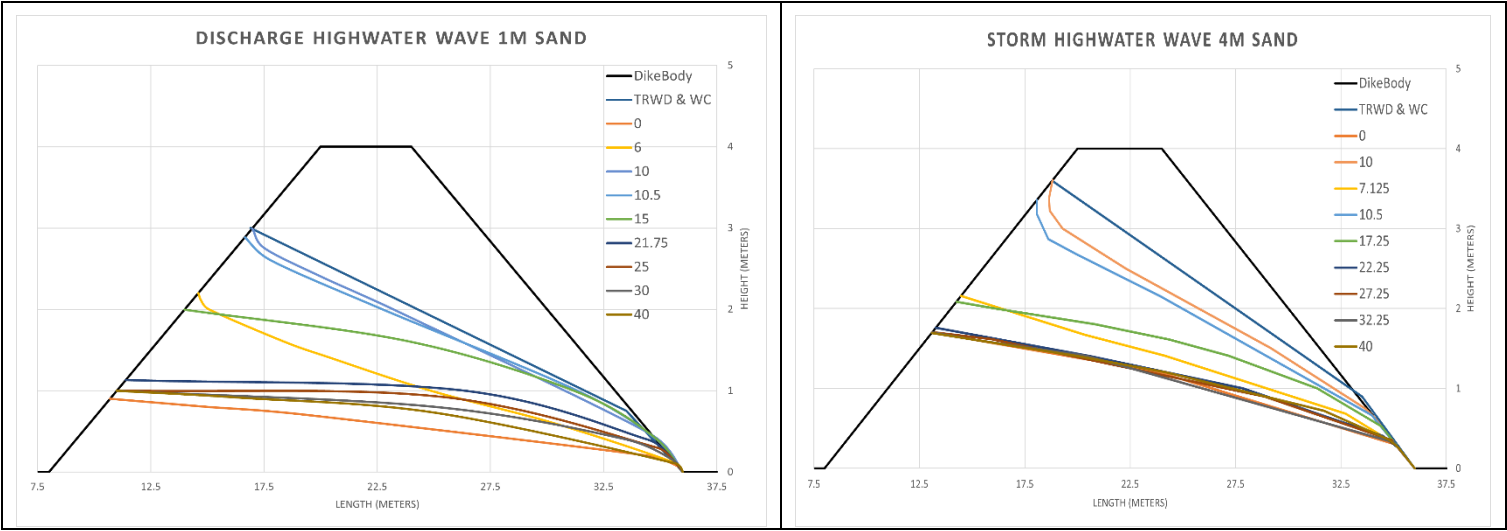


Figure A-12: The phreatic line at different time steps in days together with the dike body and the schematizations of the WC and TRWD for a sand dike with a 1 meter clay sub-soil for: (a) the discharge dominated high water wave, (b) the storm dominated high water wave.

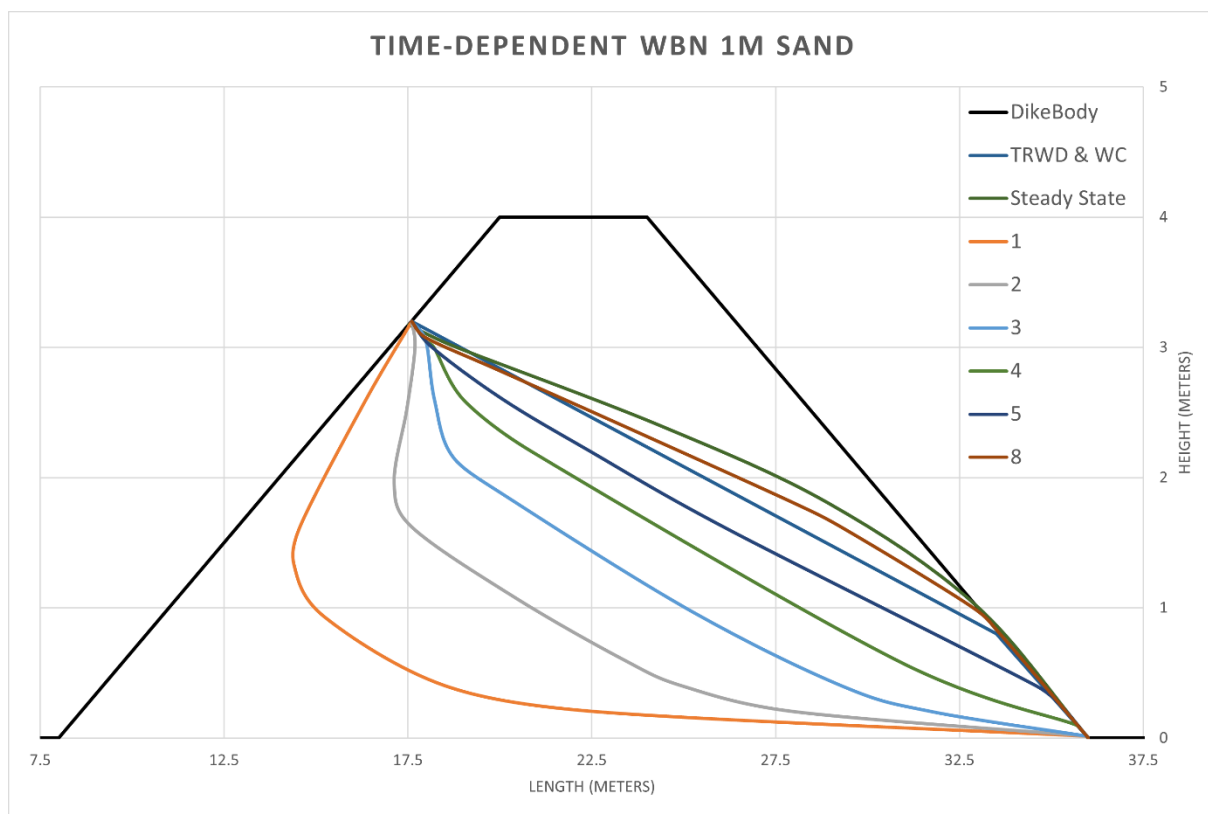


Figure A-13: The phreatic line for a normative water level at different time steps in days together with the dike body and the schematizations of the WC and the TRWD for a sand dike with a 1 meter sub-soil.

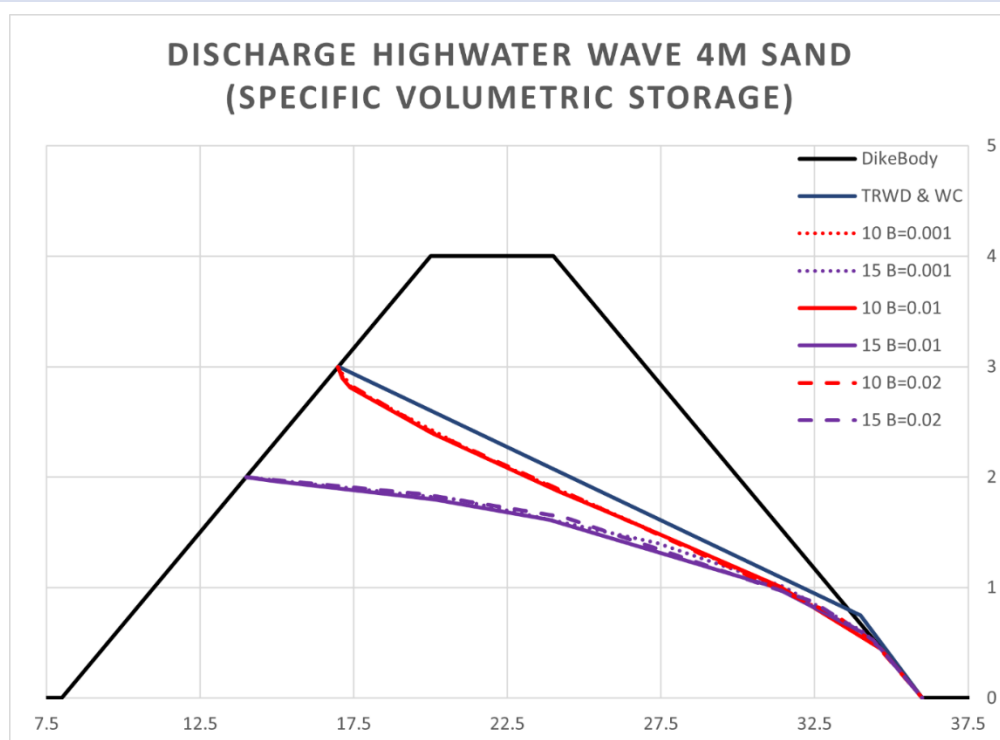
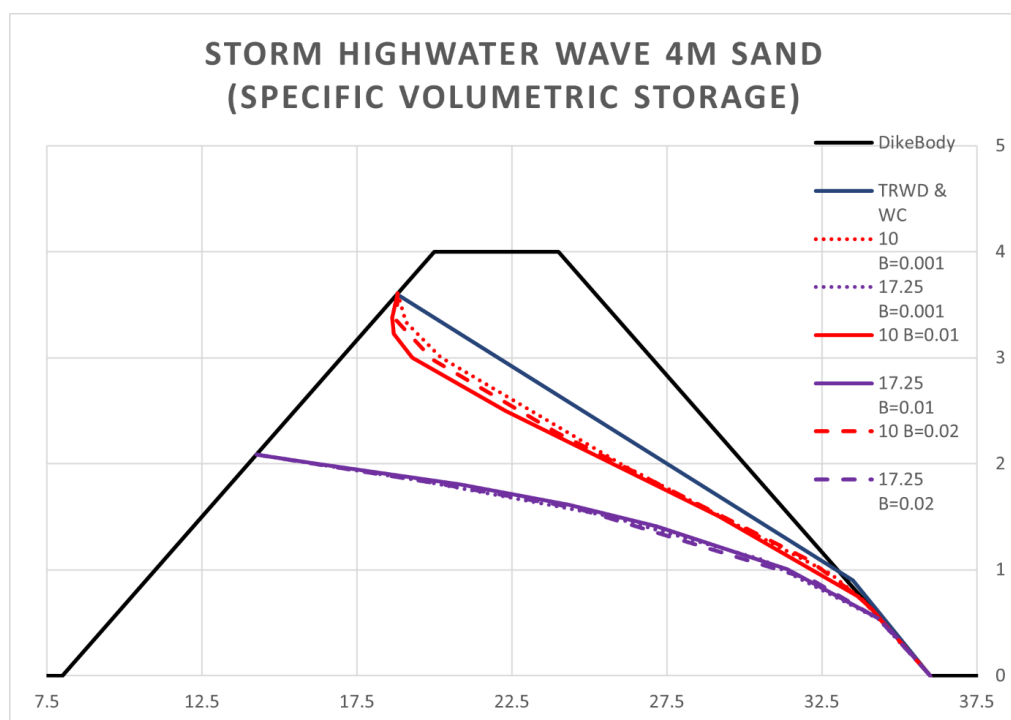


Figure A-14: The phreatic line for a discharge highwater wave with different specific volumetric storage (unit 1/m) at different time steps in days together with the dike body and the schematizations of the WC and the TRWD for a sand dike with a 4 meter sub-soil.



Figure_Apx 15: The phreatic line for a storm highwater wave with different specific volumetric storage (unit 1/m) at different time steps in days together with the dike body and the schematizations of the WC and the TRWD for a sand dike with a 4 meter sub-soil.